

โครเมียนสปีเนลจากหินอัลตราเมฟิกบางส่วนในภาคเหนือและภาคตะวันออกเฉียงของประเทศไทย



นาย วีระศักดิ์ ถิ่นวงษา

สถาบันวิทยบริการ
จุฬาลงกรณ์มหาวิทยาลัย

วิทยานิพนธ์นี้เป็นส่วนหนึ่งของการศึกษาตามหลักสูตรปริญญาวิทยาศาสตรมหาบัณฑิต

สาขาวิชาธรณีวิทยา ภาควิชาธรณีวิทยา

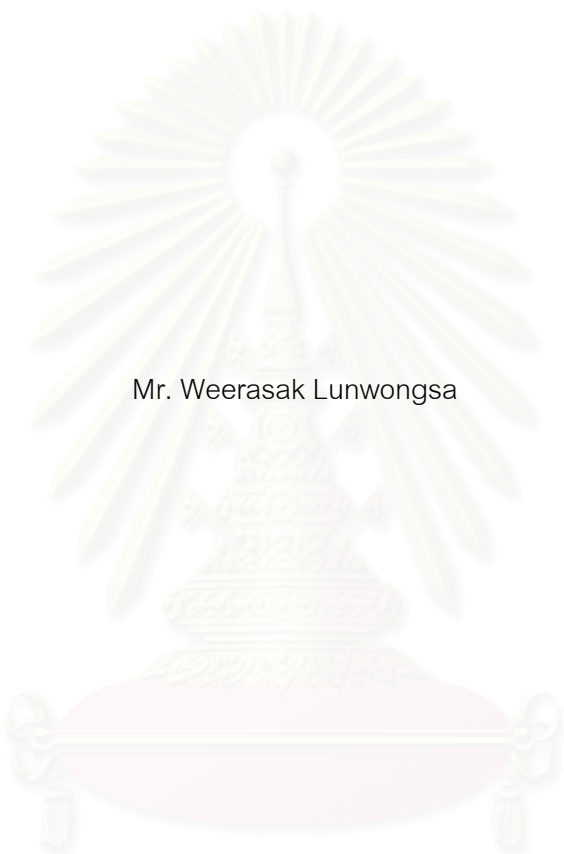
คณะวิทยาศาสตร์ จุฬาลงกรณ์มหาวิทยาลัย

ปีการศึกษา 2547

ISBN 974-53-2121-4

ลิขสิทธิ์ของจุฬาลงกรณ์มหาวิทยาลัย

CHROMIAN SPINEL FROM SOME ULTRAMAFIC IGNEOUS ROCKS IN NORTHERN
AND EASTERN THAILAND



Mr. Weerasak Lunwongsa

สถาบันวิทยบริการ
จุฬาลงกรณ์มหาวิทยาลัย

A Thesis Submitted in Partial Fulfillment of the Requirements
for the Degree of Master of Science in Geology

Department of Geology

Faculty of Science

Chulalongkorn University

Academic Year 2004

ISBN 974-53-2121 -4

Thesis Title CHROMIAN SPINEL FROM SOME ULTRAMAFIC IGNEOUS
ROCKS IN NORTHERN AND EASTERN THAILAND
By Mr. Weerasak Lunwongsa
Field of Study Geology
Thesis advisor Associate Professor Punya Charusiri, Ph.D.
Thesis Co-advisor Associate Professor Ken-ichiro Hisada, Ph.D.

Accepted by the Faculty of Science, Chulalongkorn University in Partial
Fulfillment of the Requirements for the Master's Degree

..... Deputy Dean for Administrative Affairs,
(Assoc. Prof. Tharapong Vitidsant, Ph.D.) Acting Dean, The Faculty of Science

THESIS COMMITTEE

..... Chairman
(Assistant Professor Veerote Daorerk, M.Sc.)

..... Thesis advisor
(Associate Professor Punya Charusiri, Ph.D.)

..... Thesis Co-advisor
(Associate Professor Ken-ichiro Hisada, Ph.D.)

..... Member
(Mr. Prinya Putthapiban, Ph.D.)

นาย วีระศักดิ์ ล้นวงษา: โครเมียนสปิเนลจากหินอัลตราเมฟิกบางส่วนในภาคเหนือและภาคตะวันออกของประเทศไทย (CHROMIAN SPINELS FROM SOME ULTRAMAFIC IGNEOUS ROCKS IN NORTHERN AND EASTERN THAILAND) อ. ที่ปรึกษา: รองศาสตราจารย์ ดร.ปัญญา จารุศิริ, อ.ที่ปรึกษาร่วม : รองศาสตราจารย์ ดร.เคน อิชิโร ฮิซาดะ 123 หน้า. ISBN 974-53-2121-4.

วิทยานิพนธ์ฉบับนี้ มีวัตถุประสงค์ที่จะทำการศึกษาโครเมียนสปิเนลของแร่โครเมียนสปิเนลในหินอัลตราเมฟิกของประเทศไทย และทำการเปรียบเทียบกับแร่โครเมียนสปิเนลในส่วนต่างๆของโลกที่มีความชัดเจนของกระบวนการธรณีวิทยาแปรสัณฐาน แร่โครเมียนสปิเนลจำนวน 120 ตัวอย่างจากแนวตะเข็บธรณีทั้ง 4 แนวในประเทศไทย และ 106 ตัวอย่างจากประเทศต่างๆ ได้ถูกทำการวิเคราะห์องค์ประกอบทางเคมีด้วยเครื่อง อิเล็กตรอนไมโครโพรบ โดยธาตุองค์ประกอบหลัก และ ธาตุองค์ประกอบรองที่ได้ทำการวิเคราะห์ประกอบไปด้วย แมกนีเซียม เหล็ก โครเมียม อะลูมิเนียม ซิลิกา โซเดียม โพแทสเซียม แคลเซียม ไทเทเนียม แมงกานีส และ สังกะสี แร่โครเมียนสปิเนลที่พบในหินอัลตราเมฟิกบริเวณจังหวัดเชียงรายมีลักษณะเป็นผลึกไม่สมบูรณ์ สีส้ม สีน้ำตาลถึงสีน้ำตาลแดง โดยมีกำเนิดในหิน residual harzburgite ซึ่งเกิดจากกระบวนการหลอมละลายบางส่วนระดับต่ำใน fore arc setting แร่โครเมียนสปิเนลในหินอัลตราเมฟิกบริเวณจังหวัดน่าน อุดรดิตต์ มีลักษณะเป็นผลึกกึ่งสมบูรณ์ถึงผลึกสมบูรณ์ ขนาดสม่ำเสมอ สีน้ำตาลแดงถึงสีดำอมน้ำตาล โดยมีกำเนิดในหิน dunite และหิน wehrite ในส่วนของ อัลตราเมฟิก cumulate แร่โครเมียนสปิเนลในพื้นที่นี้สามารถจำแนกออกได้เป็น 2 กลุ่ม กลุ่มแรกแสดงถึงมวลหินอัลตราเมฟิกซึ่งเกิดในบริเวณแนวแยก เหนือแนวการมุดตัวของแผ่นเปลือกโลก และกลุ่มที่สองซึ่งเกิดใน Island arc โดยมีระดับของการหลอมละลายสูงกว่ากลุ่มแรก แร่โครเมียนสปิเนลจากจังหวัดเลยสามารถแบ่งออกได้เป็น 2 กลุ่มเช่นกัน โดยกลุ่มแรกพบใน catablastic host rock แร่โครเมียนสปิเนลส่วนใหญ่เป็นผลึกกึ่งสมบูรณ์ถึงผลึกสมบูรณ์ สีดำถึงสีน้ำตาลอมส้ม หินอัลตราเมฟิกต้นกำเนิดของแร่โครเมียนสปิเนลกลุ่มนี้เป็นหิน cumulate dunite ส่วนอีกกลุ่มหนึ่งพบใน porphyroblastic host rock แร่โครเมียนสปิเนลมีลักษณะเป็นแบบกึ่งตัวนอนและผลึกประกอบ สีน้ำตาลแดงโดยเกิดในหิน residual harzburgite จากองค์ประกอบทางเคมีของแร่โครเมียนสปิเนลแสดงว่ามวลหินอัลตราเมฟิกในพื้นที่นี้จัดเป็น arc peridotite โดยมีต้นกำเนิดจากกระบวนการหลอมละลายบางส่วน ในบริเวณแนวการมุดตัวของแผ่นเปลือกโลก ส่วนแร่โครเมียนสปิเนลที่พบในหินอัลตราเมฟิกบริเวณจังหวัดสระแก้ว มีลักษณะเป็นแบบผลึกกึ่งสมบูรณ์ถึงผลึกสมบูรณ์ สีน้ำตาลแดงถึงสีน้ำตาลแดงเข้ม โดยเกิดในหิน cumulate orthopyroxenite หรือหิน residual harzburgite ที่เกิดในกระบวนการธรณีแปรสัณฐานแบบ fore arc

ภาควิชา.....ธรณีวิทยา..... ลายมือชื่อนิสิต.....

สาขาวิชา.....ธรณีวิทยา..... ลายมือชื่ออาจารย์ที่ปรึกษา.....

ปีการศึกษา.....2547..... ลายมือชื่ออาจารย์ที่ปรึกษา.....

4472411623 : MAJOR Geology

KEY WORD: chromian spinels / ultramafic / subduction / partial melting

WEERASAK LUNWONGSA: CHROMIAN SPINELS FROM SOME ULTRAMAFIC IGNEOUS ROCKS IN NORTHERN AND EASTERN THAILAND. THESIS ADVISOR: ASSOC. PROF. PUNYA CHARUSIRI, PH.D., THESIS COADVISOR : ASSOC. PROF. KEN-ICHIRO HISADA, PH.D., 123 pp. ISBN 974-53-2121 -4.

This thesis is aimed at studying petrochemistry of chromian spinels from some selected ultramafic igneous rocks in Thailand. Comparison is also made for results on Thai spinel geochemistry with those of the well know tectonic setting oversea. A total of 120 chromian spinel grains were selected to represent 4 inferred major sutures in Thailand. Additional 106 grains of other countries were determined for geochemical analysis. All of chromian spinels were analysed by an electron microprobe. Major and minor elements to be analysed were composed of Mg, Fe, Cr, Al, Si, Na, K, Ca, Ti, Mn and Zn. All Fe, Mn and Ti. Spinel found in the Chiang Rai ultramafic rocks are anhedral, orange, and brown to reddish brown. The ultramafic host rock of this area is residual harzburgite and formed by slightly low degree of partial melting within the fore arc setting. All spinels found in ultramafic rocks of the Nan-Uttaradit area are equigranular with subhedral-to-euhedral single crystals. Their color varies from reddish brown to brownish black. This ultramafic host rock should be dunite and wehrite in part of a cumulate layer. The first group represents ultramafic masses that have formed by spreading above subduction zones. The second group indicates higher degree of partial melting that formed in island arc setting. Spinel found in Loei can be divided into two groups. The first group occurs in cataclastic host rock. Spinel of this group are mostly subhedral to euhedral, black to orange brown. The ultramafic host rock of this area is considered as cumulate dunite. The other spinel group relates to porphyroblastic host rock. The spinel is subvermicular and multicrystal with reddish brown color. The ultramafic host rock of this group should be residual harzburgite. Their chemical compositions represent arc peridotite. An ultramafic source was generated by partial melting at subduction. Most spinel found in the Sra Kaeo ultramafic rocks are subhedral to euhedral single. Their color varies from moderate to dark reddish brown. The ultramafic host rock may be cumulate orthopyroxenite or residual harzburgite. A tectonic setting of ultramafic origin in this area was defined by a part of fore arc setting.

Department.....Geology.....Student's signature.....

Field of study.....Geology.....Advisor's signature.....

Academic year.....2004.....Co-advisor's signature.....

ACKNOWLEDGEMENTS

This Msc. Study is mainly sponsored by the Association of International Education, Japan (AIEJ), Japanese Ministry of Education. I am greatly indebted to my both supervisors, Associated Professor Dr.Punya Charusiri and Associated Professor Dr.Ken Ichiro Hisada for their advice, reviewing manuscripts and involve idea throughout this study. Without their helpful, this achievement would not have been possible. Grateful acknowledgements are also made to Dr.Koichi Okusawa my tutor in Japan for his extremely patient tutoring in EPMA technique and laboratory instrument support. I also thank to Chemical Analysis Center University of Tsukuba, Japan for chromian spinel chemical analysis. Special thank for all friend at institute of Geoscience University of Tsukuba especially student in Hiasda sensei laboratory for their helpful in used University facility.

Deeply thank to Mr.Rotthana Ladachard and Mr.Suchart Chinwannachot for graphic work. Mr.Nitiwut Nakchamnan and Mr.Tianpan Ampaiwan for manuscript preparation. My thanks are also due to Department of Geology Chulalongkorn University for general support.

There are of course many people, both in Thailand and in Japan that have helped me in all ways during my study. I wish to express my gratitude to all them.

สถาบันวิทยบริการ
จุฬาลงกรณ์มหาวิทยาลัย

CONTENTS

	PAGE
ABSTRACT IN THAI.....	iv
ABSTRACT IN ENGLISH.....	v
ACKNOWLEDGEMENTS.....	vi
LIST OF TABLES.....	xi
LIST OF FIGURES.....	xii
CHAPTER I INTRODUCTION.....	1
1.1 Background.....	1
1.2 Spinel review.....	6
1.2 Objectives and Scope of Work.....	7
1.3 Methodology.....	10
1.4 Study areas.....	10
1.5 Previous works of Cr-spinels in Thailand.....	12
CHAPTER II GEOLOGICAL SETTING.....	16
2.1 Regional geology.....	16
2.2 Detailed geology.....	19
2.2.1 Area A: Ban Pong Noi.....	19
2.2.2 Area B: Mae Charim, Nan-Tha Pla, Uttaradit.....	23
2.2.3 Area C: Na Klang, Loei.....	30
2.2.4 Area D: Sra Kaeo.....	33
CHAPTER III PETROGRAPHIC INVESTIGATION.....	37
3.1 Petrography of Ultramafic Rock.....	37
3.1.1 Chiang Rai Area.....	40
3.1.2 Nan-Uttaradit Area.....	40
3.1.3 Loei.....	40
3.1.4 Sra Kaeo.....	44
3.2 Spinel Petrography.....	44
3.2.1 Chiang Rai spinel.....	44
3.2.2 Nan-Uttaradit spinel.....	46

	PAGE
3.2.3 Loei spinel.....	46
3.2.4 Sra Kaeo spinel.....	51
CHAPTER IV GEOCHEMISTRY.....	56
4.1 EPMA Method.....	56
4.2 Geochemical results.....	56
4.2.1 Chiang Rai Spinel.....	56
4.2.2 Nan-Uttaradit spinel.....	57
4.2.3 Loei spinel.....	57
4.2.4 Sra Kaeo spinel.....	60
CHAPTER V INTERPRETATION.....	63
5.1 Geochemical Correlation Diagram.....	63
5.1.1 Chiang Rai Spinel.....	63
5.1.2 Nan-Uttaradit spinel.....	63
5.1.3 Loei spinel.....	67
5.1.4 Sra Kaeo spinel.....	67
5.2 Petrographic Interpretation.....	67
5.2.1 Chiang Rai Spinel.....	71
5.2.2 Nan-Uttaradit spinel.....	73
5.2.3 Loei spinel.....	73
5.2.4 Sra Kaeo spinel.....	76
CHAPTER VI DISCUSSION.....	78
6.1 Implication to tectonic setting.....	78
6.1.1 Abyssal peridotites.....	81
6.1.2 Fore arc peridotites.....	81
6.1.3 Back arc peridotites.....	81
6.1.4 Subcontinental peridotite.....	82
6.1.5 A alpine type peridoties.....	82
6.2 Comparison with other studies areas.....	83
6.2.1 Sohar, Oman.....	85

	PAGE
6.2.2 Davos, Switzerland.....	89
6.2.3 Song Ma, Viet Nam.....	90
6.2.4 Indus, Tibet.....	97
6.3 Comparison of the results between Thai and overseas spinels....	101
6.3.1 Nan-Uttaradit VS Song Ma Viet Nam.....	101
6.3.2 Sra Kaeo VS Sohar Oman.....	101
6.4 Tectonic setting of individual suture.....	103
6.4.1 Chiang Mai.....	103
6.4.2 Sra Kaeo.....	104
6.4.3 Nan-Uttaradit.....	105
6.4.4 Loei.....	105
CHAPTER VII CONCLUSION.....	107
7.1 Chiang Rai.....	107
7.2 Nan-Uttaradit.....	107
7.3 Loei.....	109
7.4 Sra Kaeo.....	109
REFERENCES.....	110
APPENDICES.....	116
APPENDIX I.....	117
How to calculate ferric and ferrous in chromian spinel by spinel By spinel stoichiometry.....	113
APPENDIX II.....	118
Table II.1 Representative microprobe analyses of detrital chromian spinels from Sohar, Oman.....	119
Table II.2 Representative microprobe analyses of detrital chromian Spinels from Davas, Switzerland.....	120
Table II.3 Representative microprobe analyses of detrital chromian Spinels from Indus, Tibet.....	121
Table II.4 Representative microprobe analyses of detrital chromian	

	PAGE
Spinels from Song Ma, Vietnam.....	122
BIOGRAPHY.....	123



สถาบันวิทยบริการ
จุฬาลงกรณ์มหาวิทยาลัย

LIST OF TABLES

TABLE		PAGE
1.1	Detailed locations of ultramafic rocks collected for Cr spinel analyses.....	12
4.1	Representative microprobe analyses of chromian spinels in ultramafic rock from Chiang Rai.	58
4.2	Representative microprobe analyses of chromian spinels in ultramafic rock from Nan-Uttaradit.....	59
4.3	Representative microprobe analyses of chromian spinels in ultramafic rock from Loei.....	61
4.4	Representative microprobe analyses of chromian spinels in ultramafic rock from Sra Kaeo.....	62
7.1	Classified ultramafic host rocks and tectonic setting of each areas from Thailand by chromian spinel chemistry.....	109



สถาบันวิทยบริการ
จุฬาลงกรณ์มหาวิทยาลัย

LIST OF FIGURES

FIGURES		PAGE
1.1	Outline map of Southeast Asia showing branch suture and major tectonic element referred in text. CSZ = Changning-Shuangjiang zone, TZ = Tengjiaohe zone, BRZ = Bentong-Raub zone (modified after Barr and Macdonald, 1987 and Charusiri et al., 2002).....	2
1.2	Distribution of principal continental terranes and structures of East and Southeast Asia. EM = East Malaya, WB = west Burma, SWB = South West Borneo, S = Semitau Terrane, L = Lhasa Terrance, HT = Hainan Island Terranes, QT = Qiangtang Terrane, QS = Qamdo-Simao Terrane, SI = Simao Terrane, SG = Songpan Ganzi accretionary complex, KT = Kurosegawa Terrane, KL = Kunlun Terrane, QD = Qaidam Terrane, AL = Ala Shan Terrane, LC = Lampang-Chiang Rai, and NT = Nakhon Thai (modified after Metcalfe et al, 1999).....	3
1.3	The tectonic interpretation map of Thailand based on the results of airborne geophysical and geological data, showing five sutures and two microplates Nakhon Thai and Lampang-Chiang Rai between Shan Thai and Indochina terrane (modified after Tulyatid and Charusiri, 1999 and Charusiri et. al., 2002).....	4
1.4	Model for the emplacement of certain alpine ultramafics A) during and early stage of alpine orogenic cycle, oceanic crust is subducted beneath the continental margin at low angle. B) weakened serpentinite (ultramafic rise upward along a fault. C) as subduction continues, angle of plate junction steepens and rate of subduction may quicken, higher pressure than before any given temperature (lockwood, 1972).....	8
1.5	Alternative tectonic models for the setting of ophiolite genesis A) fast-spreading ridge (left) and slow-spreading ridge (right) B) spreading ridge between continental fragment C) a fracture zone is converted into a subduction zone followed by SSZ-type spreading above D) collapse of spreading ridge (Robertson, 2004).....	9
1.6	Methodology chart of this study.....	11

FIGURES	PAGE
1.7 Map illustrate four substudy areas; A = Chiang Rai, B = Nan-Uttaradit, C = Loei and D = Sra Kaeo, red solid star represent ultramafic sample locations (Geology by DMR, 1991).....	13
2.1 Simplified geological map of Thailand showing the distribution of rocks of various ages, significant tectonic plates and major sutures/faults system (Charusiri et al., 2002).....	18
2.2 Geologic map of Ban Pong Noi, Amphoe Chiang Khong Changwat Chiang Rai (Department of mineral resource, 1989), red solid star represent ultramafic sample locations.....	21
2.3 Geologic map of Amphoe Mae Chan, Changwat Chiang Rai (Department of mineral resource, 2000), red solid star represent detrital spinel sample locations.....	22
2.4 Geologic map of Amphoe Mae Charim, Changwat Nan (Department of mineral resource, 1987), red solid star represent ultramafic sample locations.....	24
2.5 Geologic map of Amphoe Tha Pla, Changwat Uttaradit (Department of mineral resource, 1987), red solid star represent ultramafic sample locations.....	27
2.6 Geologic map of the Nan-Uttaradit area(A) in northern Thailand(B) showing distribution of rock units (after Charusiri et al, 2005) and geological structure and sample locations (red solid star).....	29
2.7 Geologic map of Ban Khok, Amphoe Na Klang Changwat Loei (Department of mineral resource, 1985), red solid star represent ultramafic sample locations.....	31
2.8 Geologic map of Amphoe Wang Nam Yen, Changwat Sra Kaeo (Department of mineral resource, 1997), red solid star represent ultramafic sample locations.....	34
3.1 Graph showing relationship between compositional field of spinels from	

FIGURES	PAGE
ultramafic rock types (Pober and Faupl, 1983).....	38
3.2 Ternary plots of Cr#, Al# and Fe# for spinels of different of ultramafic host rock; Abyssal and Alpine-type peridotite, Stratiform complexes and Tulameen alaskan-type complex (Cookenboo et al., 1997).....	38
3.3 Simplified model of ultramafic origin (Arai, 2000).....	39
3.4 Photomicrograph of Chiang Rai ultramafic host rock showing; rounded orthopyroxene relicts and serpentine disseminated in glass-rich ground mass. Note that rock is cross cut by talc veinlet (long axis of photo is 2 mm).....	41
3.5 Photomicrograph of Chiang Rai ultramafic host rock showing; lensoid-shaped clinopyroxene replaced by deuteric subhedral calcite aggregate (long axis of photo is 2 mm).....	41
3.6 Photomicrograph of Nan ultramafic host rock showing altered clinopyroxene at the right side enclosed by antigorite mesh. The rock also shows cataclastic texture (long axis is 2 mm).....	42
3.7 Photomicrograph of Uttaradit ultramafic host rock showing euhedral spinel (black) disseminated in mesh of antigorite and lizardite groundmass (long axis of photo is 2 mm).....	42
3.8 Photomicrograph of Loei ultramafic host rock showing altered olivine patches surrounded by polygonal serpentine. Note that some olivine patches replaced by calcite (long axis of photo is 2 mm).....	43
3.9 Photomicrograph of Loei ultramafic host rock showing fibrous chrysotile altered from orthopyroxene in central part, and lens shape of pyroxene squeezed was replaced by calcite on top (long axis of photo is 2 mm).....	43
3.10 Photomicrograph of Sra Kaeo ultramafic host rock showing deformed orthopyroxene clast and porphyroblastic texture and two directions perfect cleavage system of antigorite called real mesh (reticulate) structure (long axis of photo is 2 mm).....	45

FIGURE	PAGE
3.11 Sketch of the morphological characteristic of chromian spinels of Chiang Rai.....	47
3.12 Photomicrographs of spinels from Chiang Rai ultramafic rocks showing isolated single crystals (A and G) and crystalline aggregate (B, C, D, E, and F). Mostly spinels are anhedral.....	48
3.13 Sketch of the morphological characteristic of chromian spinels of Nan-Uttaradit.....	49
3.14 Photomicrographs of spinels from Nan-Uttaradit ultramafic host rocks showing isolated grains (A and I) and equigranular (G and J), with subhedral (C, D, F, and H) to euhedral (B, G, and I) shapes.....	50
3.15 Sketch of the morphological characteristic of chromian spinels of Loei.....	52
3.16 Photomicrographs of spinels from Loei ultramafic host rocks showing single rounded anhedral (A, B, C, and D), equigranular euhedral (E and F) and large multicrystalline (G).....	53
3.17 Sketch of the morphological characteristic of chromian spinels of Sra Kaeo.....	54
3.18 Photomicrographs of spinels from Sra Kaeo ultramafic host rocks showing isolated grains (E) subhedral (A and C) to euhedral (B, D, and F).....	55
5.1 Cr# and Mg# plots of spinels from Chiang Rai mostly within Alpine type peridotite and some in stratiform complex field of ultramafic bodies (Irvine, 1974).....	64
5.2 Cr#-TiO ₂ relationship of chromian spinels from Chiang Rai mostly indicating fore-arc setting field (modified from Arai, 1992 and Charusiri 2000).....	64
5.3 Cr# and Mg# plots of spinels from Nan-Uttaradit mostly outside but close to Alpine type peridotite with some minor stratiform complex ultramafic bodies (Irvine, 1974).....	65

FIGURE	PAGE
5.4 Cr#-TiO ₂ relationship of chromian spinel from Nan-Uttaradit mostly within the island arc tectonic setting field (modified from Arai, 1992 and Charusiri, 2000).....	65
5.5 Cr# and Mg# plots of spinels from Thailand (left with red dots) in comparison with several models of spinel in ultramafic origin (black in right diagrams) from different tectonic setting (Haggerty, 1976).....	66
5.6 Cr# and Mg# plots of spinels from Loei mostly within the stratiform complex and some in Alpine-type peridotite ultramafic bodies (Irvine, 1974).....	68
5.7 Cr#-TiO ₂ relationship of chromian spinel from Loei mostly within the island-arc field and some in fore-arc tectonic setting field (modified form Arai, 1992 and Charusiri, 2000).....	68
5.8 Cr# and Mg# plots of spinels from Sra Kaeo almost all within the Alpine-type peridotite and stratiform complex bodies, only few are out side these two field (Irvine, 1974).....	69
5.9 Cr#-TiO ₂ relationship of chromian spinels from Sra Kaeo mostly located within fore-arc tectonic setting field (modified from Arai, 1992 and Charusiri, 2000).....	69
5.10 Schematic diagrams to show relationship between morphological change of chromian spinel and lithological variation due to mantle/melt interaction (Matsumoto and Arai, 2001).....	70
5.11 Cr# and Mg# plots of spinels from Chiang Rai plots in the compositional fields of Iherzolite, harzburgite, and cumulate of spinels from ultramafic rock types (Pober and Faupl, 1988).....	72
5.12 Trivalent partition plot of spinels from Chiang Rai showing trivalent plot mostly in arc setting (Cookenboo et al., 1997).....	72
5.13 Cr# and Mg# relation of spinel from Nan-Uttaradit howing plots in the compositional field of cumulates of spinels from ultramafic rock types (Pober and Faupl, 1988).....	74

FIGURE	PAGE
5.14 Trivalent partition plot of spinels from Nan-Uttaradit showing trivalent plot mostly in stratiform complex (Cookenboo et al., 1997).....	74
5.15 Cr# and Mg# plots of spinels from Loei showing plots in compositional field of cumulates and some in harzburgite of spinels from ultramafic rock types (Pober and Faupl, 1988).....	75
5.16 Trivalent partition plot of spinels from Loei showing trivalent plot mostly in stratiform complex and some in Alpine-type peridotite (Cookenboo et al., 1997).....	75
5.17 Cr# and Mg# plots of spinels from Sra Kaeo plotted mostly in cumulates field on compositional field of spinels from ultramafic rock types (Pober and Faupl, 1988).....	77
5.18 Trivalent partition plot of spinels from Sra Kaeo showing trivalent plot mostly in overlap zone between stratiform complex and Alpine-type peridotite (Cookenboo et al., 1997).....	77
6.1 Variation of Cr# and Mg# in spinels during partial melting of mantle materials and during fractionation of extracted melt (primary magma). Arrow present trend of chemical variation.....	79
6.2 Variation of trivalent partition in spinels during partial melting of mantle materials and during fractionation of extracted melt (primary magma). Arrows present trend of chemical variation.....	79
6.3 Relationship Cr#-TiO ₂ contents of mafic and ultramafic origins for the classification of tectonic setting (after Arai, 1992).....	80
6.4 Diagram showing ranges of Cr# of spinel in peridotites from different tectonic settings. The heavy--line represents the majority of data plots.....	80
6.5 Geographic map of Asia showing locations where spinel-bearing ultramafic rocks were collected	84
6.6 Photomicrographs of spinel from Oman.....	87
6.7 Chemical relation plots of spinels from Oman. A) Ternary plot of the major	

FIGURE	PAGE
trivalent cation, B) Cr# and Mg# plot on compositional field of spinel from ultramafic rock type, C) Cr# and Mg# relation plot with Alpine type peridotite and stratiform complex ultramafic bodies, and D) Cr#-TiO ₂ relationship compared with tectonic-setting field.....	88
6.8 Photomicrographs of spinels from Switzerland ultramafic rocks.....	91
6.9 Chemical relation plots of spinels from Switzerland. A) Ternary plot of the major trivalent cation, B) Cr# and Mg# plot on compositional field of spinel from ultramafic rock type, C) Cr# and Mg# relation plot with Alpine type peridotite and stratiform complex ultramafic bodies, and D) Cr#-TiO ₂ relationship compared with tectonic-setting field.....	92
6.10 Photomicrographs of spinels from VietNam ultramafic rocks.....	94
6.11 Chemical relation plots of spinels from Vietnam. A) Ternary plot of the major trivalent cation, B) Cr# and Mg# plot on compositional field of spinel from ultramafic rock type, C) Cr# and Mg# relation plot with Alpine type peridotite and stratiform complex ultramafic bodies, and D) Cr#-TiO ₂ relationship compared with tectonic-setting field.....	95
6.12 Cr# and Mg# relation plot of spinels from several countries (left with red dots) in comparison with several models of spinel in ultramafic origin (Black in right diagrams) from different tectonic setting (Haggerty, 1976).....	96
6.13 Photomicrographs of spinels from Tibet ultramafic rocks.....	98
6.14 Chemical relation plots of spinels from Oman. A) Ternary plot of the major trivalent cation, B) Cr# and Mg# plot on compositional field of spinel from ultramafic rock type, C) Cr# and Mg# relation plot with Alpine type peridotite and stratiform complex ultramafic bodies, and D) Cr#-TiO ₂ Relationship compared with tectonic-setting field.....	99
6.15 Diagram showing Cr# plot of all areas compare range of Cr# of spinel in	

FIGURE	PAGE
peridotites from different tectonic settings (Arai, 1994). The heavy-line part represents the majority of data plots.....	102
7.1 The conclusive model of ultramafic origins from each interpreted suture zone A) Chiang Rai; Fore arc setting B) Nan-Uttaradit; (1) SSZ ultramafic and (2) Island arc peridotite C) Loei; Fore arc or island arc ultramafic peridotite D) Sra Kaeo; Fore arc peridotite.....	108



สถาบันวิทยบริการ
จุฬาลงกรณ์มหาวิทยาลัย

CHAPTER I

INTRODUCTION

1.1 Background

Since nineteenth century, many geoscientists have widely studied geologic evolution of Thailand. Based on Bunopas (1992), Thailand was comprised of a complex assembly of two alloctonous microcontinents, namely Shan-Thai in the west and Indochina in the east, with the N-Strending linear Nan-Sra Kaeo suture as their entity. Additionally, Charusiri et al. (2002) proposed the other two tectonic blocks, viz. Lampang-Chiang Rai and Nakhon Thai, immediately western and eastern sides of the Nan-Sra Kaeo suture, respectively. Both Shan-thai and Indochina microcontinents were thought to possibly be cratonic fragments of the Southern Hemisphere supercontinent, "Gondwana". These two microcontinents were rifted from their parent craton possibly Australia (Bunopas, 1981) during Middle Paleozoic and then moved up to lower southern latitudes in Late Paleozoic and across the equator to lower northern hemisphere by middle Permian (Charusiri et al., 2002). Late Paleozoic tectonism may have caused the pair "Benioff" subduction of the paleotethys-one subducted westward beneath Shan-Thai and the other eastward beneath Indochina (Bunopas and Vella, 1978, 1991) which may have triggered the development of Lampang-Chiang Rai and Nakhon Thai mainly oceanic plates. Magmatism at plate margins and subsequent collision of individual plates may have occurred in Permo-Triassic to Late Triassic periods. Later the appearance of mountain ranges along the sutures which in response to the uplifted plutonic and volcanic rocks forming long sinuous tectonic belts, were widely distributed throughout plate boundaries (Charusiri et al., 1993).

Suture zones in Thailand occurred as branch sutures or tectonic lines (Charusiri et al., 2002) and are inferred to correlate with Langcangjiang and Changning-Menglian sutures in Tibet and Yunnan (Figure 1.1 and Figure1.2). Numbers of sutures zones were highly possible to preserve remnants of the Paleotethys (Barr and MacDonald, 1987 and Metcalfe, 1999). The advent of the two newly proposed smaller tectonic blocks between Shan-Thai and Indochina, namely the paleotethys Nakhon Thai oceanic crust in the east

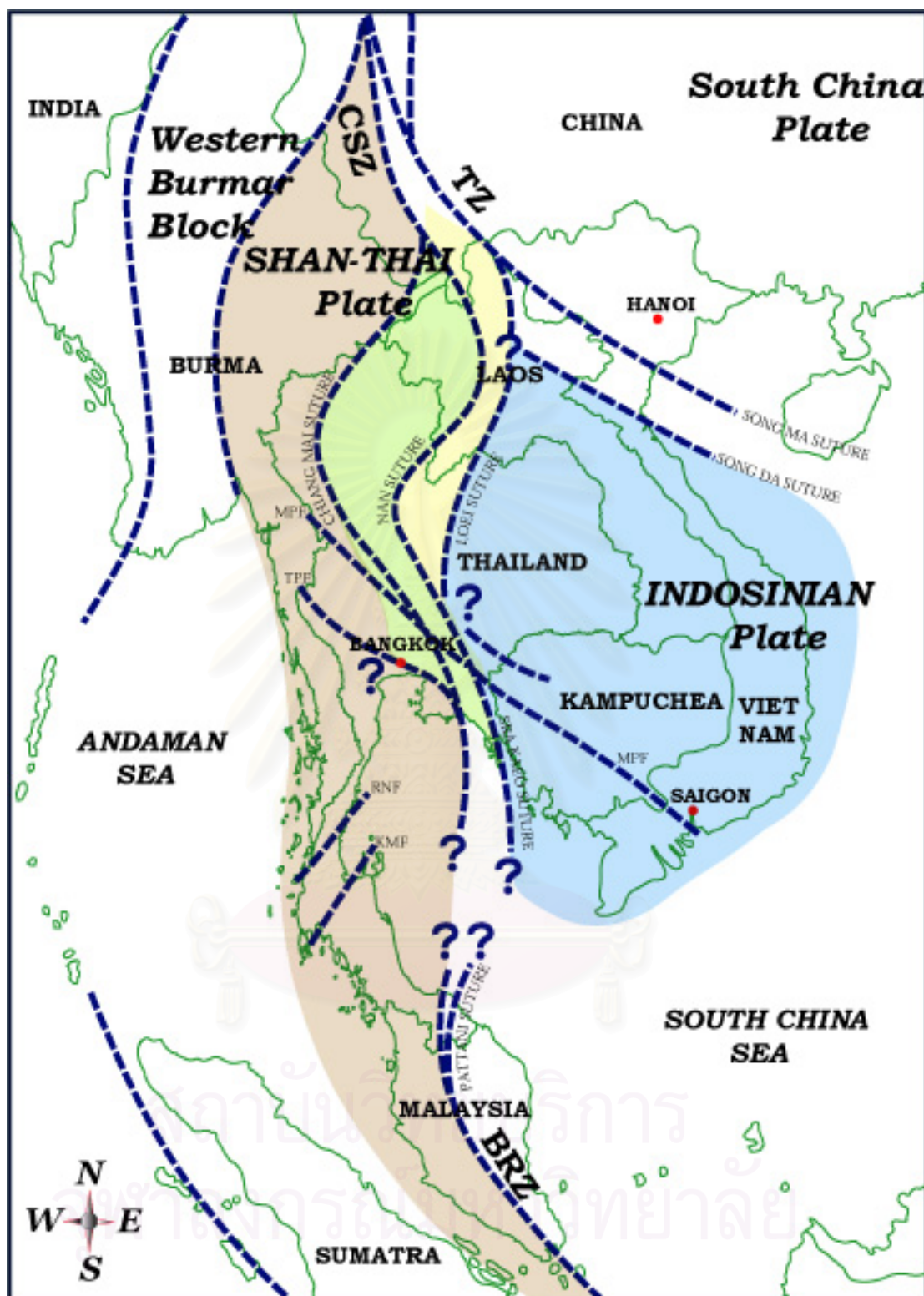


Figure 1.1 Outline map of Southeast Asia showing branch suture and major tectonic element referred in text. CSZ = Changning-Shuangjiang zone, TZ = Tengiaohu zone, BRZ = Bentong-Raub zone (modified after Barr and Macdonald, 1987 and Charusiri et al., 2002).

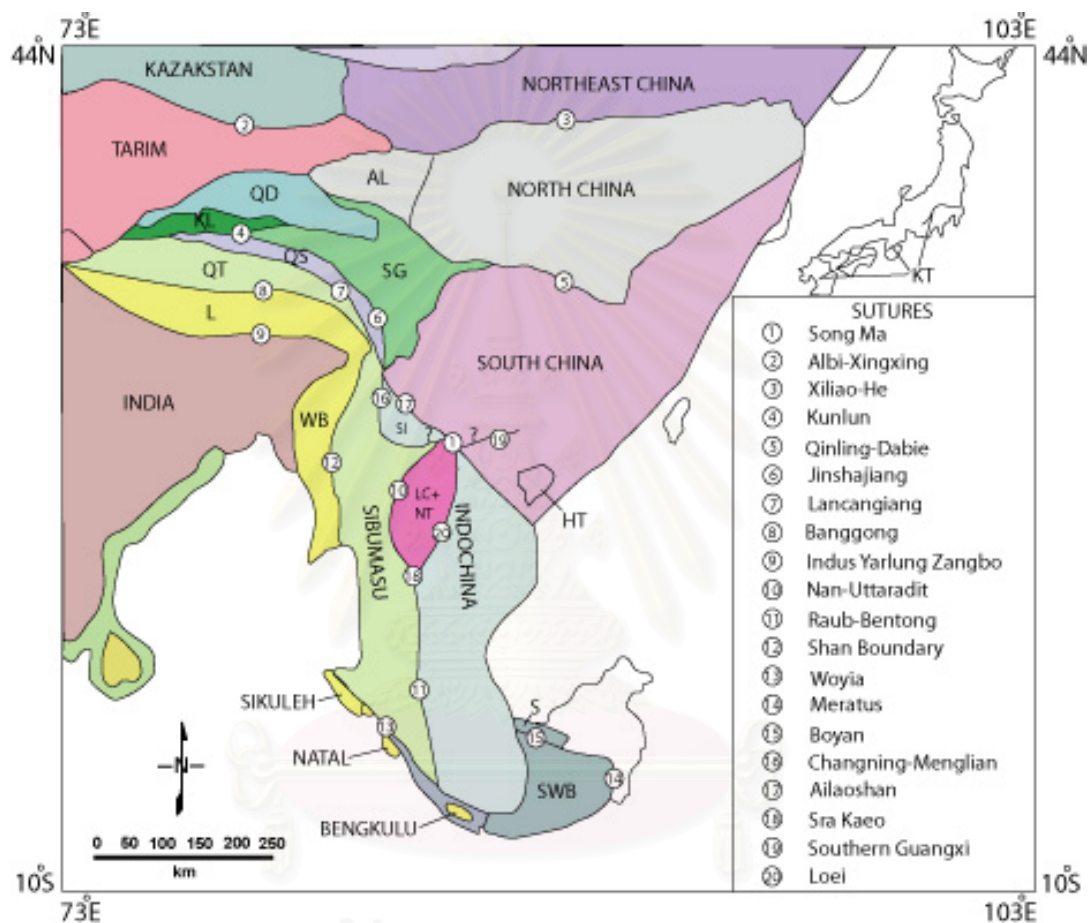


Figure 1.2 Distribution of principal continental terranes and major structures of East and Southeast Asia. EM = East Malaya, WB = west Burma, SWB = South West Borneo, S = Semitau Terrane, L = Lhasa Terrance, HT = Hainan Island Terranes, QT = Qiangtang Terrane, QS = Qamdo-Simao Terrane, SI = Simao Terrane, SG = Songpan Ganzi accretionary complex, KT = Kurosegawa Terrane, KL = Kunlun Terrane, QD = Qaidam Terrane, AL = Ala Shan Terrane, LC = Lampang-Chiang Rai, and NT = Nakhon Thai (modified after Metcalfe et al, 1999).

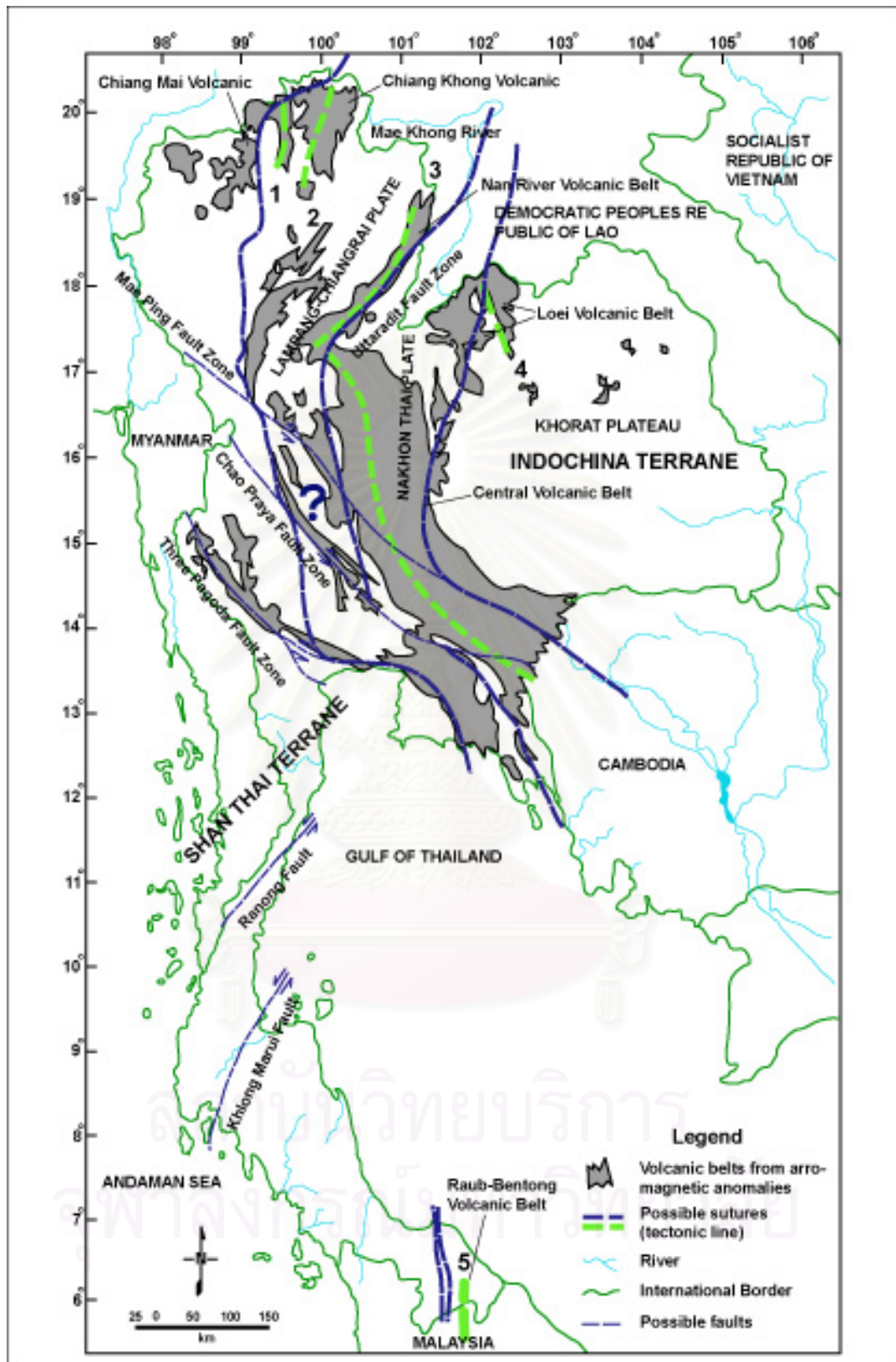


Figure 1.3 The tectonic interpretation map of Thailand based on the results of airborne geophysical and geological data, showing five sutures and two microplates Nakhon Thai and Lampang-Chiang Rai between Shan Thai and Indochina terrane (modified after Tulyatid and Charusiri, 1999 and Charusiri et al., 2002).

and Lampang-Chiang Rai volcanic arc in the west (Figure 1.3), significantly changed geological components and tectonic evolution model of Thailand and mainland SE Asia, particularly numbers and positions of suture zones. As inferred from many kinds of available geological, geochemical and geophysical data (see also Figure 1.3). Three suture zones of Thailand are proposed by Charusiri et al. (op. cit.) called Chiang Mai-Chiang Rai, Nan-Uttaradit and Loei sutures. The Chiang Mai-Chiang Rai suture zone trended northeast-southwest ward and extended from northeast of Chiang Rai to eastern parts of Chiang Mai and eastern Tak (Vicharn Arunsrisanchai, 2003, personal communication). The Nan-Uttaradit suture commenced in Nan and continued southwestward to Uttaradit along the Nan River and disappeared in the Chao Phraya Central Plain due to the continuous interaction of the Mae Ping Fault. The north-south trending Loei suture extended from Loei southward along the western margin of the Khorat Plateau, including Nakhon Nayok, Prachinburi and Sra Kaeo in southeastern Thailand. Moreover, there is the suture zone near the boundary between Thailand and Malaysia namely Bentong-Raub (Tan, 1996) or Pattani (Charusiri et al., 2002) suture zone, which was widely interpreted to join either Nan-Uttaradit suture (Barr and MacDonald, 1991 and Bunopas, 1994) or Chiang Mai-Chiang Rai suture (Mitchell, 1988, 1992). The margins of these belts are regarded as the tectonic lines or sutures (Charusiri et al., 2000) and have been interpreted as paleo-subduction zones (see also Tan, 1996). However, these tectonic setting interpretations were discussed based on limited geological evidences of few good exposures. Geological belt correlation from the northern part eastward and southward is very difficult due to the limitation of various geological data. This makes the tectonic setting of several suture zones in Thailand an interesting topic of investigation.

This thesis is aimed at studying petrochemistry of chromian spinels from some selected ultramafic igneous rocks in Thailand. Since it is considered that the petrochemical data of Cr-spinels can unravel the tectonic setting of the country. Comparison is also made for results on Thai spinel geochemistry with those of the overseas well-know tectonic setting.

1.2 Spinel review

Chromian spinel's principle constituents behave very differently during fractional crystallization or partial melting, with Cr and Mg strongly partitioned into the solid, and Al strongly partitioned into the melt. In addition, partitioning of Mg and Fe^{2+} between spinel and silicate melts and minerals is strongly temperature dependent and the ratio of Fe^{2+} to Fe^{3+} varies according to $f\text{O}_2$. As early magmatic mineral chromian spinels reflects magmatic conditions, such as pressure, temperature and melt composition. Due to these characteristics, chromian spinel is a good indicator of the physiochemical condition of a host rock.

Earlier works have been done for chromian spinels. Good example is shown below. Till present, chromian spinel has been a focus of interest for unravelling tectonic setting by several geoscientists. Irvine (1974) used worldwide chromian spinel compositions from ultramafic bodies to define fields of alpine-type peridotites and stratiform complex based on chrome partition ($\text{Cr}/\text{Cr}+\text{Al}$) and magnesium partition ($\text{Mg}/\text{Mg}+\text{Fe}^{2+}$).

In USA, Dick and Bullen (1984) reported that chemical compositions of chromian spinel from a variety of ultramafic complexes can be discriminated by trivalent plotting of Cr^{3+} , Al^{3+} and Fe^{3+} partition and useful for distinguishing alpine-type peridotites from stratiform peridotites and Alaskan type. Detrital chromian spinels have been also proved to be an excellent tracer for tectonic setting even in the areas with poorly defined geology.

In Europe, Pober and Faupl (1988) presented relationship between chrome and magnesium partitions of chromian spinel implicated to ultramafic host rocks (such as lherzolites, harzburgites, ultramafic cumulates and podiform chromitites) for the geodynamic evolution of the eastern Alps.

In Japan, Arai (1992) studied chemical characteristic of chromian spinel in volcanic rocks, mainly basalt, and suggested that the TiO_2 content of spinel compared at similar $\text{Fe}^{3+}/(\text{Cr}+\text{Al}+\text{Fe}^{3+})$ or $\text{Cr}^{3+}/(\text{Cr}+\text{Al}+\text{Fe}^{3+})$ can distinguish island arc basalts from intraplate basalts and mid-oceanic ridge basalts. He researched variation of olivine-chromian spinel in Mg-rich magmas and concluded that a restite for the magma can be

assessed by extrapolating the olivine-chromian spinel fractionation line back to the olivine-spinel mantle array.

From the above-mentioned researches, chromian spinel is one of the important accessory and refractory minerals in mafic to ultramafic rocks. These rocks usually occur in several types of tectonic settings (Presr, 1986, Sigurdsson and Schilling, 1979, Lee, 1999). And the chemical composition of the accessory chromian spinel is an excellent indicator for the inference of their source rocks in different tectonic settings and conditions in the parental melt. Due to its mechanical and chemical resistant, chromian spinel becomes an important index mineral in paleotectonic reconstruction work. Most of ultramafic rocks in Thailand are strongly weathered, but fortunately chromian spinels are still remained and their geochemical data are therefore available for solving the tectonic setting within suture zones in Thailand.

Regarding to the genesis of ophiolite suits, Lockwood (1972) proposed the ultramafic genesis related to compressive tectonic by subduction mechanism (Figure 1.4). However recently, Robertson (2004) generated several models for genesis of ultramafic rocks by extension and compression tectonic of mid-oceanic ridge and subduction-related features (Figure 1.5).

1.3 Objectives and Scope of Work

The main goal of this research is to study the geochemistry and petrography of chromian spinels in ultramafic rocks, collected from several areas nearby main tectonic lines or sutures of Thailand. The geochemical data are useful for determining the tectonic setting during the formation of chromian spinels and mafic-ultramafic masses. The scope of work is therefore limited to spinel chemistry and does not include the geochemistry of ultramafic rocks collected in the areas. In addition, the research also referred to the studies on geochemistry and petrography of chromian spinels from several places outside Thailand where their tectonic settings have been known and widely accepted. Physical and chemical properties of chromian spinels and tectonic setting will be discussed, compared and combined with other geological data to construct the tectonic evolution of ultramafic masses in the main tectonic lines of Thailand.

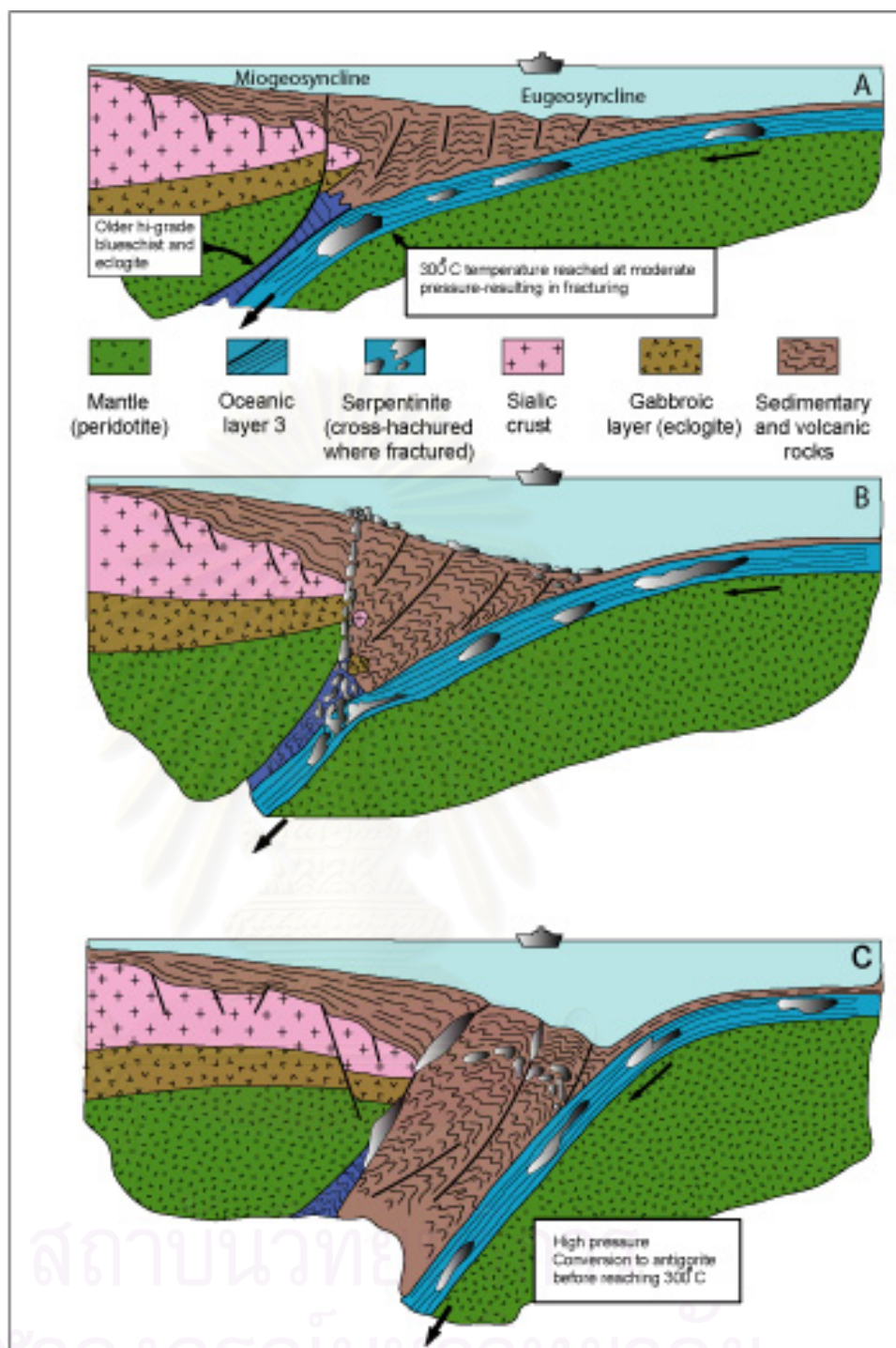
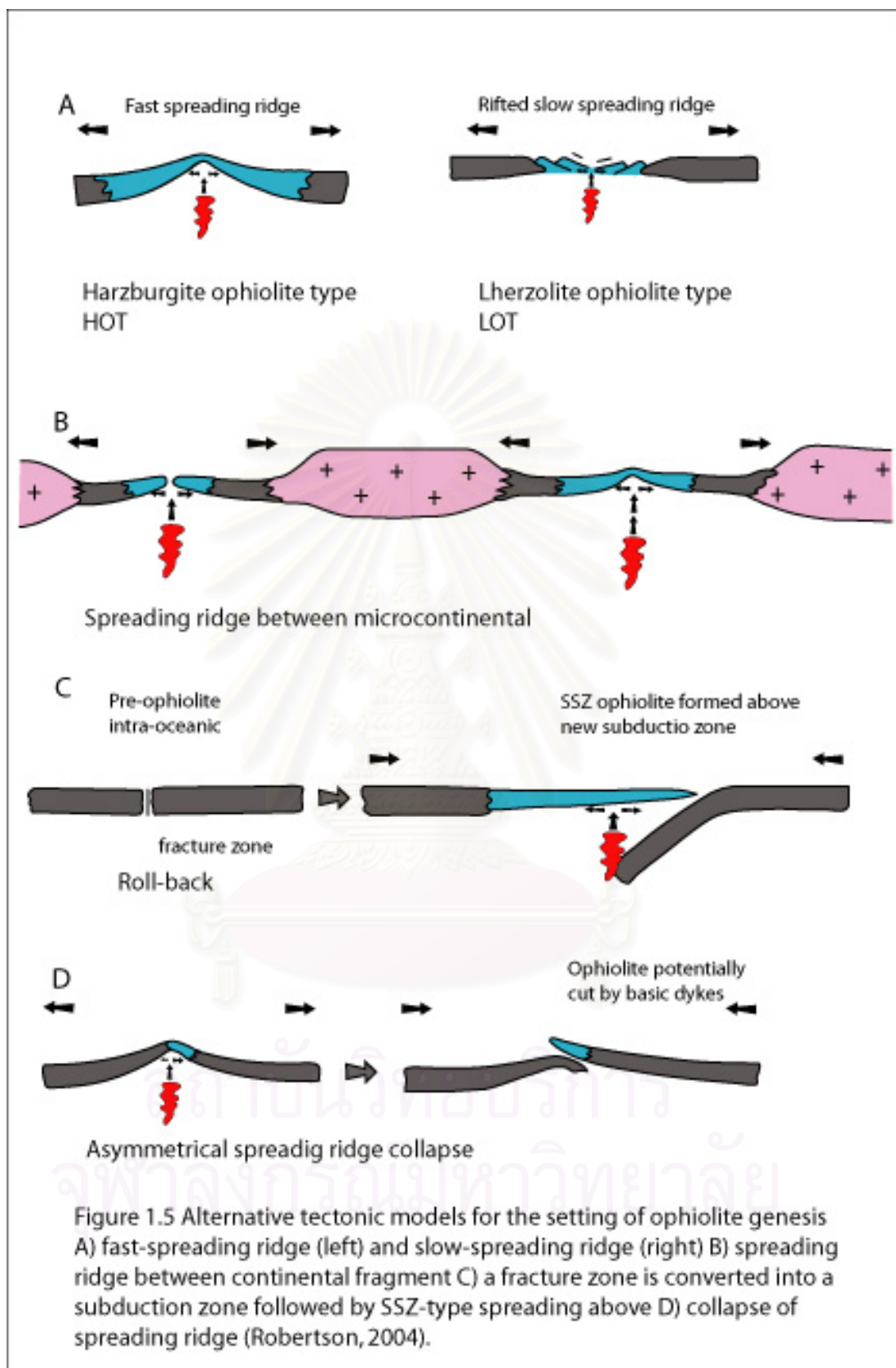


Figure 1.4 Model for the emplacement of certain alpine ultramafics. A) during an early stage of alpine orogenic cycle, oceanic crust is subducted beneath the continental margin at low angle. B) weakened serpentinite (ultramafic) rises upward along a fault. C) as subduction continues, angle of plate junction steepens and rate of subduction may quicken, higher pressure than before for any given temperature (Lockwood, 1972).



1.4 Methodology

Geological work from the main sutures in Thailand were carefully compiled and analysed along with Landsat TM5 images. Fieldworks were carried out in two short-period seasons in 2001, some samples from Chiang Rai and Nan-Uttaradit study areas were provided by K.Hisada. About 30 ultramafic rocks were collected and petrographically studied.

A total of 120 chromian spinel grains from 34 ultramafic samples within 6 locations in Thailand were selected to represent 4 inferred major sutures. Additional 106 grains from 16 samples of other countries were determined for geochemical analysis. Polished thin-sections of ultramafic rocks were prepared carefully for polarizing microscopic studies. High populations of chromian spinel sample were selected during petrographic investigation. Physical characteristics, such as size, color and shape, were recorded by sketching and taking photographs before chemical analysis stage. All of chromian spinels were analysed in the cores on polished thin-section using an electron microprobe, JEOL Model JXA 8261, at the Chemical Analysis Center, University of Tsukuba. Major and minor elements to be analysed consists of Mg, Fe, Cr, Al, Si, Na, K, Ca, Ti, Mn and Zn. All Fe, Mn and Ti (as ulvospinel molecule, $\text{Fe}^{2+}\text{TiO}_4$) were added and displayed as FeO. After subtraction ferrous ion from ulvospinel molecule, the cation partitions of Mg, Fe^{2+} , Cr, Al and Fe^{3+} were calculated with the assumption of ideal spinel stoichiometry. These cation partitions were plotted on coordinate standard diagrams to define types of tectonic setting that ultramafic host rocks occurred. The overall methodology of this study is summarized in Figure 1.4 Interpretation the moult was done in comparison with those of the other countries where tectonic setting was well known.

1.5 Study areas

Ultramafic rock samples were collected from 6 selected locations in 4 subareas (A, B, C and D) which were inferred to locate within suture zones of the country (Figure 1.6). Detailed locations of ultramafic masses are shown below (Table 1.1).

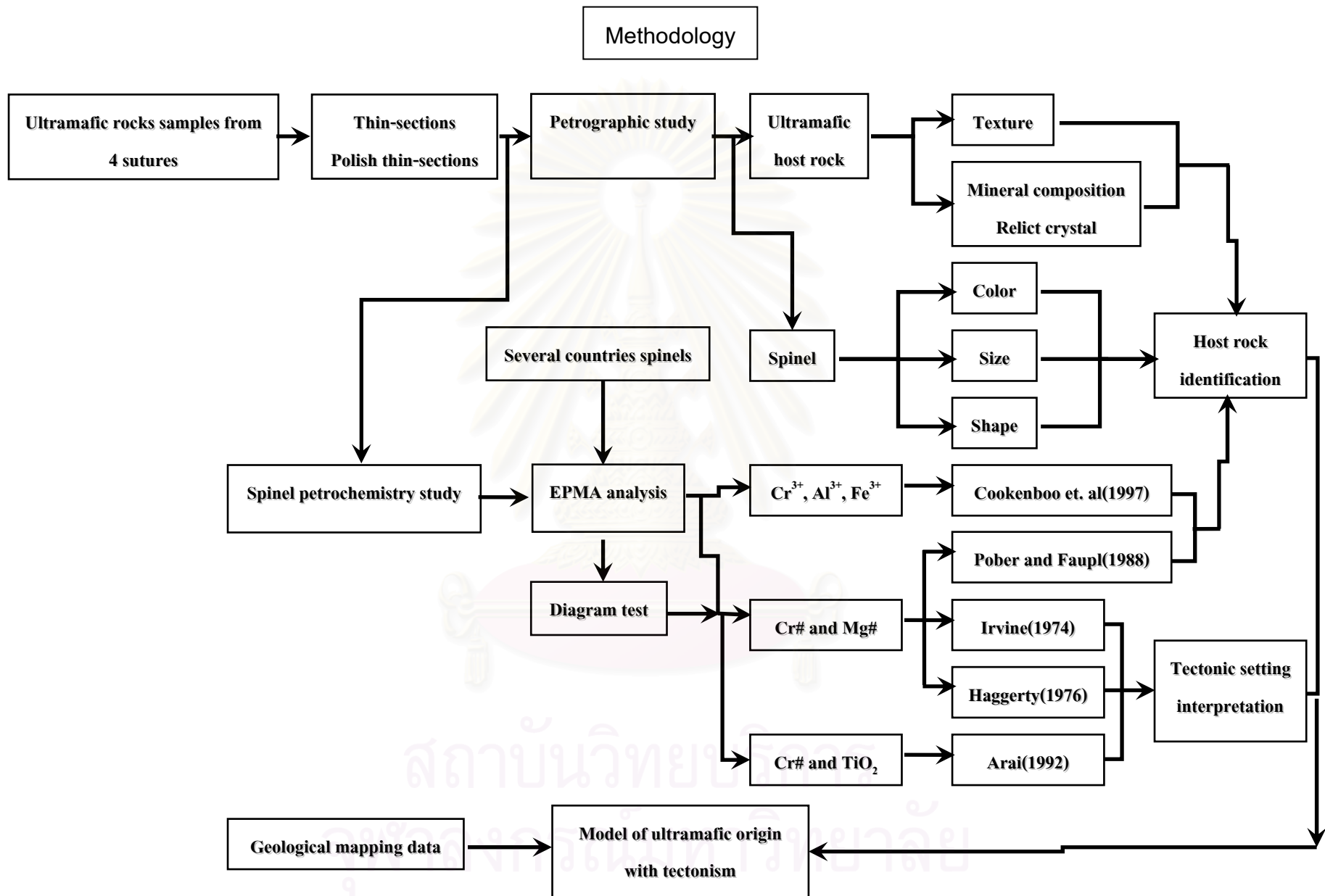


Figure 1.6 Methodology chart of this study

Table 1.1 Detailed locations of ultramafic rocks collected for Cr spinel analyses.

Area No.	Geographic locations	Geographic coordination	No. of samples	No. of analyzed cr spinel
1	Ban Pong Noi, Amphoe Chiang Khong, Changwat Chiang Rai	at latitude 20° 12' 07" and longitude 100° 10' 23"	8	25
2	Area near Amhpoe Chiang Saen and Amphoe Mae Chan boundary, Changwat Chiang Rai	at latitude 20° 02' 33" and longitude 99° 54' 05"	1	5
3	Doi Kaeo, King Amphoe Mae Charim, Changwat Nan	at latitude 18° 39' 20" and longitude 101° 02' 30"	5	14
4	South of Sirikit Dam, Amphoe Tha Pla, Changwat Uttaradit	at latitude 17° 46' 30" and longitude 100° 26' 20"	4	16
5	Area near Changwat Loei and Changwat Nong Bua Lum Phu boundary, Ban Khok, Amphoe Nan Som, Changwat Loei	at latitude 17° 32' 26" and longitude 102° 10' 32"	8	29
6	Suan Pha Khao Plu Hip, King Amphoe Khao Chakan, Changwat Sra Kaeo	at latitude 13° 34' 22" and longitude 102° 06' 20"	8	31

All sample locations are shown solid stars in the tectonic base map (Figure 1.7).

1.6 Previous works of Cr-spinels in Thailand

At present, there are a few reports concerned about the spinel studies in Thailand. Mostly their works are on detrital chromian spinels more than spinels from ultramafic rocks.

Panjasawatwong (1991) first studied some chromian-spinel in basaltic lavas around Nan-Uttaradit area. Most spinel crystals are subhedral to anhedral, and occur either as inclusions in olivine or as discrete small crystals outside olivine grains. The analysed spinels are chromitite and have relatively low Fe³⁺ contents, suggestive of low oxygen faculcity during crystallization. A plot of compositions on Cr# and Fe³⁺ versus Mg#

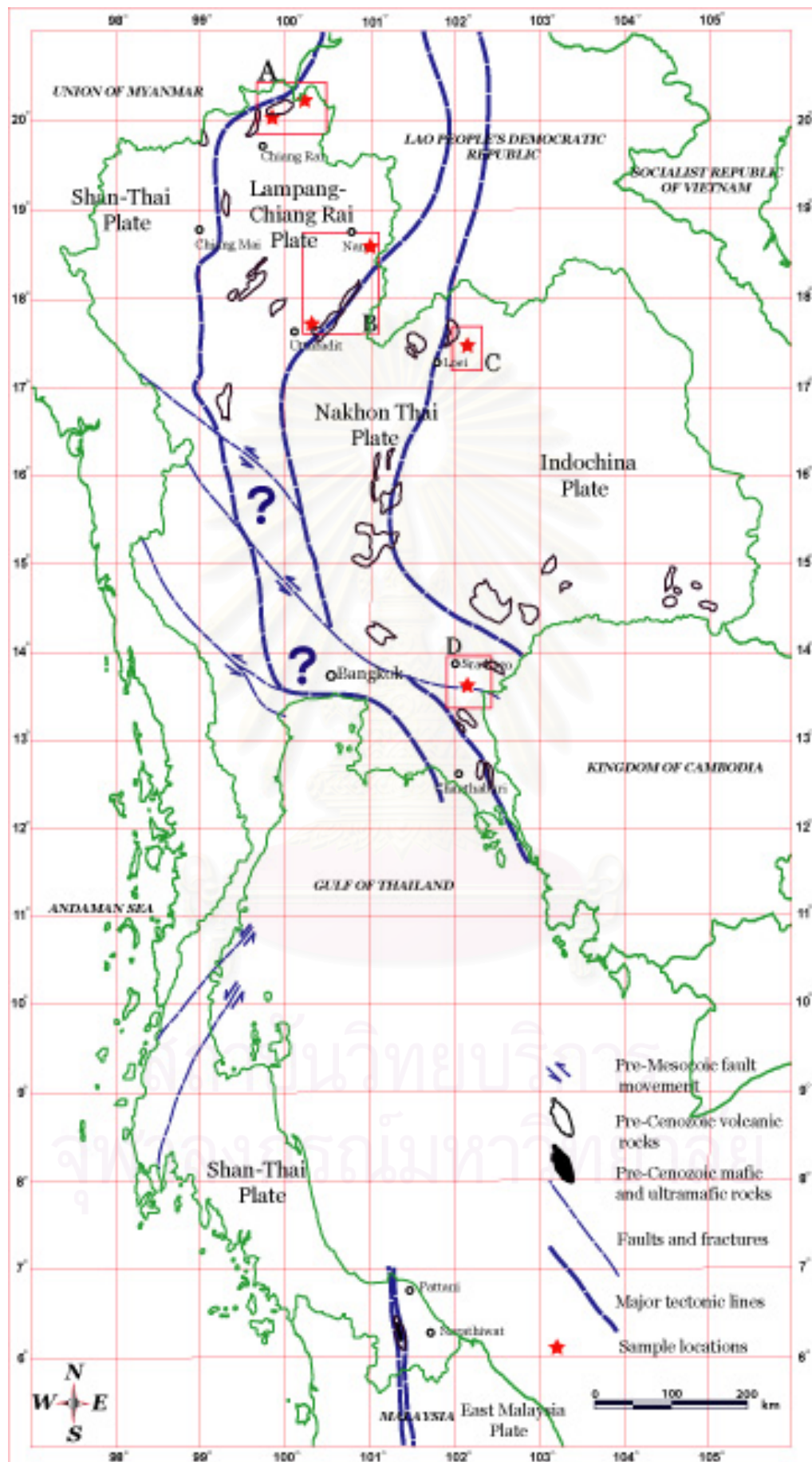


Figure 1.7 Map illustrate four substudy areas; A = Chiang Rai, B = Nan-Uttaradit, C = Loei and D = Sra Kaeo, red solid star represent ultramafic sample locations (Geology by DMR, 1991).

overlaps the compositional field of chromitites from Hawaiian tholeiites. Their TiO_2 contents are also comparable to those in the Hawaiian tholeiitic spinels.

Sugiyama (1999) reported geochemistry of detrital chromian spinels in the Triassic sandstones along the Mae Yuam Fault, Mae Hong Son. Three groups of spinel were classified. They are (1) low TiO_2 (less than about 1 wt%) and low Cr# (less than about 0.6), (2) low TiO_2 and high Cr# (higher than about 0.6), and (3) high TiO_2 (higher than about 1.0 wt%). Cr-spinels of the first group are thought to have originated in intraplate type basalt. Cr-spinels of the second group are probably derived from peridotites, which are highly correlated with arc and possible fore-arc setting derivation. Cr-spinels of the third group appear to have been derived from oceanic mantle type peridotite. This result leads Hisada et al. (2003) to propose the existence of subduction along the margin of Shan-Thai along the Mae Yuam Fault.

Charusiri et al. (2000) studied chromian spinels from mafic/ultramafic igneous rocks and clastic sedimentary rocks at six locations from five inferred geosutures of Thailand (Mae Yuam Suture, Nan-Uttaradit Suture, Loei Suture, Sra Kaeo-Chanthaburi Suture and Narathiwat-Pattani Suture). Their petrochemical and geochemical results on chromian spinels in ultramafic rocks suggest the chromian spinels from mafic/ultramafic rocks from the Nan-Uttaradit, Sra Kaeo and Narathiwat-Pattani sutures illustrate the quite similar pattern. Their plots are distributed within the field of island arc setting.

Chutakositkanon et al. (2001) studied detrital chromian spinels from turbiditic sandstones in the Permian Nam Duk Formation, central Thailand. The spinels have relatively high Cr content, the Cr# being mostly higher than 0.5 and up to 0.83. TiO_2 are generally low but variable from 0.02-1.16 wt% and Fe^{3+} are consistently low. The relatively high Cr# and low TiO_2 contents of the Nam Duk detrital chromian spinels in the Permian sediments indicate their derivation from mafic-ultramafic rocks of the arc origin. The relatively small and euhedral to subhedral spinels with undetermined inclusions strongly suggest their provenance from volcanic rocks. It is strongly inferred that igneous rocks (namely volcanics and peridotites) of arc origin were exposed in region at

the Late Permian. Therefore, the Loei-Petchabun-Ko Chang volcanic belt interpreted to have been constructed by several magmatic episodes (Devonian, Permian, Triassic, and late Tertiary) (see also Charusiri et al., 2002), could be a good candidate for the source of detrital chromian spinels in Nam Duk Formation.

Chutakositkanon (2004) studied detrital chromian spinels in the upper Permian volcanic clastic, Triassic sandstone and conglomerate blocks in the mélangé zone and sandstone of Middle Triassic Pong Nam Ron Formation around Sra Kaeo-Chanthaburi accretionary complex. The chemistry of spinels in volcanic clastics indicates two types of tectonic setting: intraplate or volcanic seamount and Island arc whereas those in Triassic sequences suggest an island arc origin only. He constructed an uppermost Permian-Middle Triassic tectonic evolution model of the area. A volcanic seamount was active in the west on paleo-oceanic plate. Contemporaneously paleo-oceanic plate was subducted to the east beneath the Indochina continental plate and became a volcanic arc. This volcanic arc still active until Middle Triassic but a western volcanic seamount activity was ceased in this age.



สถาบันวิทยบริการ
จุฬาลงกรณ์มหาวิทยาลัย

CHAPTER II

GEOLOGICAL SETTING

In this chapter four selected areas of study are geologically compiled and reported in the generalized tectonic map of Thailand showing major rock units and locations of the study areas (Figure. 1.5). The areas under study are located mostly in northern, northeastern and eastern parts of Thailand. They are described separately as areas A, B, C and D.

2.1 Regional geology

Area A (or Chiang Rai area) is located within the tectonomagmatic belt called “Chiang Mai Volcanic Belt” (Barr, 1990) and “Central Granitoid Belt” (Charusiri, 1993). Two locations are inferred to location 1 and is close to the Thai-Laos boundary whereas location 2 is about 7 km far from the south the of Mae Chan fault. In the northeast-southwest of the area, all rock units lie in the northeast-southwest direction. Generally, these rocks are Permo-Triassic volcanic rocks and volcanic tuffs with rhyolitic to andesitic composition, interbeds of Lower Jurassic clastic tuffaceous rock strata. To the western part the rocks are mainly biotite-hornblende granite, biotite granite and granodiorite porphyry with few fine-grained diorite.

Structurally, major faults mostly assumed as rock boundaries, are in the northeast-southwest direction, and younger minor faults are along the northwest-southeast. (Sukvattananunt and Assavapatchara, 1989). The southwestern part of this area is dominated by Triassic batholiths of equigranular to porphyry biotite granite and hornblende-biotite granite, with a long and narrow belt of gabbro to diorite, orientating approximately in the northeast direction. Sedimentary and metamorphic rocks can also be found as Devonian-Carboniferous phyllite and Triassic tuffaceous shale interbedded with thin bedded fine-grained sandstone. Main rock unit is chiefly intercepted by the eastnortheast – westsouthwest trending. Mae Chan fault (Paengkaew and Kittisarn, 2000). Mafic and ultramafic masses trend in the northeast-southwest direction, conforming to the Mae Chan fault.

Area B (or Nan-Uttaradit area) is situated in the Nan River mafic-ultramafic belt or the so-called Nan River Suture Zone (Barr and Macdonald, 1987). Mafic and ultramafic rocks are exposed extensively along the northeast-trending core of the major anticlinal structure with the length of approximately 100 km. Permian-to-Triassic undifferentiated sedimentary unit and Jurassic silt to sandstone in the north of the area constitute the main rock unit and orient in the northeast-southwest trend. In the south, the major rocks are Middle to Late Palaeozoic low grade metamorphic rocks (slate and phyllite) and Carboniferous chert and tuffaceous sandstone. Rock boundaries are generally controlled by the northeast-southwest trending faults (Sukvattananunt and Prasittikarnkul, 1985, Wunapeera and Kosuwan, 1987, and Singharajwarapan and Berry, 1999).

Area C is in the northern part of the Loei Volcanic Belt (Intasopa and Dunn, 1993), and in Eastern granitoid belt (Charusiri, 1993). Its major structure aligned in the northwest-southwest direction. The area is occupied by two main rock groups. Rocks of Carboniferous Group are mainly shale, sandstone, bedded chert with limestone lenses which are slight dynamothermally metamorphosed. The major thrust fault in this western part is westward thrusting and made Carboniferous (meta-)sediments overlain by Middle to Late Palaeozoic low grade metamorphic rocks. The other rock group is Permo-Triassic group of tuff, andesite and rhyolite. The eastern most of the region is constituted by Permo-Triassic tuff, andesite and rhyolite. Ultramafic rock bodies were found the new location within Permo-Triassic volcanic area.

The last area D belongs to the so-called Central Volcanic Belt (Intasopa and Dunn, 1990). The area extends southward from Loei to Phetchabun area, along the western margin of Khorat Plateau. The study area D also belongs to the Eastern Granitoid Belt (Charusiri, 1993), and Sra Kaeo-Chanthaburi accretionary complex (Hada, 1994, Chuthakosikanont, 2004). All rock units align in the northwest-southeast direction, bounded by the major fault of the same direction and minor faults in the northeast-southwest direction can also be found. In the northeastern part of the area D, rocks are mainly Permo-Triassic volcanic mass of rhyolite to andesite composition, extending to the central, while the southeast is characterized by Devonian-to-Triassic (meta-) clastic sedimentary rocks. The older Devonian-Permian rocks have steep

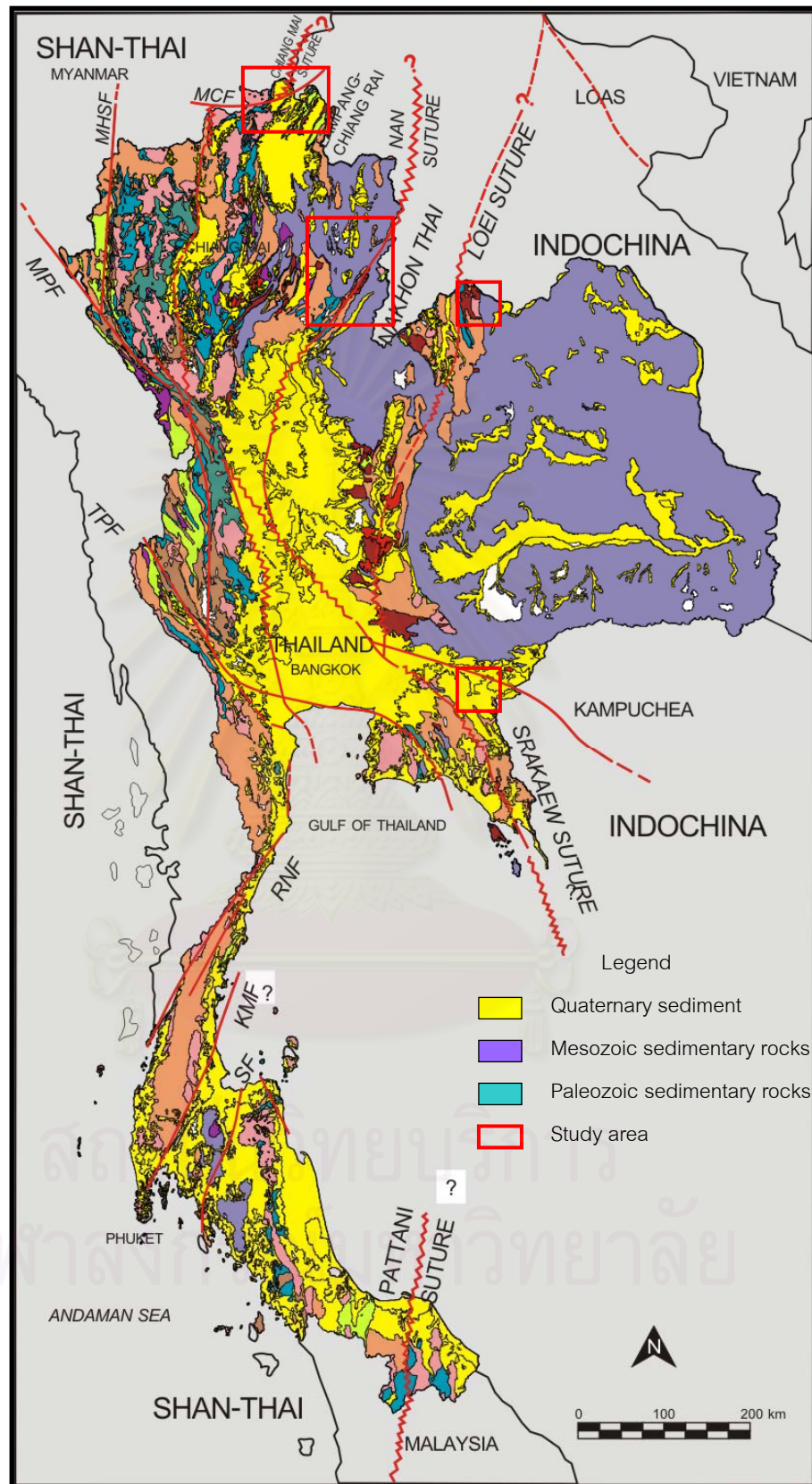


Figure 2.1 Simplified geological map of Thailand showing the distribution of rocks of various ages, significant tectonic plates and major sutures/faults system (Charusiri et al., 2002).

northeast dipping and are overlain by (volcanic) clastic sediments of Pong Nam Ron Formation which distributes widely throughout the area. Ultramafic masses, found as huge blocks, align northwest-southeast and controlled by faults on both sides of the boundaries. Sedimentary rocks bounding ultramafic rocks are possibly in the age of Permo-Triassic.

2.2 Detailed Geology

2.2.1 Area A: Ban Pong Noi, Chiang Rai (see Figure 2.2 and 2.3)

Geology

Based on the work of Sukvattananunt and Assavapatchara (1989), the Ban Pong Noi area in Mae Chan District, of Chiang Rai Province, is covered by Permo-Triassic rocks (30%), Triassic rocks (20 %), and Tertiary and Quaternary sediments (40%). Over fifty percents of the area are covered by the Permo-Triassic rocks which are composed largely of sedimentary, volcanic and plutonic rocks. The Permo-Triassic sedimentary rocks are characterized by intercalation of greenish gray sandstone, greenish gray siltstone, dark gray shale and black mudstone, and are associated with reddish purple agglomerate and conglomerate. The sedimentary rocks, which overlay the Permo-Triassic volcanic rocks, consist of rhyolite, andesite and tuff. In the northern part of the area, the Permo-Triassic plutonic rocks, i.e. gabbro and gabbro-diorite, are widely exposed. The western part of the area is covered by the Triassic plutonic rocks: granite, grano-diorite and diorite. The Tertiary rocks superimpose the Permo-Triassic and Triassic rocks. The Tertiary rocks are composed of semi-consolidated deposits of conglomerate, sandstone, siltstone, and shale with peat fragments. They are exposed in the northwestern part of the area. The Quaternary sediments can be divided into two categories: terrace sediments and floodplain sediments. The terrace sediment consists largely of sand to gravel size and laterite. The floodplain sediment comprises sand and mud.

Main geological structures of the area are two major faults, in the northeast-southwest and northwest-southeast directions. Anticlinal fold with northeast-southwest trending and southwestward plunging is observed in the central part of the study area minor structure is folding in Permo-Triassic sedimentary rocks.

Stratigraphy

Permo-Triassic rocks can be grouped into 2 formations including Mae Bong and Doi Huai Sala Formations (Sukvattananunt and Assavapatchara, 1989).

The Mae Bong Formation is characterized by shale and tuff without fossils. It overlies the Permian marine rocks. The age of Mae Bong Formation has been assigned as Permo-Triassic based on stratigraphic correlation. In this area, this formation is a sequence of sandstone, greenish gray shale and sandstone intercalated with tuff. On the top of the sequence, conglomerate can be observed in some parts of the area. The thickness of this formation is over 1,000 meters.

The Doi Huai Sala Formation is exposed along the eastern side. This formation is typified by volcanic conglomerate and intercalations of sandstone, shale and conglomerate. The total thickness of the formation is about 300 meters. This formation was deposited in non-marine environment during the Triassic.

The Tertiary rocks are composed of intercalation of semi consolidated conglomerate, sandstone and siltstone. Pebble size clasts in the conglomerate are chiefly the Pre-Tertiary rocks around this area. The age of this formation is the Neogene.

Igneous rocks

Igneous rocks in the area consist of intrusive (40 %) and extrusive (60 %) rocks. The intrusive rocks can be divided into two groups: Doi Sango Suite, and Chiang Saen Suite. The Doi Sango Suite includes (meta-)ultramafic rocks dominated by weathered dark green serpentinite. The serpentinite shows relic textures of pyroxene and olivine. It has been retrograde metamorphosed from peridotite. It has been assumed that the ultrabasic rocks formed during the Triassic. The Doi Sango Suite is a group of mafic igneous rocks that is characterized by gray to black color and fine- to coarse-grained crystalline texture. It is composed of gabbro, gabbro-diorite and diorite. Hornblende, pyroxene, olivine, magnetite, quartz and plagioclase, are major mineral constituents. The Doi Sango Suite crosscut the Permo-Carboniferous sedimentary sequence only, so the age of the Doi Sango suite has been assigned as the Permo-Triassic. The Chiang Saen Granite – Granodiorite Suite is a group of felsic to intermediate plutonic rocks

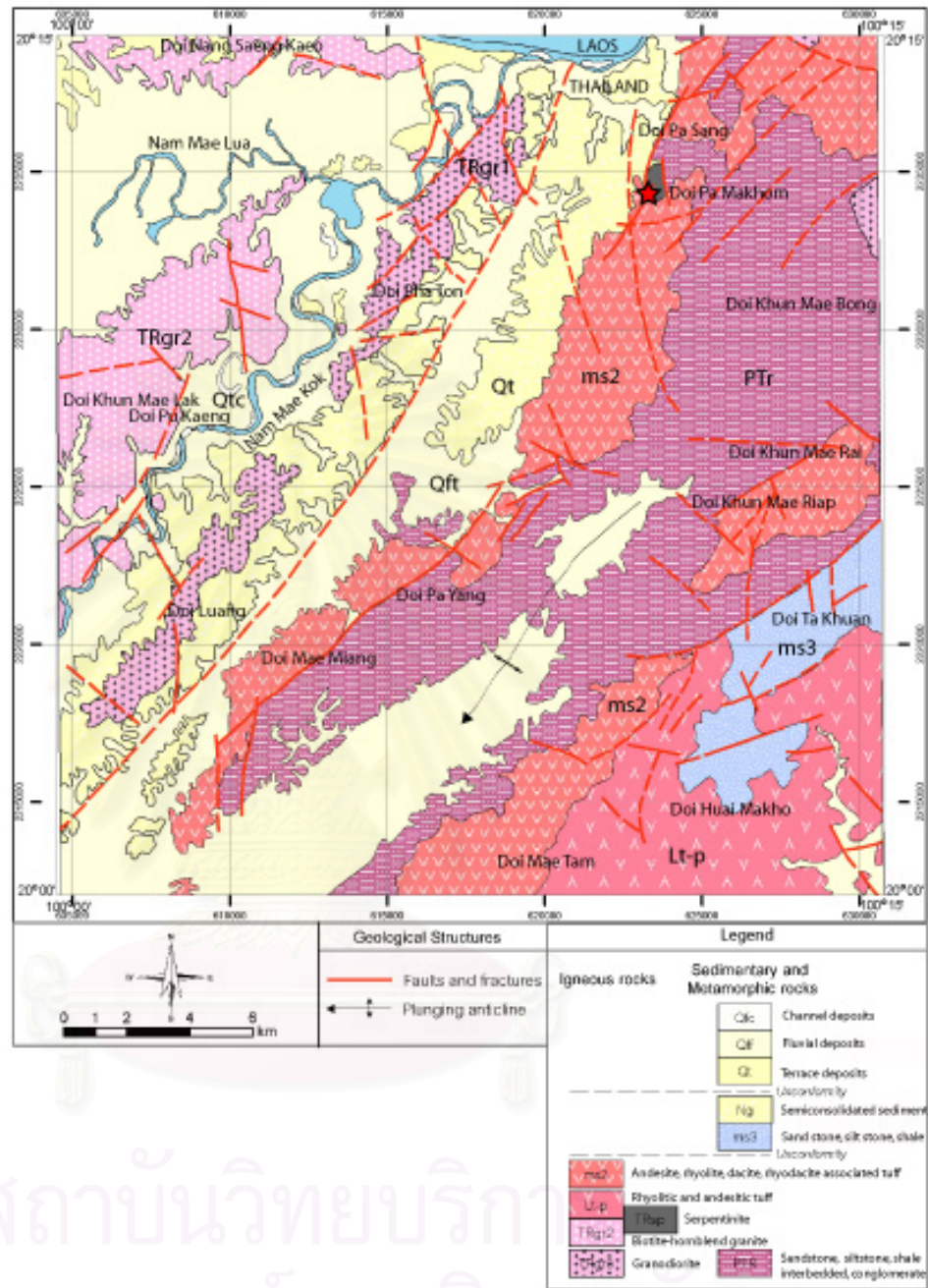


Figure 2.2 Geologic map of Ban Pong Noi, Amphoe Chiang Khong, Changwat Chiang Rai (Department of Mineral Resource, 1989). Red solid stars represent ultramafic sample locations.

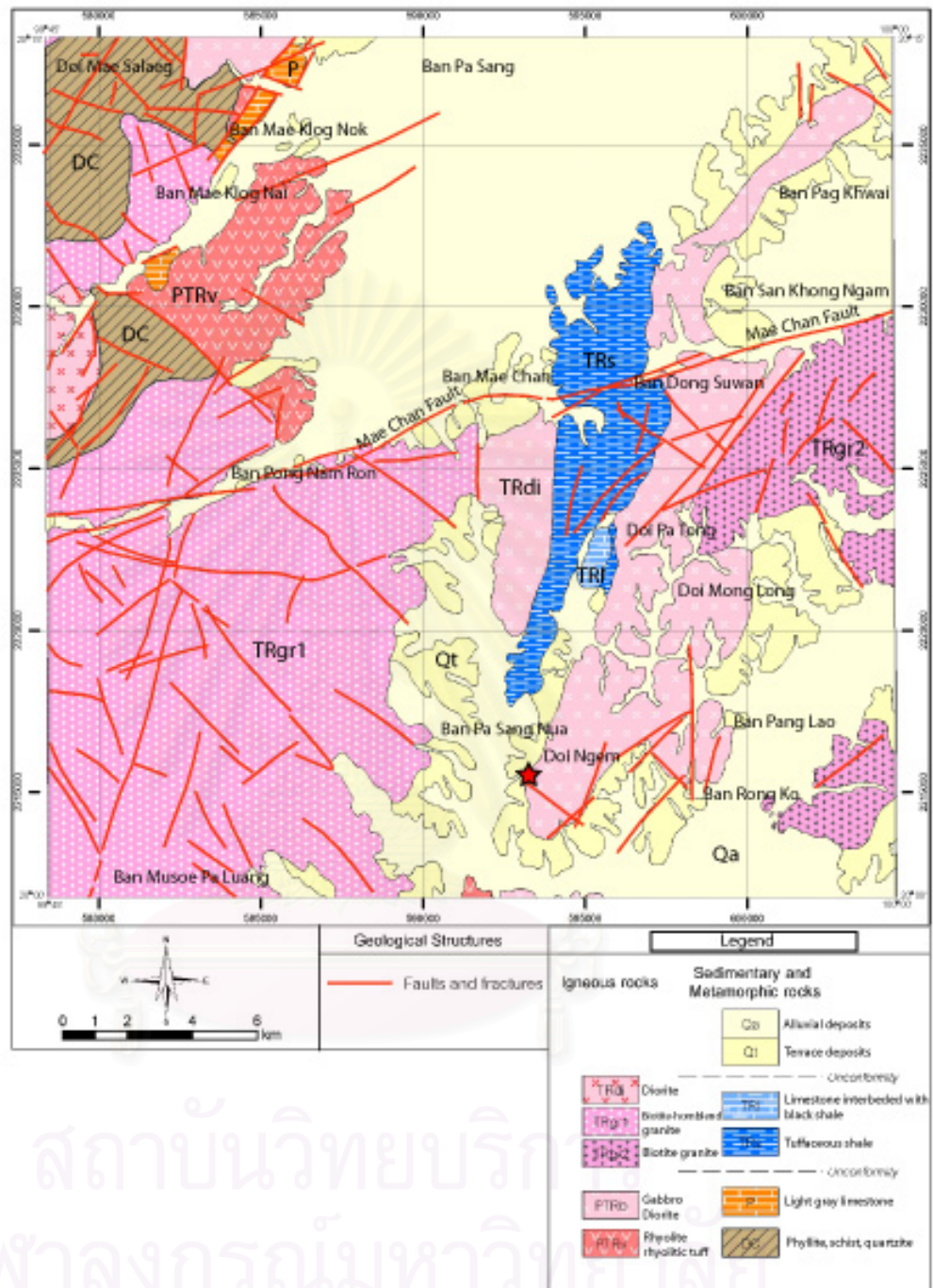


Figure 2.3 Geologic map of Amphoe Mae Chan, Changwat Chiang Rai (Department of Mineral Resource, 2000). Red solid star represents spinel-bearing sample locations.

dominated by granite, granodiorite and diorite. It distributes along the western part of the area.

The extrusive igneous rocks can be observed along the eastern side of the mapped area. Two units are recognized, including the Lt-p and the Ms units (Sukvattananunt and Assavapatchara, 1989). The Lt-p unit is characterized by volcanic rocks, such as tuff, rhyolite, and andesite. This unit unconformably underlies the Doi Huai Sa La formation so its age has been designated as the Permo-Triassic. Well exposures of this unit are found in the southeastern area of Ban Pong Noi. The Ms unit is the Triassic-Jurassic intermediate to felsic extrusive rocks and their volcanoclastic equivalent. Stratigraphically, the Ms unit is found unconformably over the sediments of the Doi Huai Sa La formation.

Structural Geology

Main structures in this area are faults, folds, and lineaments oriented in the northeast-southwest direction. Most of the faults are high-angled normal faults that cut across the Permo-Triassic rocks. Some minor faults which are mainly in the northwest-southeast direction cut the major northeast-trending faults. Moreover there are some faults in the north-south direction. Based up Sukvattananunt and Assavapatchara (1989) they were probably formed at the latest period of structural development in this area. Major folds, such as anticlines and synclines, are commonly found in the Permo-Triassic rocks. These structures are considered to have been caused by igneous intrusions in this area.

2.2.2 Area B: Mae Charim, Nan –Tha Pla, Uttaradit (see Figure 2.4 and 2.5)

2.2.2.1 Mae Charim, Nan Geology

The study area is mainly occupied by lithological sequences of various ages from Carboniferous to Quaternary age. Sediments and sedimentary rocks are quite dominated and oriented in the northeast-southwest trend, following major structures. Small exposures of felsic to mafic rocks are found along the major northeast-trending fault.

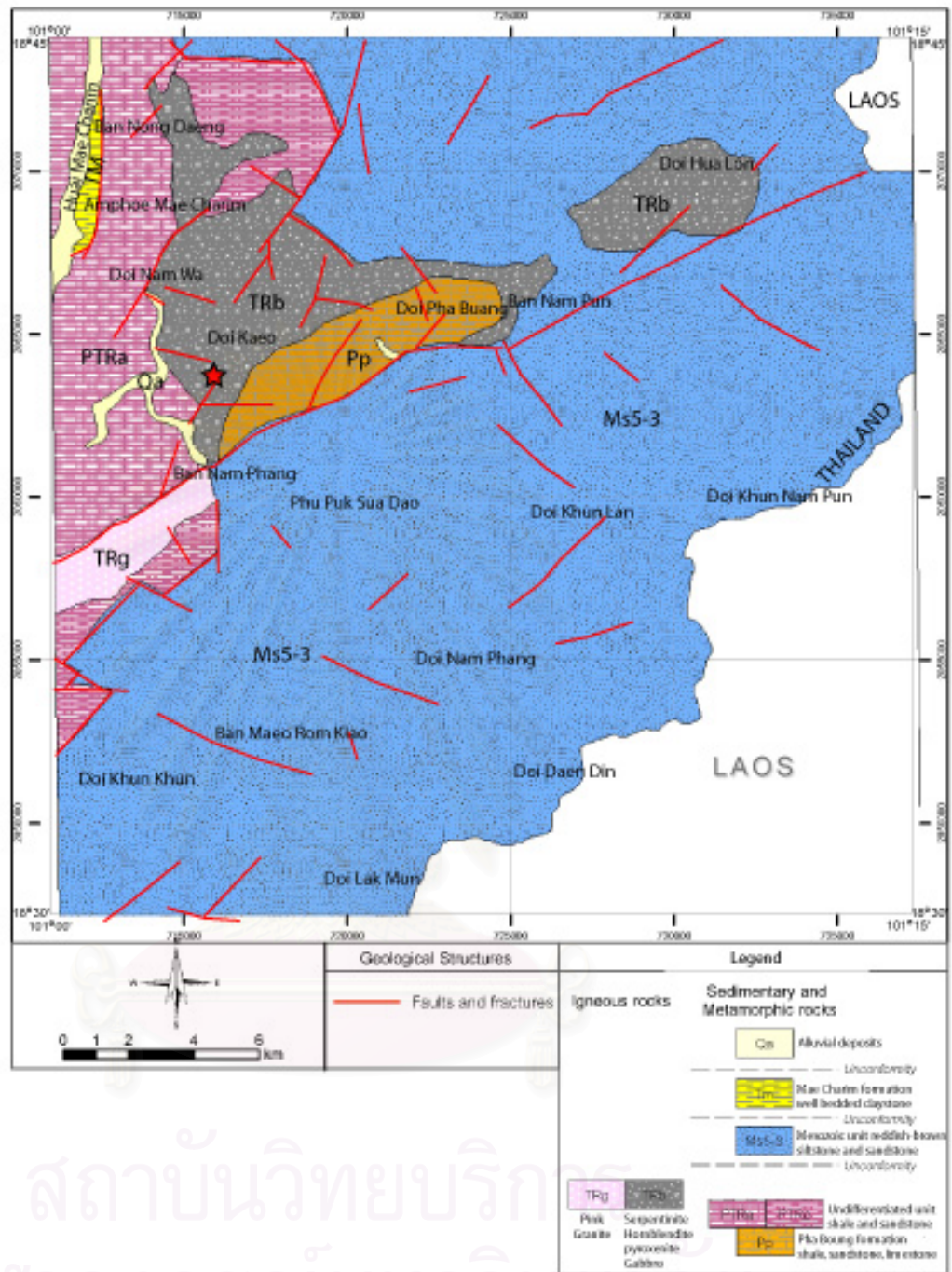


Figure 2.4 Geologic map of Amphoe Mae Charim, Changwat Nan (Department of Mineral Resource, 1987). Red solid star represent ultramafic sample locations.

Stratigraphy

Three major groups of sedimentary rocks are recognized, including the Phrae Group of the Carboniferous to Triassic age, the Lampang Group of the Triassic age, and the Nakhon Thai Group of the Jurassic to Cretaceous age. As shown in figure. 2.4, no Carboniferous strata are found in the study area. The oldest strata are the Permian rock of the Pha Boun Formation by Wunapeera and Kosuwan (1987) which is equivalent to the Rong Kwang Formation of the Phrae Group by Charusiri et al., (2003). This (Permian) formation consists of interbedded sequence of gray and brown shale and sandstone in the lower part and fusulinid and algae-rich limestone is intercalated in the upper part. Overlying the Rong Kwang formation is the youngest formation of the Phrae Group. Nathannang formation of Permo-Triassic age includes greenish gray to brown greywacke sandstone interbedded with shale, mudstone, and discontinuous limestone. The youngest marine strata are the Lampang Group of Triassic age. The rock sequences are mainly interbeds of gray to brown shale and sandstone with intercalated calcareous sandstone containing unidentified pelecypods.

The Mesozoic non-marine clastic rocks belong to the Nakhon Thai Group (Charusiri et al., 2003) and can be subdivided into two units. The older unit is composed mainly of red to reddish brown siltstone, sandstone, and subordinated conglomerate with pebble of limestone, chert, and volcanics. The younger unit comprises white to grayish white fine- to medium-grained quartzitic and arkosic sandstone with intercalated siltstone.

The Tertiary rocks, designated as Mae Charim Formation by Wunapeera and Kosuwan (1987), are of grayish white claystone overlain by clay and silt of semiconsolidated lake deposit. The Quaternary sediments are normally unconsolidated deposits of gravel, sand, silt, and clay along current streams and their tributaries in the western part of the study area.

Igneous rocks

The Mae Sanan and Nam Pu granitic rocks, belonging to the so-called Uttaradit Plutons of Triassic age (Charusiri et al., 2003), comprise medium-to coarse-grained pink ± white granite as well as dark green granodiorite and diorite with fine-grained

xenoliths. Ultramafic rocks at Doi Kaew, Doi Hua Lon and Ban Ko, of the Phasom Ophiolite (Permian-Carboniferous age; Charusiri et al., 2003) are composed largely of serpentinite, hornblendite, gabbro and pyroxenite. Very small extent of unmappable rhyolitic and adesitic rocks are present at Ban Nam Paeng, south of Ban Num Pu.

Structural Geology

The Upper Paleozoic rocks are more intensely folded and fractured than the Mesozoic rocks. In the middle portion of the area, a dominant fault trends in the northeast-southwest direction and seems to cross-cut most of the study area. The Permo-Triassic rocks generally develop moderate to good cleavage. The Unconformities are recognized in the area. The Mesozoic non-marine sequence unconformably overlies the Permo-Triassic sequence. The Tertiary sequence is unconformably underlain by the non-marine Jurassic Cretaceous sequences and subsequently unconformably overlain by the Quaternary sediments.

2.2.2.2 Tha Pla, Uttaradit

Geology

There are three kinds of rocks of various ages in this area: metamorphic (50%), igneous (20%) and sedimentary rocks (30%). Most of the rock units are aligned in northeast-southwest direction. The rock strata were deformed and metamorphosed. Small-scale of anticlinal and synclinal folds are dominant within the area, steep dipping fault much form as a lithological boundary. Rocks units can be divided into 3 sedimentary rocks units and 3 igneous rocks units.

Stratigraphy

Silurian-Devonian unit (about 40% total area) is distributed in the central and southeastern parts of the area. It consists chiefly of brown phyllite, black slate, quartzite with miority of talc schist, rhyolite and andesite tuff schist. Preferred orientation is mostly in the northeast-southwest direction with irregular dipping but mostly to the northwest direction. The rock sequences are quite obvious due to their complex fold structures.

The Carboniferous unit covers the area of about 40% almost similar to that of the SD unit. The Carboniferous unit comprises dark gray chert interbedded with shale and

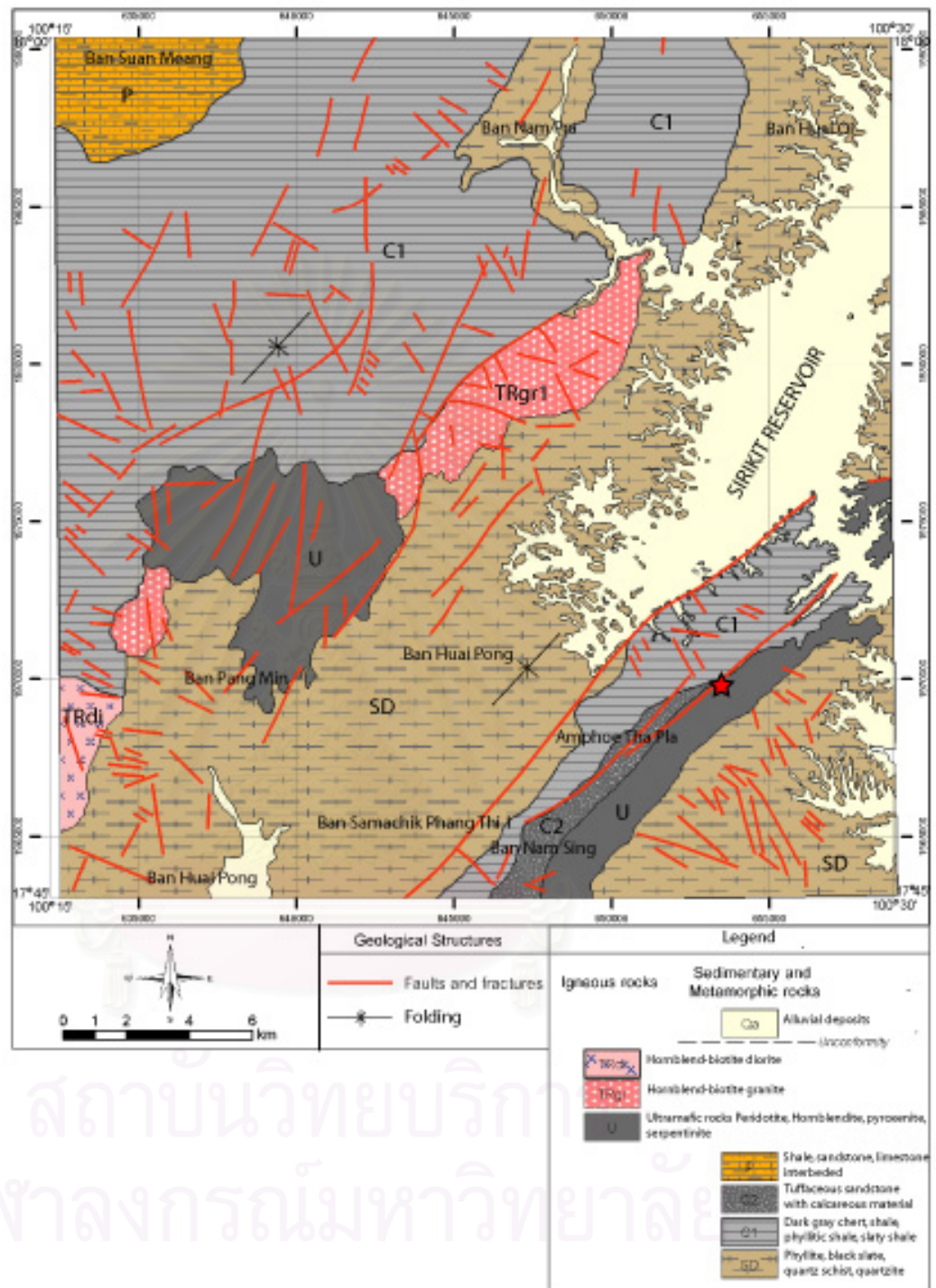


Figure 2.5 Geologic map of Amphoe Tha Pla, Changwat Uttaradit (Department of Mineral Resource, 1987). Red solid star represent ultramafic sample locations.

sandstone, phyllitic to slaty shale with chert augen, quartz schist, chlorite schist, quartzite, rhyolitic and andesitic tuff, tuffaceous sandstone and tuffaceous conglomerate. The regional trend of unit follows that of the SD unit. The Permian unit with fusulinids in some horizons exposed at few locations only in northwestern part of the area. Major rock type contains deformed shale interbedded with sandstone in lower part and mixed with limestone lens graded to limestone beds in the upper part. The orientation of Permian rock unit is still conformable with that of the Carboniferous unit.

Igneous rocks

Igneous rocks in this area can be divided into 3 main types; ultramafic, intermediate and felsic rocks. Ultramafic mass appears as a long and narrow belt trending in the northeast-southwest direction. This unit mass was partially affected by shear sense with the shear mostly along the fault. Most rocks are hornblendite, pyroxenite, peridotite and some mafic rocks such as gabbro and basalt are also present in much smaller amount. Because the ultramafic rocks intruded into Permian rocks but not into the Mesozoic non-marine sediment, so their age is estimated to be Triassic to Permo-Triassic age. Felsic intrusions located in the central of the area. They are mostly hornblend-biotite granite, granodiorite, and biotite granite, hornblend and biotite are slightly altered to chlorite. Texture that dominant is equigranular texture, whereas a porphyritic texture occurs locally. These felsic intrusive cut into rocks are similar to those of the ultramafic rocks, so the age of felsic rocks are assigned to be Triassic. Intermediate rocks of mainly dioritic to tonalitic (?) composition, are also widely distributed in the central part of the area. They formed as extensional northeast-trending mass from felsic stocks. The rocks have microporphyritic textures of which most phenocrysts are Ca-Na plagioclase. Hornblende and biotite are important mafic minerals, the forms being slightly more abundant. Transition zones around contact between felsic and intermediate rocks are also present, suggesting that both rocks have the same age.

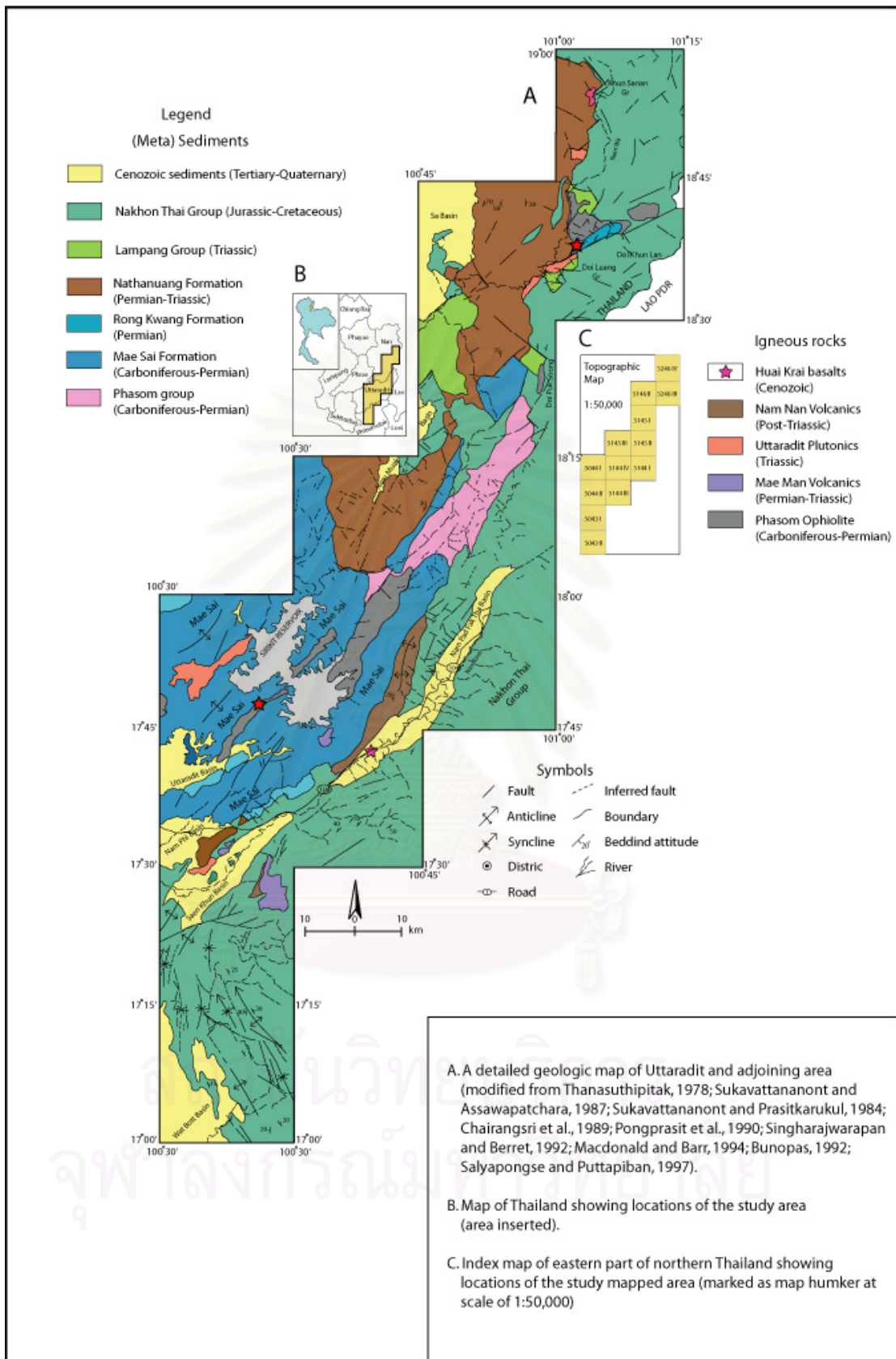


Figure 2.6 Geologic map of the Nan-Uttaradit area(A) in northern Thailand(B) showing distribution of rock units (after Charusiri et al., 2005) and geological structure and sample locations (red solid star).

Structural Geology

Major structures in this area are faults and folds mainly in the northeast-southwest direction. Tight synclinal and anticlinal folds are dominant in Middle Paleozoic sedimentary strata. Steep-angle faults with east-dipping were formed in the fold axes.

2.2.3 Area C: Na Klang, Loei (see Figure. 2.7)

Stratigraphy

Sedimentary rocks in this area can be divided into 6 units in ascending order.

1. Na Mo Formation

The formation is distributed in the central part of the study mapped area in Ban Na Klang. It consists mainly of the weakly metamorphosed sediments, i.e. phyllite, quartzite, schist, quartz schist and slate. This formation is relatively more resistant than the other formations exposed in the area. The age of this formation can be assigned based on the presence of Silurian-Devonian corals found in the Ban Nong Member which overlies the Na Mo Formation. Moreover, the formation is highly deformed and contained no fossils. Thus the formation is assigned by DMR (1985) as Silurian. Sediment of this formation may have occurred in marine shelf environment (Charusiri et al., 2002).

2. Ban Nong Member

The member comprises the lower part of the Pak Chom Formation. It is exposed in a limited area, just east of Amphoe Pak Chom. This member consists mainly of shale and minor limestone and is formerly called "Ban Nong Shale" (Bunopas, 1981) occurring in the outer shelf environment. From several index fossils in many localities, the member is considered to be Late Silurian (?) - Devonian in age.

3. Nong Dok Bua Member

This member is part of the Wang Saphung Formation. It consists largely of sandstone, conglomerate and thin-bedded grey limestone. This rocks member trends in the northwest-southeast direction in the proximity of Khao Pha Viang Udon Graphite Mine in Amphoe Na Klang. The middle part of this member consists essentially of grey limestone interbedded with greenish grey shale. Numerous fossils (e.g. corals, crinoids,

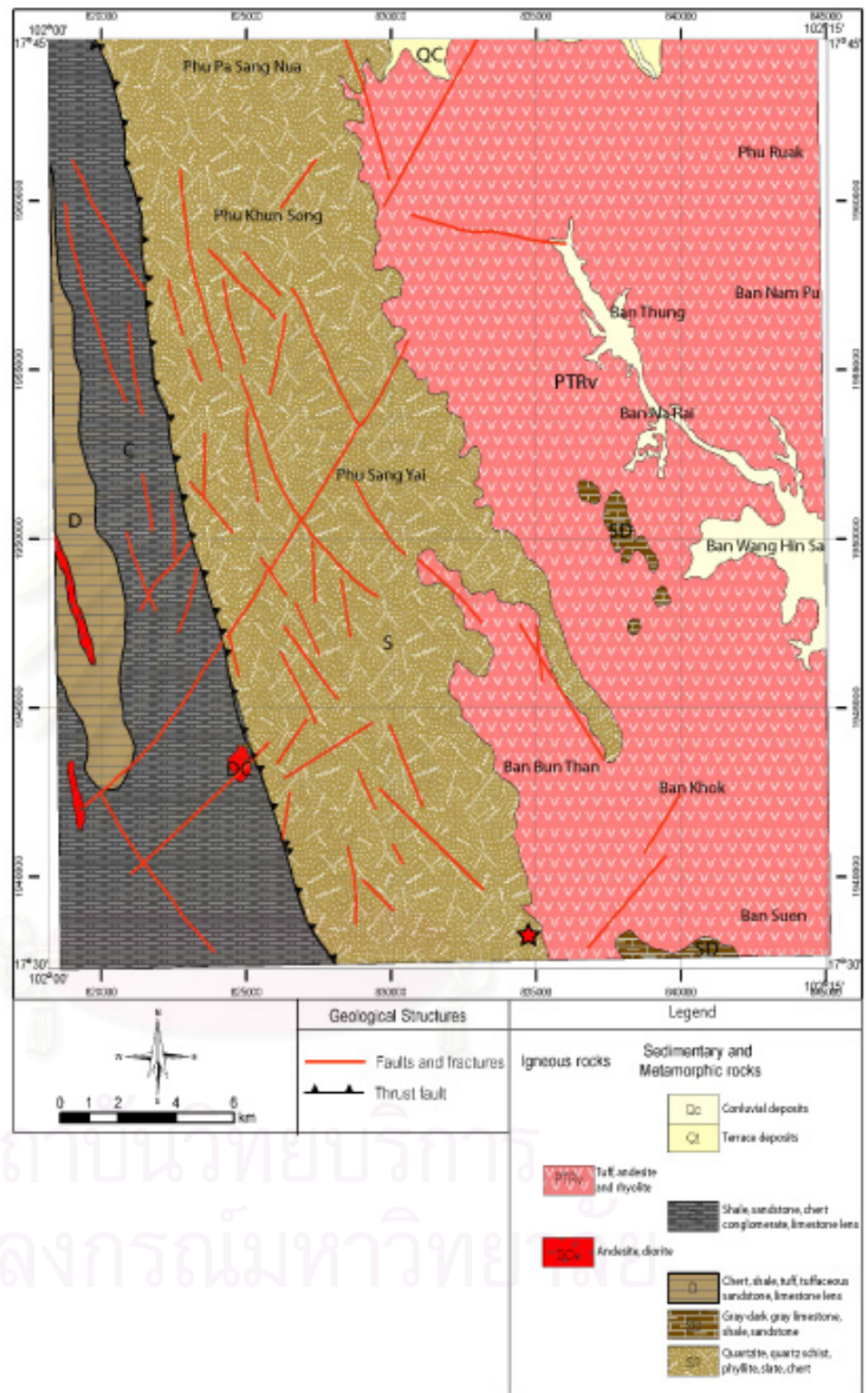


Figure 2.7 Geologic map of Ban Khok, Amphoe Na Klang Changwat Loei (Department of Mineral Resource, 1985). Red solid star represents ultramafic sample locations.

brachiopods and pelecypods) are found in the limestone. The corals (*Paleosilia* sp.) indicate a Late Visean age, Late Carboniferous.

4. Wang Saphung Member

The member consists of coarse-grained sandstone and conglomeratic sandstone which are underlain by greenish grey shale with limestone lens, suggesting shelf environment. Moreover, a portion of the sequence is interbedded with red shale which indicates the tidal flat environment of deposition.

5. Tham Nam Mahoran Formation

This formation is distributed in the western part of the study area. It consists predominantly of light grey massive limestone. In some area, the limestone is interbedded with late diagenetic chert beds and some limestones contain chert nodules. Fusulinids, corals and brachiopods are found in limestone along the road between Wang Saphung and Udon Thani. Lower Permian fossils (Asselian-Sakmarian) are found in limestone.

6. Cenozoic Deposit

Quaternary deposits are mainly unconsolidated deposits of active river system. Most sediments are sand, silt, clay and gravel. The Tertiary rocks have not been found in this area.

Igneous rocks

The igneous rocks of this area can be divided into two groups, felsic and intermediate volcanic units with their volcanoclastic affinities. Their age is mostly Permian-Triassic. Based on stratigraphic correlation but Kittisarn and Kenvised (1985) proposed that these volcanic units are of Devonian to Carboniferous age.

1. Intermediate unit

The unit are exposed as stocks (possibly equivalent to shallow intrusive), east of Ban Khok Sa-ad, Phu Pleak and north of Ban Sum Juang. Main rocks are fine-grained andesite porphyry and andesite tuff. The porphyry has abundant phenocrysts which are usually Ca-Na plagioclase and hornblende phenocrysts. Groundmass consists largely of sericite, kaolinite, plagioclase, chloritoid minerals and glass.

2. Felsic unit

The unit is distributed in Nam Som and Huai Khop quadrangle map. The unit is dominated by agglomerate and tuff of rhyolitic and andesitic compositions.

Structural Geology

The pronounced north-trending synclinal structure of the Tham Nam Mahoran Formation in Wang Saphung area can be clearly observed by aerial photographs and airborne geophysical data (Newsuparb, 2005). The contact between Nong Dok Bua Member and Wang Saphung Member is marked by a north-trending reversed fault. The older Na Mo Formation has been moved up overlying the younger Wang Saphung Formation. Most major faults in this area are reversed faults, but some are strike-slip faults (Newsuparb, 2005). They lie in a northwest-southeast direction, but the minor faults which are younger lie in a northeast-southwest direction.

2.2.4 Area D: Sra Kaeo (see Figure. 2.8)

General Geology of Eastern Thailand

Due to the fact that this study area is quite large comparing to the other study area, so geology is herein explained in the more regional scale than the others, Much of the geology are modified from Chutakosikanon (2003). Geology of eastern Thailand is described in accordance with the tectonostratigraphic terrane (Bunopas and Vella, 1978 and Charusiri et al., 2002). The Shan-Thai with the adjoining Lampang-Chiang Rai arc terrane was welded with the Nakhon Thai oceanic and Indosinian Terranes in late Triassic (Charusiri et al., 2003). Within the Shan-Thai Terrane, the Precambrian amphibolite facies was formed as the oldest crystalline basement rocks. The Cambrian-Ordovician siliciclastic-carbonate rocks, as usually observed in the western Thailand, have not been definitely proved here (Salyapongse, 1992). So the oldest sequence is possibly Silurian-Devonian age and it may have overlaid unconformably on the Precambrian metamorphic rocks. The Silurian-Devonian rocks appear to be transitional to the Carboniferous sandstone-shale-chert-limestone and the Permian sandstone-shale-chert-limestone (Bonopas, 1983). The Permian-Triassic volcanic rocks show their appearance when approaching the Lampang-Chiang Rai arc terrane. The Lower

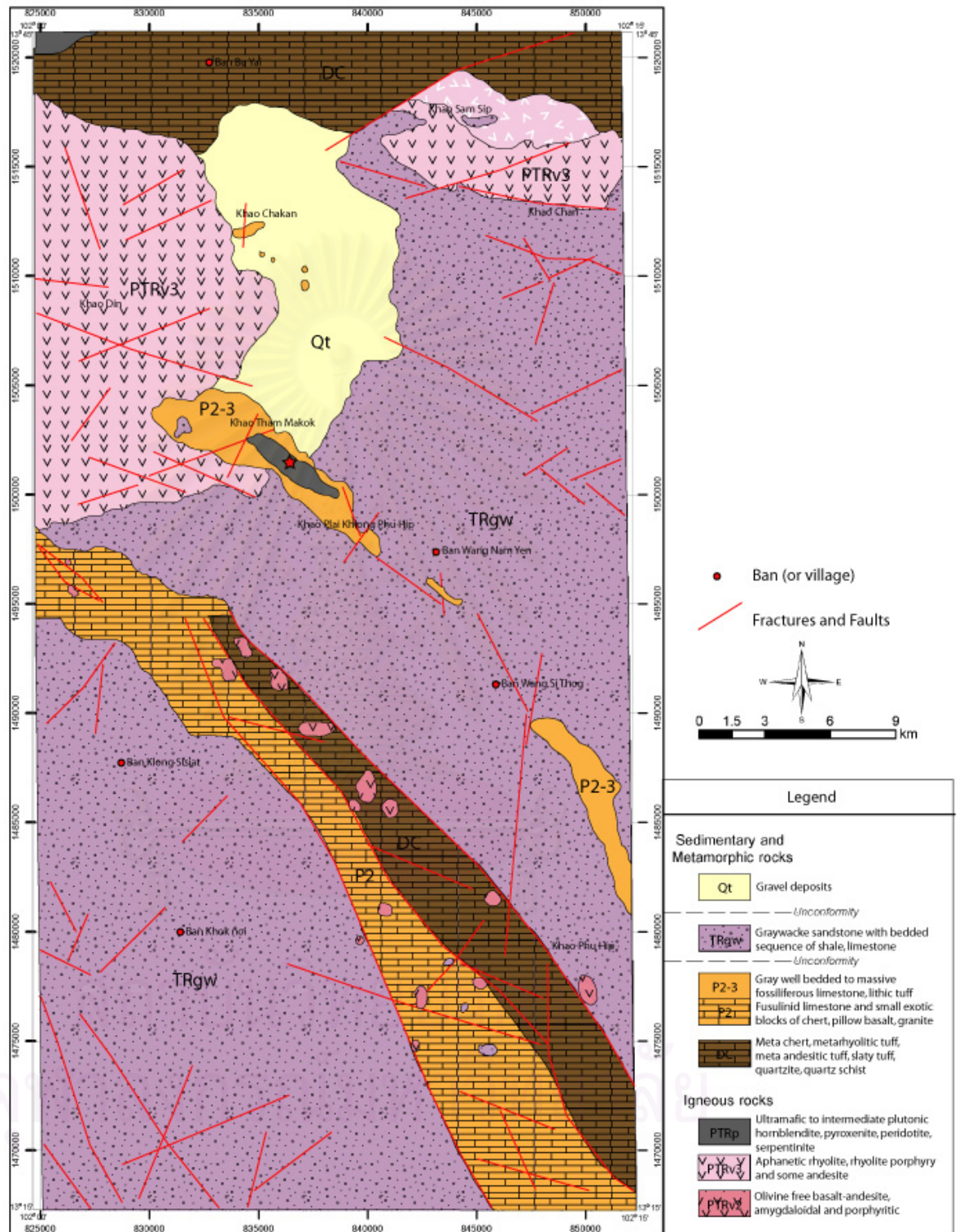


Figure 2.8 Geologic map of Amphoe Wang Nam Yen, Changwat Sra Kaeo (Department of Mineral Resource, 1997). Red solid star represents ultramafic sample locations.

Triassic rocks are quite clearly indicated very shallow marine facies whereas further to the east the Middle Triassic bedded chert and intraformational basaltic rocks are explicitly very deep marine facies. The Jurassic-Cretaceous non-marine red beds and the Tertiary sediments within the Shan-Thai terrane and associated terranes are related to the events after Triassic collision between these afore-mentioned terranes.

Sra Kaeo-Chanthaburi Suture

Geology of the area between the Sra Kaeo-Chanthaburi sutures is divided into two parallel belts: a western belt of chert-clastic sequence and an eastern belt of serpentinite mélangé (Hada, 1998). These rock assemblages include a wide variety of rock types characteristic of oceanic plate stratigraphy including chert and other siliceous sedimentary rocks with deep water or pelagic and hemipelagic faunas and carbonate rocks with associated shallow water faunas.

Chanthaburi chert-clastic sequence

The Chanthaburi chert-clastic sequence as proposed by Chutakosikanont (2004) is mainly composed of chert unit, siliceous mudstone unit and coarse clastic unit in ascending order, and generally is tectonically piled up to form an eastward, steeply dipping imbricate structure. Chert unit, and coarse clastic unit are predominant in sequence, comprise many stacked slices, however, each of which shows a coarsening upward succession. Vertical lithologic change within the chert-clastic sequence has been considered to indicate a shifting of sedimentary environment which reflects the landward drift of ocean floor from pelagic through hemipelagic to terrigenous environment in the trench. The imbricate chert-clastic sequence is formed by a successive off-scraping process of an oceanic plate in the subduction zone similar to western Honshu Island, Japan (Matsuoka 1984).

The western belt of the suture zone in the Sra Kaeo-Chanthaburi area is characterized by alternations of a red bedded chert unit and coarse clastic unit. All chert unit which occurred repeatedly in this belt are of similar age. Greenstone basalt, locally pillow, is recognized at one locality intimately accompanied with chert. It may be assumed safely that the most likely explanation for this belt is an offscraped accretionary complex made of the chert-clastic sequence resulting from the convergence of the

Paleo-Tethys ocean with the greenstone rocks interpreted as former ocean floor basalt.

Thung Kabin melange

An eastern belt designated as the Thung Kabin *mélange* (Hada et al., 1994) is a serpentinite matrix *mélange* which is characterized by strongly foliated serpentinite which includes various kinds of inclusions. At the outcrops, the foliation occurs only in serpentinite matrices and distinctively anastomoses around the more competent tectonic inclusions, resulting in a characteristic rock mixture of chaotic blocks in matrix appearance. Greenstone, limestone and chert are the dominant rock types of inclusions but sandstone, conglomerate, metamorphic rocks and granitic rock also occur as tectonic inclusions.

Greenstone commonly occurs as large blocks (several meters to several hundred meters in length). The rock is dark brownish gray basaltic tuff and green to dark greenish gray pillow lava. Basaltic tuff locally carries chert or limestone inclusions. Petrochemical and geochemical data of greenstone in this area suggests that the basaltic rocks resemble E-type MORB reported from anomalous ridge segment and hot spot-related ocean islands (Yoshikura et al. 1999). Chert and limestone occur as large blocks or as smaller clasts in serpentinite matrices. Red bedded chert is often accompanied by greenstone and limestone is sometimes interbedded with chert or enclosed in basaltic tuff. Inclusions of exotic metamorphic rocks have been found only from the eastern half of the belt as larger slivers. Those include not only meta-sedimentary rocks like meta-chert, but also a mylonitic gneissic rock with distinctive boudinaged leucocratic veins. They have been found at the eastern margin of the belt. Strongly weathered granitic rock was found as an inclusion in the serpentinite matrix. It is medium grained tonalite or granodiorite and consists essentially of plagioclase and quartz. Shearing effects are indicated by undulatory extinction of quartz and plagioclase. Quartz is commonly recrystallized to fine aggregates of secondary quartz with suture outlines. Anyway the original structure relationship between the suture zone and Indochina block is difficult to confirm definitely due to deep weathering condition. However, the tectonic line or suture must be located within the Sra Kaeo-Chanthaburi study area.

CHAPTER III

PETROGRAPHIC INVESTIGATION

As stated earlier, the total of 34 rock samples used in this study were collected from 4 main suture zones. They are mainly ultramafic rocks and most of them are physically weathered and undergone by the low-temperature thermal alteration. Major minerals, such as olivine, orthopyroxene, clinopyroxene, and minor minerals, such as calcic plagioclase were altered to be hydrous minerals. Various habits of serpentine were clearly shown under thin sections. Talc, chlorite, magnetite, and chromian spinel are minor and/or accessory minerals. Therefore, the most important point of this chapter is to observe relicts of the original mineral composition of these ultramafic rocks. This observation was done for petrography of the whole rock samples and chromian spinels (EPMA). The following step is to find out chemical analysis of chromian spinel using electron probe-microanalysis (EPMA), which is then used for calculating various partitions of $Cr\# = Cr/(Cr + Al)$, $Mg\# = Mg/(Mg^{2+} + Fe^{2+})$, trivalent element proportion of Cr^{3+} , Al^{3+} and Fe^{3+} . Based on the classification of ultramafic host rock characterization of Pober and Faupl (1983) (Figure. 3.1), Cookenboo et al. (1997) (Figure. 3.2) and model of ultramafic origin of Arai (2000) (Figure. 3.3), the identification of chromian spinel-bearing ultramafic host rocks can be identified.

Thin and polished-thin sections were carefully made in order to avoid the damage of original textures by using blue epoxy, which can bear the heat higher than 700° – $1,000^{\circ}$ C. It can protect the sample from the corrosion by electron beam from electron microprobe. The surfaces of polished-thin sections were polished by 3-micron diamond polishing powder and were examined their smoothness under reflected light microscope. All methods of petrographic study, spinel mapping, spinel sketching and photomicrograph were done before the process of chemical analysis by EPMA.

3.1 Petrography of ultramafic Rocks

Petrograph of ultramafic rock was described respectively for the investigated area in Chiang Rai, Nan-Uttaradit, Loei and Sra Kaeo using the IUGS classification of ultramafic rocks (Streckeisen, 1976) and serpentine varieties of William (1999).

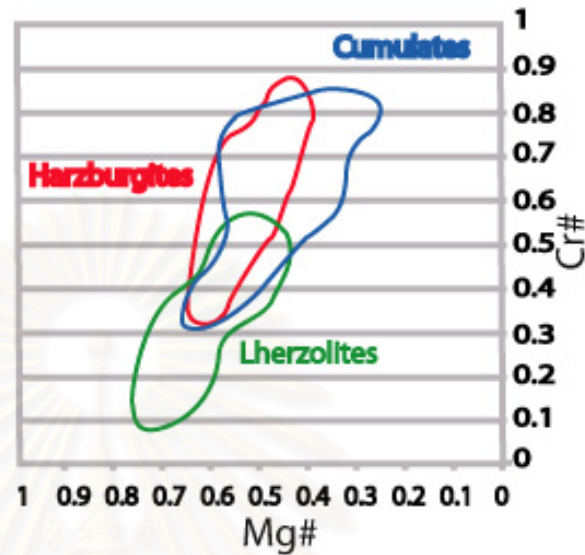


Figure 3.1 Graph showing relationship between compositional field of spinels from ultramafic rock types (Pober and Faupl, 1983).

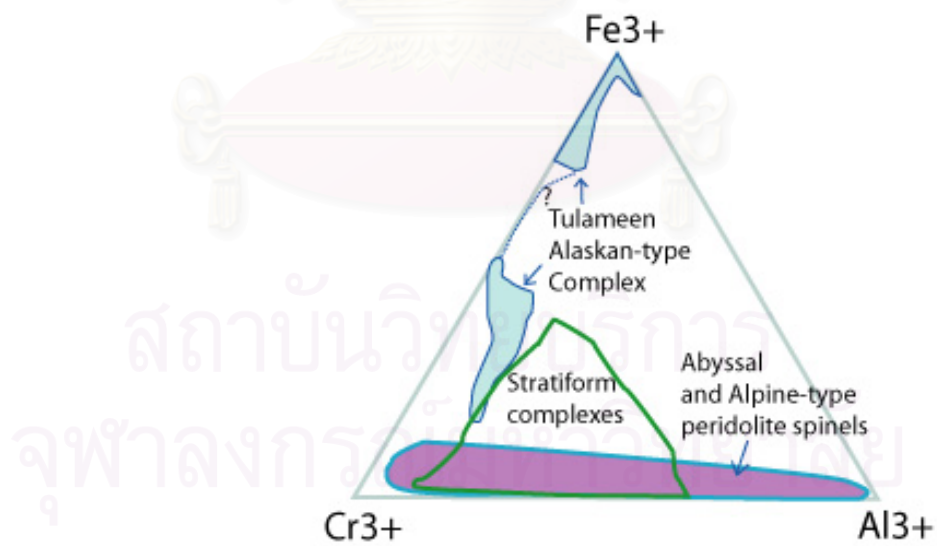


Figure 3.2 Ternary plots of Cr#, Al# and Fe# for spinels of different of ultramafic host rock ; Abyssal and Alpine-type peridotite, Stratiform complexes and Tulameen alaskan-type complex (Cookenboo et al., 1997).

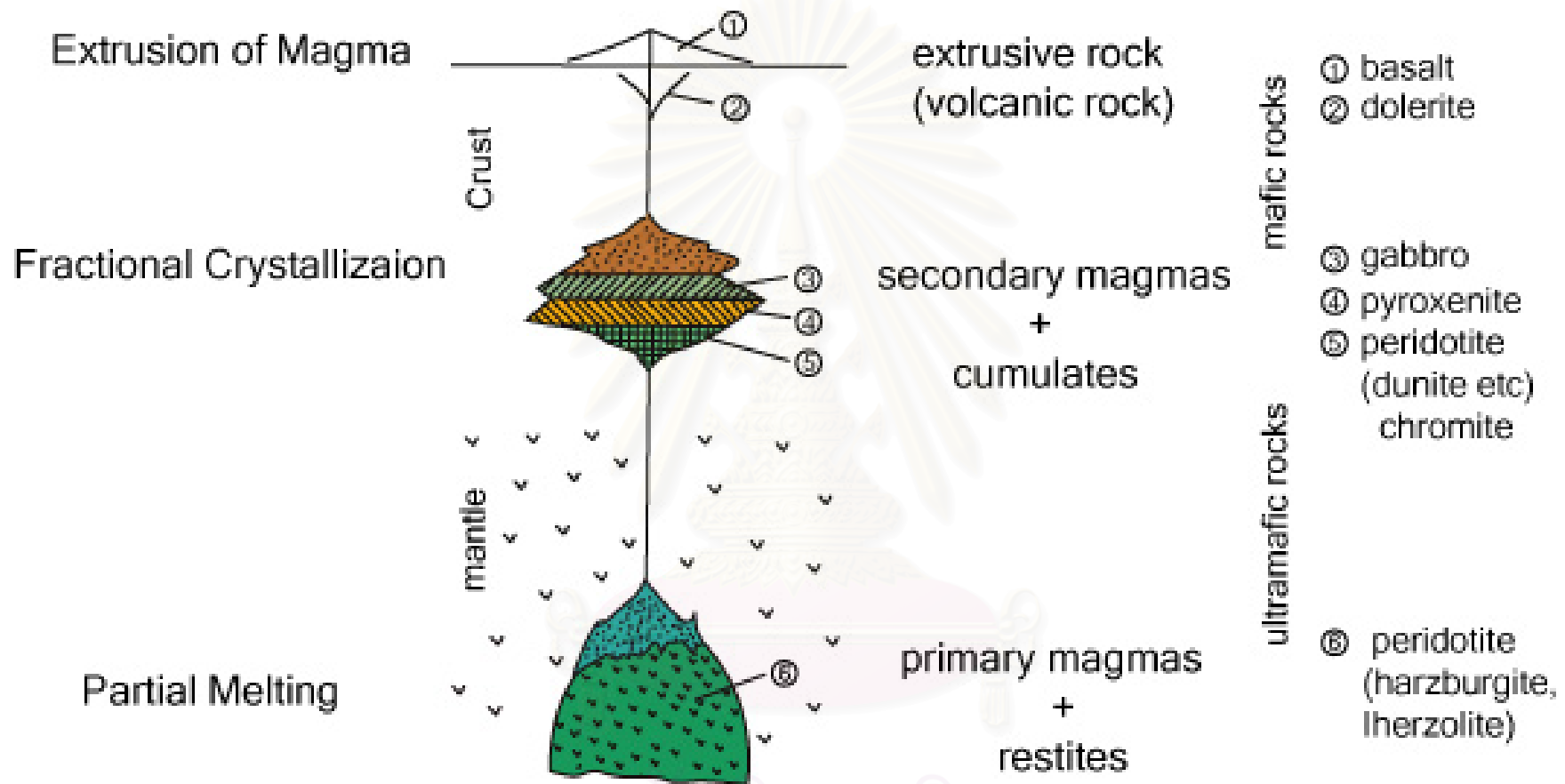


Figure 3.3 Simplified model of ultramafic origin (Arai, 2000)

3.1.1 Chiang Rai Area

Ultramafic host rocks of the Chiang Rai area is mostly serpentized and show porphyroblastic texture. Serpentine groundmass is difficult to be used because of its cryptocrystalline size. The texture is slightly /mesh and partially fibrous texture with irregular-shape veinlets of talc cutting all over the section. Talc, previously observed from hand specimen, is usually green but under thin section, this talc does not obviously show many optical properties. It is colorless, irregular and grain-mounted. Figure 3.4 shows the relict of subrounded to rounded, yellow orthopyroxene distributing equally in serpentine groundmass. Magnetite is also observed disseminated within grains of orthopyroxene. Both orthopyroxene and clinopyroxene are generally present as, the latter porphyroblasts normally occurs as lenses. Orthopyroxene is always yellow, shows high birefringence and exhibit polygonal shape. Clinopyroxene is found as small relict crystals and mostly replaced by calcite, (Figure 3.5).

3.1.2 Nan-Uttaradit Area

Ultramafic host rocks are mainly serpentinite with deformational structures. Serpentine in groundmass (Figure 3.6) are generally polygonal and show the main characteristic of both cataclastic and cataclastic textures. In Nan area, clinopyroxene is observed as relicts associated with magnetite grain. In the middle part, the dark-color area is antigorite. Crystal-rim feature of bright microfibrillar texture is exsolution lamellae of lizardite which is a platy mineral of hydrous magnesium silicate-a polymorph of chrysotile. Also in Uttaradit area (Figure 3.7), there are small amounts of varieties of long fibrous chrysotile. Due to our limited samples no chlorite and talc is found in this area.

3.1.3 Loei

In Loei area Ultramafic host rocks can be differentiated into 2 main types including cataclastic rocks and porphyroblastic rocks.

The cataclastic rocks contain groundmass of polygonal of antigorite, surrounded by lizardite lamellae. Within the groundmass, fractures are always semi-systematic, and show preferred orientation, called "mesh texture" (Figure 3.8). The mesh texture is therefore an ultramafic texture in which crystals are partially altered to a secondary

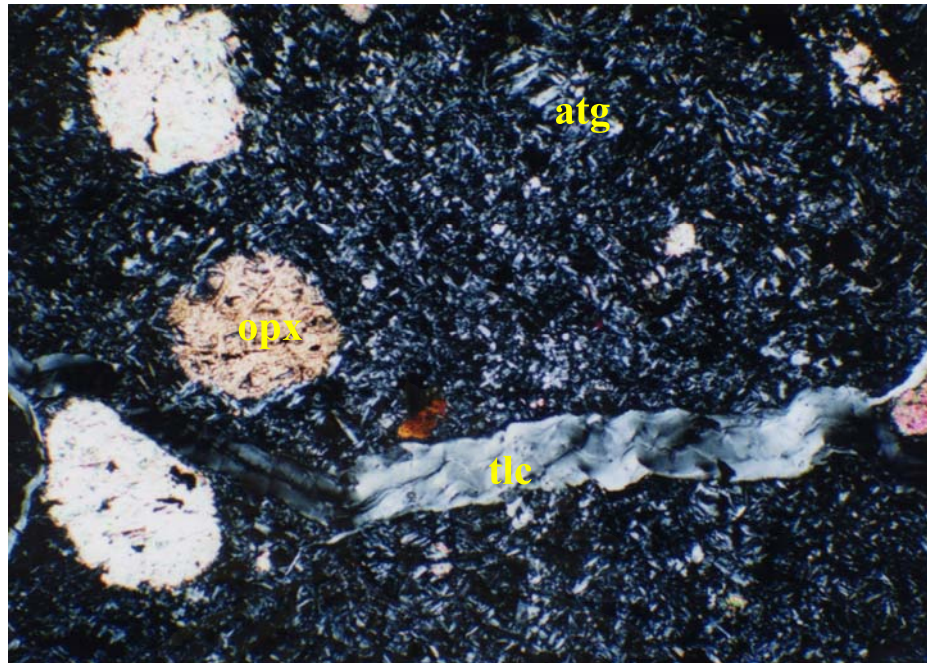


Figure 3.4 Photomicrograph of Chiang Rai ultramafic host rock showing; rounded orthopyroxene relicts and serpentine disseminated in glass-rich ground mass. Note that the rock is cross cut by talc veinlets (long axis of photo is 2 mm).

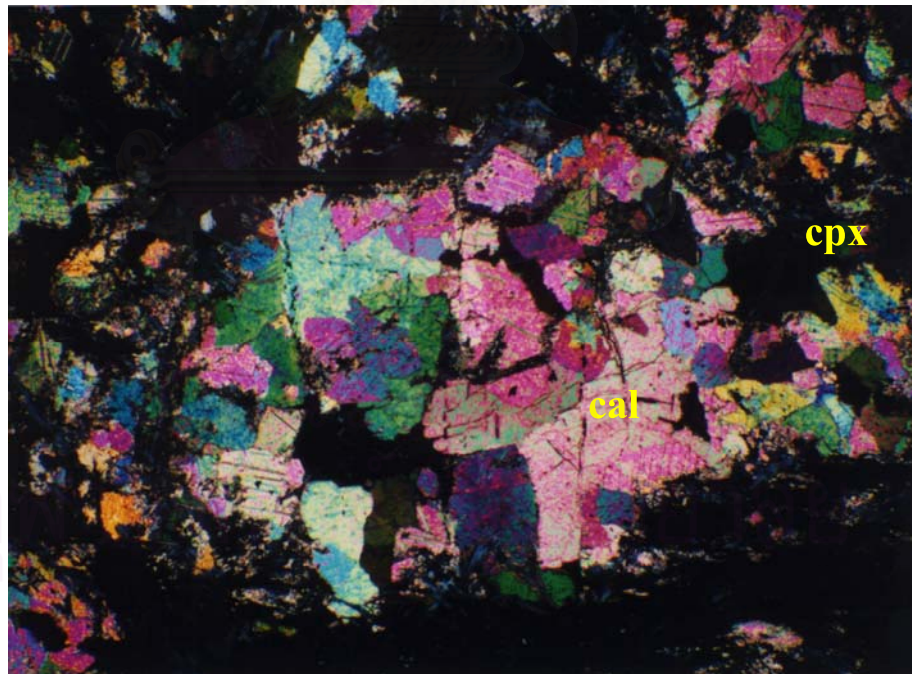


Figure 3.5 Photomicrograph of Chiang Rai ultramafic host rock showing; lensoid-shaped clinopyroxene replaced by deuteritic subhedral calcite aggregate (long axis of photo is 2 mm).

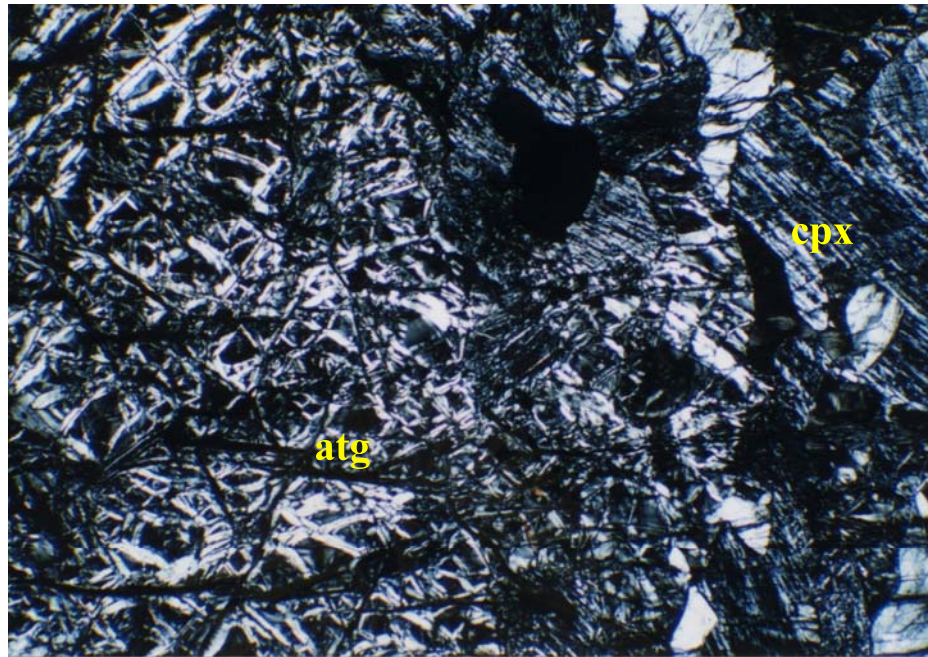


Figure 3.6 Photomicrograph of Nan ultramafic host rock showing altered clinopyroxene at the right side enclosed by antigorite mesh. The rock also shows cataclastic texture (long axis of photo is 2 mm).

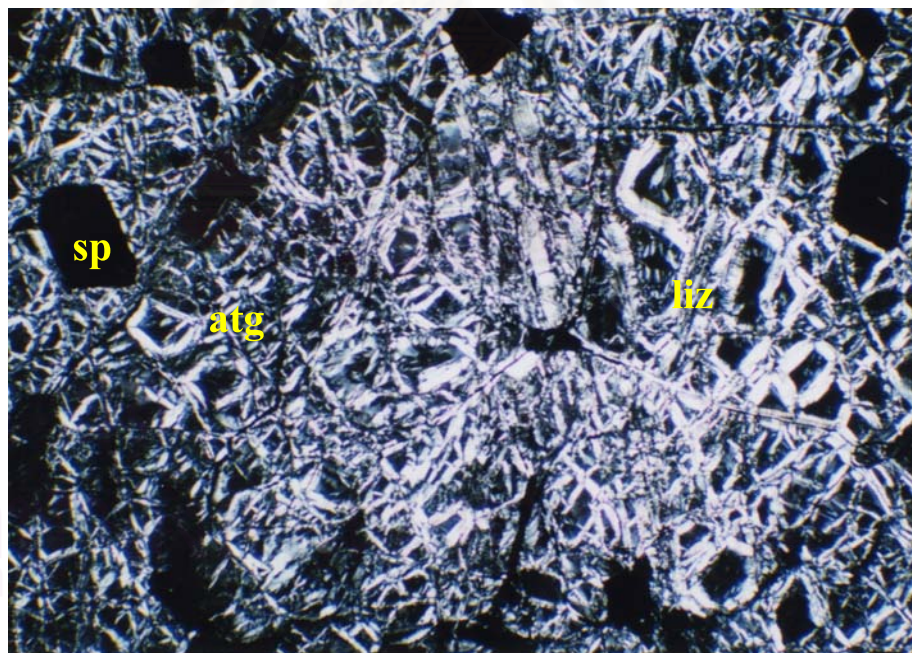


Figure 3.7 Photomicrograph of Uttaradit ultramafic host rock showing euhedral spinel (black) disseminated in mesh of antigorite and lizardite groundmass (long axis of photo is 2 mm).

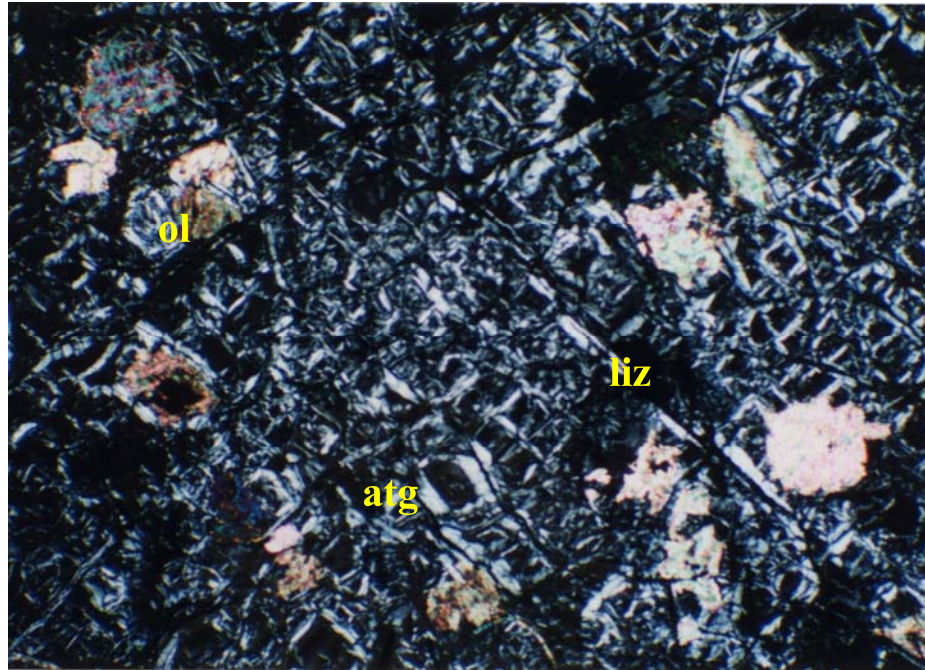


Figure 3.8 Photomicrograph of Loei ultramafic host rock showing altered olivine patches surrounded by polygonal serpentine. Note that some olivine patches replaced by calcite (long axis of photo is 2 mm).

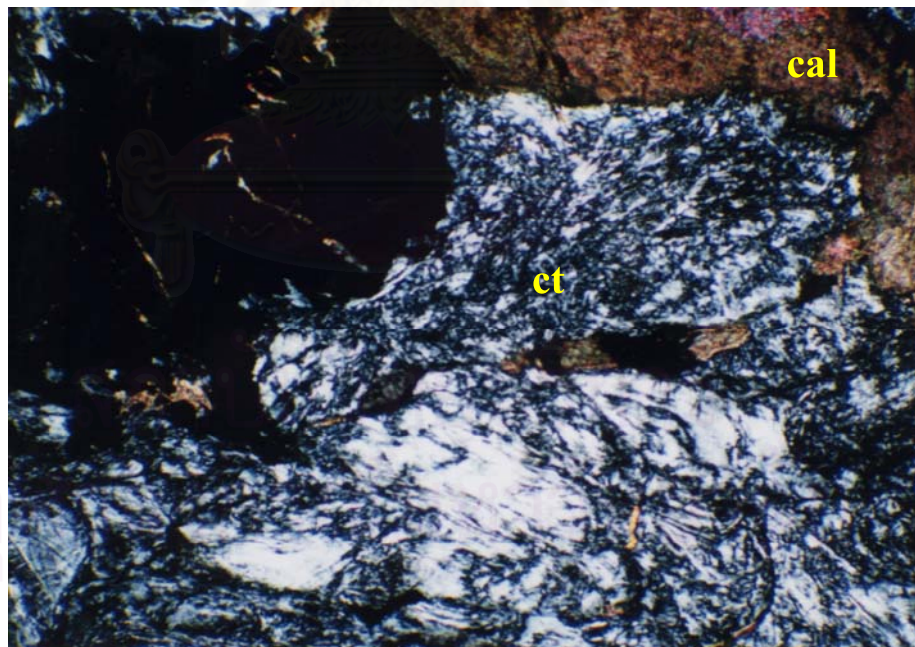


Figure 3.9 Photomicrograph of Loei ultramafic host rock showing fibrous chrysotile altered from orthopyroxene in central part, and lens shape of pyroxene squeeze was replaced by calcite on top (long axis of photo is 2 mm).

mineral (lizardite), forming a network that encloses the remnant of original mineral (olivine). Chlorite is rarely found while talc is absent. The relict of olivine patches is outstanding variety whose size is somewhat equal, distributing continuously in groundmass. Many grains of olivine were partially replaced by calcite.

The porphyroblastic rocks (Figure 3.9) show relicts of pyroxene squeezed into lens-shape and replaced by other minerals, resulting in high difficulty in identification of pyroxene variety. However, in some parts of thin sections, it was noticed that orthopyroxene was altered into fibrous chrysotile and chlorite. Clinopyroxene was replaced by very fine-grained crystals of calcite.

3.1.4 Sra Kaeo

Ultramafic host rocks of Sra Kaeo area obviously show porphyroblastic textures with various forms of parallel extinction. Orthopyroxene relicts although are small are really contrast from serpentine groundmass. Cleavages of orthopyroxene are distinctively razor-shaped. Pyroxene crystals are partially altered to serpentine especially around crystal rims and insides with parallel cleavage space. Serpentine in groundmass are slightly fine-grained and preferred 2 perfect cleavage systems that can be called "real mesh" structure. Most of serpentine varieties are antigorite and a few combined with microfibrinous lizardite on walls of serpentine veins (Figure 3.10).

3.2 Spinel Petrography

3.2.1 Chiang Rai spinel

Spinel found in the Chiang Rai ultramafic rocks are both isolated single crystals and crystalline aggregates. All of the crystals are anhedral \pm subhedral, orange, and brown to reddish brown. Crystal size ranges from 0.05 to 1 mm and average size is 0.5 mm. Grain shape are mainly long irregular with some rounded grains. These crystals were mechanically cracked, and they were clearly seen within the grains. Crystal rims were invariably changed to magnetite possibly under the influences of alteration and weathering processes. Several spinel crystals also have preferred orientation conforming to the direction of mineral grains in groundmass. There are only 1-2% of all spinel specimens that are subhedral. Inner crystal shows physical properties of spinel

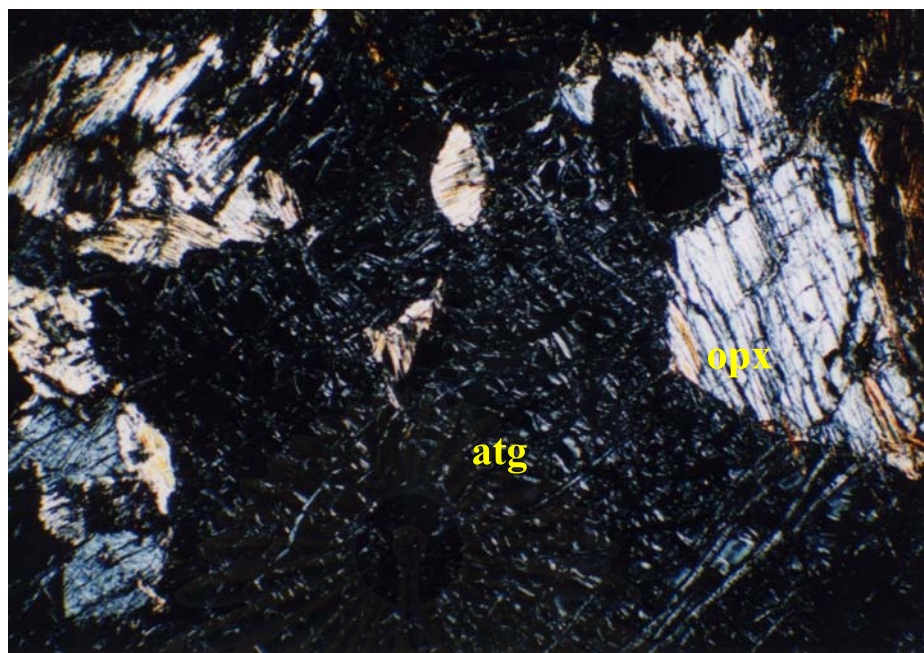


Figure 3.10 Photomicrograph of Sra Kaeo ultramafic host rock showing deformed orthopyroxene clast and porphyroblastic texture and two directions perfect cleavage system of antigorite called real mesh (reticulate) structure (long axis of photo is 2 mm).

สถาบันวิทยบริการ
จุฬาลงกรณ์มหาวิทยาลัย

obviously and its characteristics change transitionally to magnetite at crystal rim together with a small amount of chlorite. In some spinel crystals, small inclusions of silicate minerals are found which are unable to identify (Figure. 3.11, 3.12).

3.2.2 Nan-Uttaradit spinel

All spinels found in ultramafic rocks of the Nan-Uttaradit area are somewhat equigranular, with subhedral-to-euhedral single crystals distributing throughout the works. The sizes of the crystals range approximately from 0.1 to 0.3 mm. Their color varies from reddish brown to brownish black. Important feature of spinels in this area is their clean and highly homogeneous internal texture. Spinel of Nan-Uttaradit were free from mechanical break. Crystal rims are quite sharp and lack of magnetite rims. From the shape of crystals and their characteristic rims, it is assumed that they were not affected by any alteration. Magnetite is small and black in color, both magnetite patches and chains occur between serpentine. This character may have formed by the exsolution process from weathering of mafic minerals in host rocks (Figure. 3.13, 3.14).

3.2.3 Loei spinel

Spinel can be divided into 2 groups based on the relation and characteristics of ultramafic host rocks.

The first group occurs in catablastic host. Spinel of this group are mostly subhedral to euhedral, black to orange brown. Crystal sizes vary from 0.1 to 0.5 mm and average 0.2 mm. Many micro-inclusions were observed in spinel crystals. Besides, magnetite patches were also found throughout the groundmass.

The other spinel group relates to porphyroblastic host. The spinel is subvermicular, but its crystallinity is quite good and shows the feature of combination between many crystals, so-called multicrystal. The color is reddish brown. General spinel size is 1 to 2 mm in size and always show some cracks in the crystals. They are like jigsaw phase of surrounding minerals in groundmass with the same variety of mineral filled in the crack. This texture clearly shows the sequence of mineral crystallization. Spinel crystallization was the first, then the crystals were cracked and filled in by the crystallization of pyroxene. Another feature of subvermicular spin of this



Figure 3.11 Sketch of the morphological characteristic of chromian spinels of Chiag Rai.

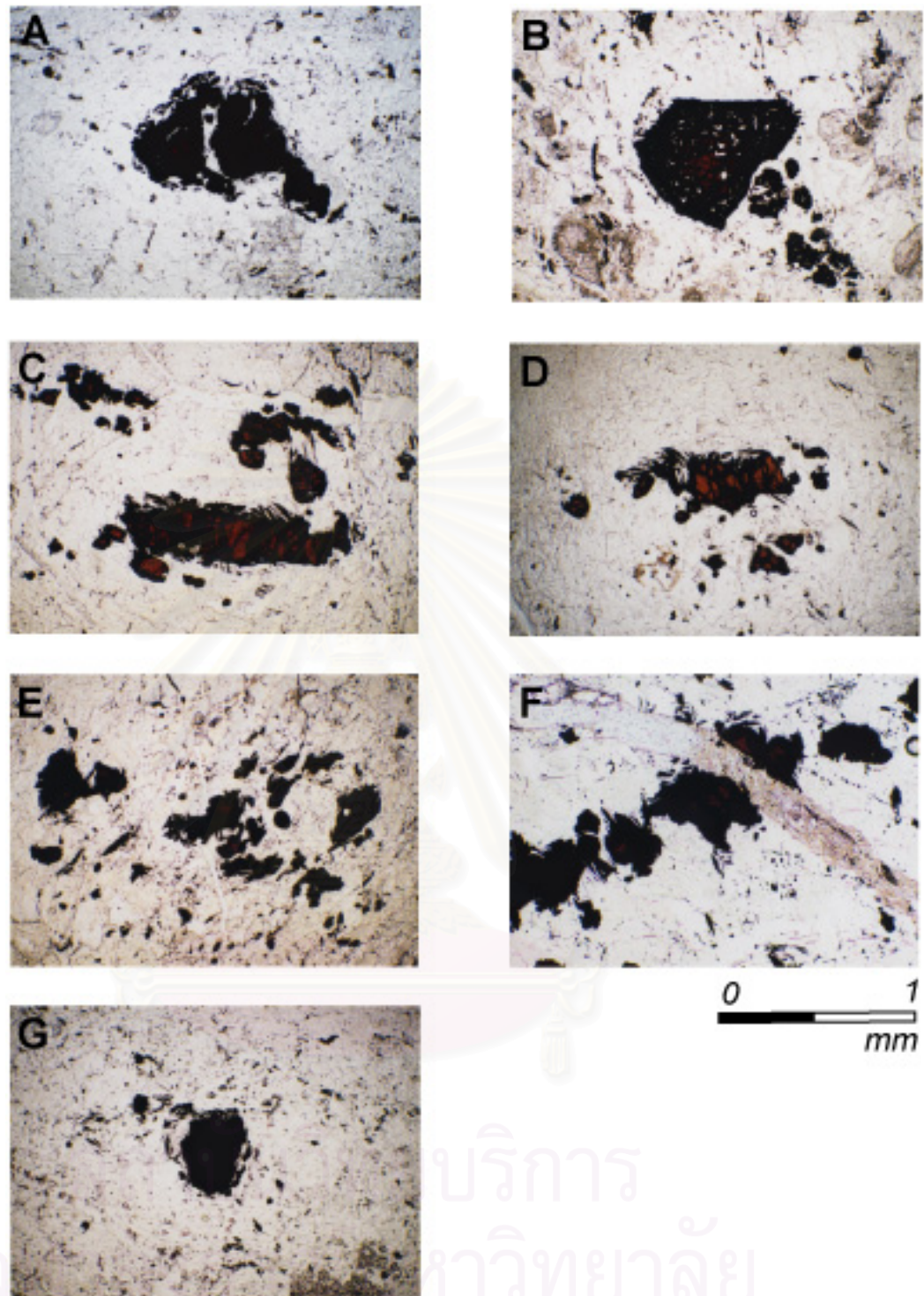


Figure 3.12 Photomicrographs of spinels from Chiang Rai ultramafic rocks showing isolated single crystals (A and G) and crystalline aggregate (B, C, D, E, and F) Mostly spinels are anhedral.

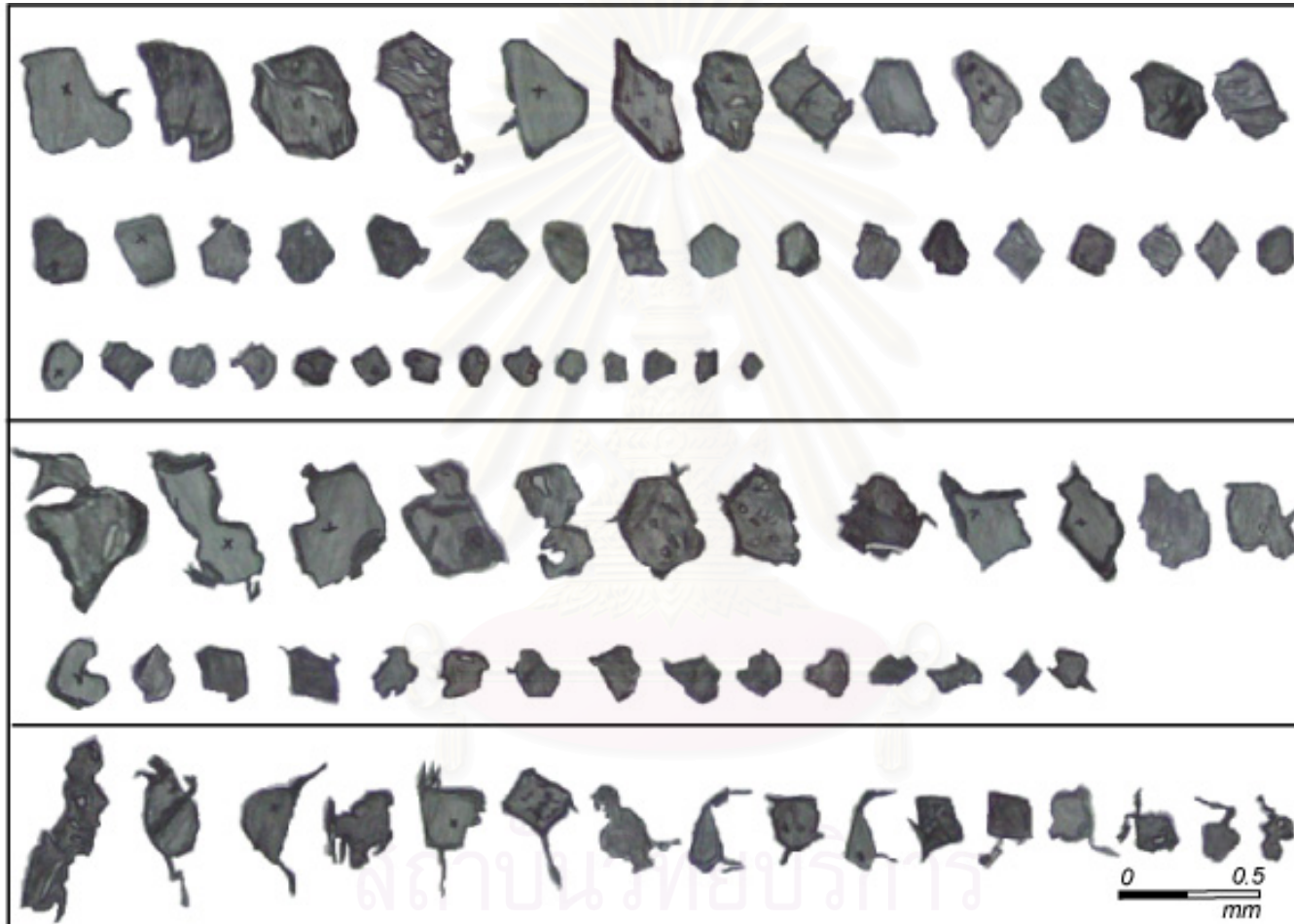


Figure 3.13 Sketch of the morphological characteristic of chromian spinels of Nan-Uttaradit.

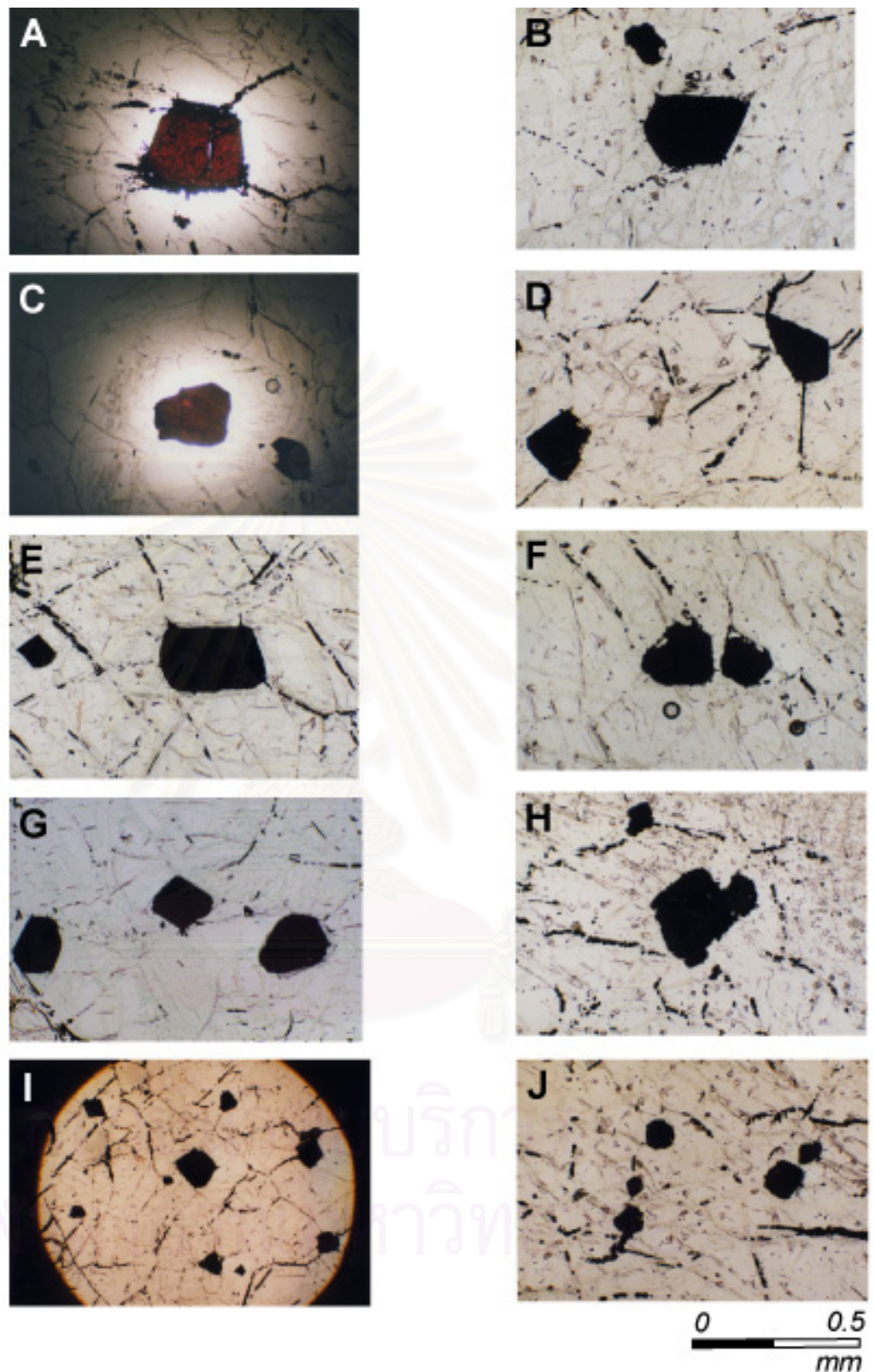


Figure 3.14 Photomicrographs of spinels from Nan-Uttaradit ultramafic host rocks showing isolated grains (A and I) and equigranular (G and J), with subhedral (C, D, F, and H) to euhedral (B, G, and I) shapes.

area is that the crystal rims are very sharp but they are obviously found as thin band of magnetite while clean homogeneous spinel is within crystal. The inner part of spinel and thin-banded magnetite can be easily separate and visibly seen under reflected light (Figure. 3.15, 3.16).

3.2.4 Sra Kaeo spinel

Most spinel found in the Sra Kaeo ultramafic rocks are subhedral to euhedral single crystals. Their colour varies from moderate to dark reddish brown. Crystal size of spinel ranges from 0.2 to 0.5 mm and it always has sharp crystal rim. Most of crystal faces, such as basal, tetrahedral and octahedral faces, are usually polygonal, and very few percent occur as rounded grains. Important feature should be notice of spinel in this area is a large size inclusion. Although without any EPMA analysis, the inclusion is interpreted as one kind of silicate minerals. Moreover, chlorite corona was founded around some spinel crystal rims. Magnetite is also distributed as patches similar to those observed in other areas (Figure. 3.17, 3.18).

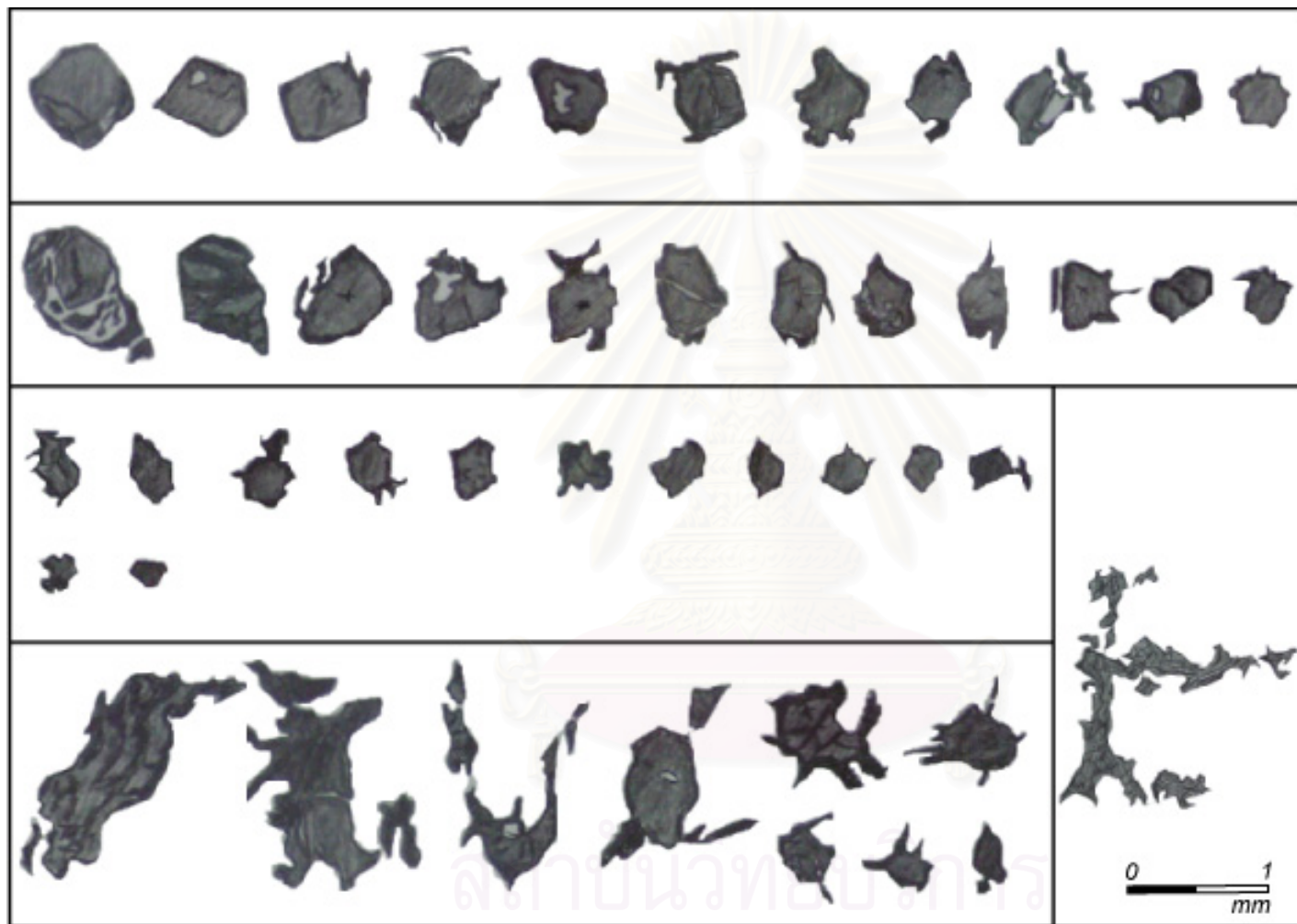


Figure 3.15 Sketch of the morphological characteristic of chromian spinels of Loei.

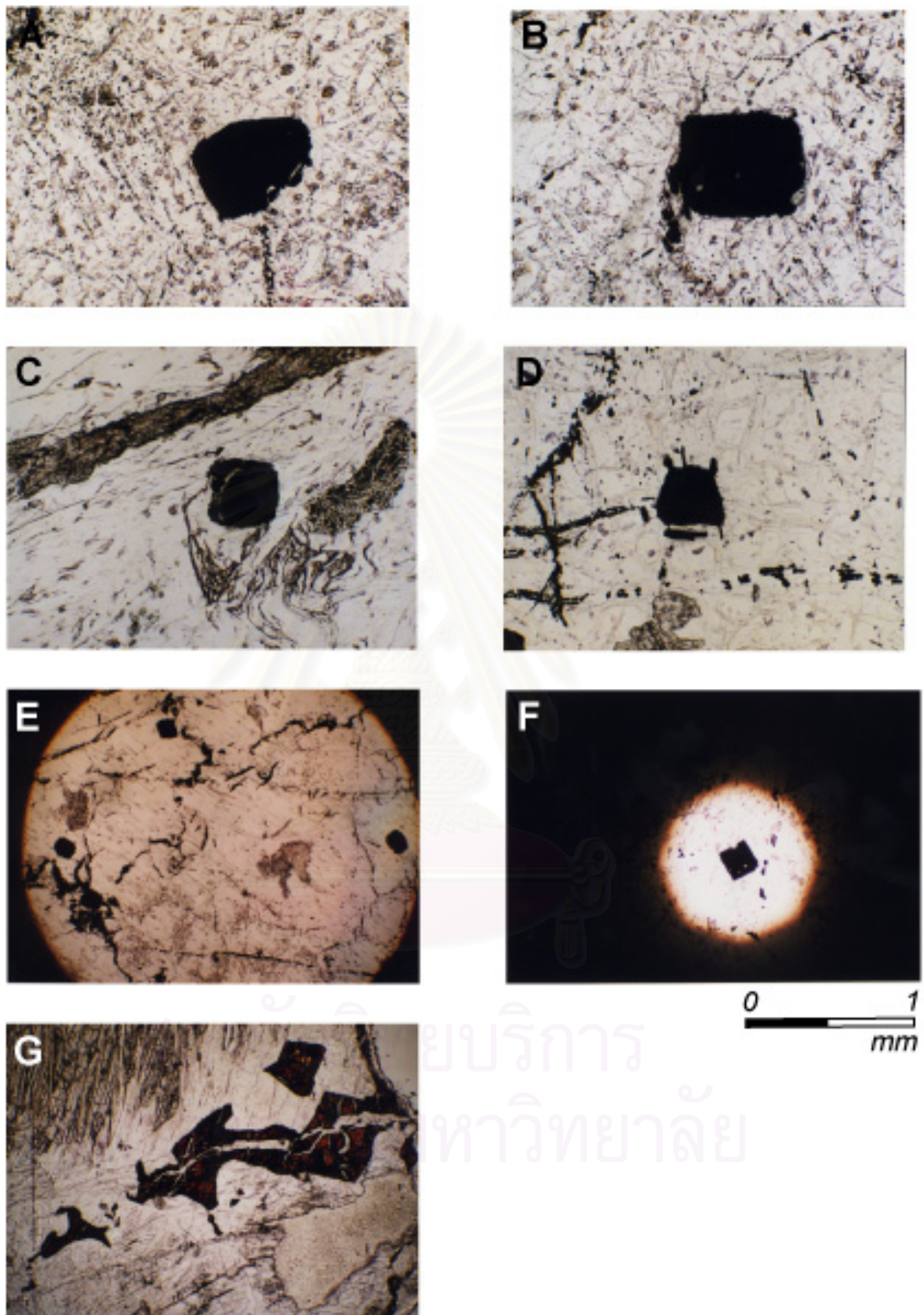


Figure 3.16 Photomicrographs of spinels from Loei ultramafic host rocks showing single rounded anhedral (A, B, C, and D), equigranular euhedral (E and F) and large multicrystalline (G).

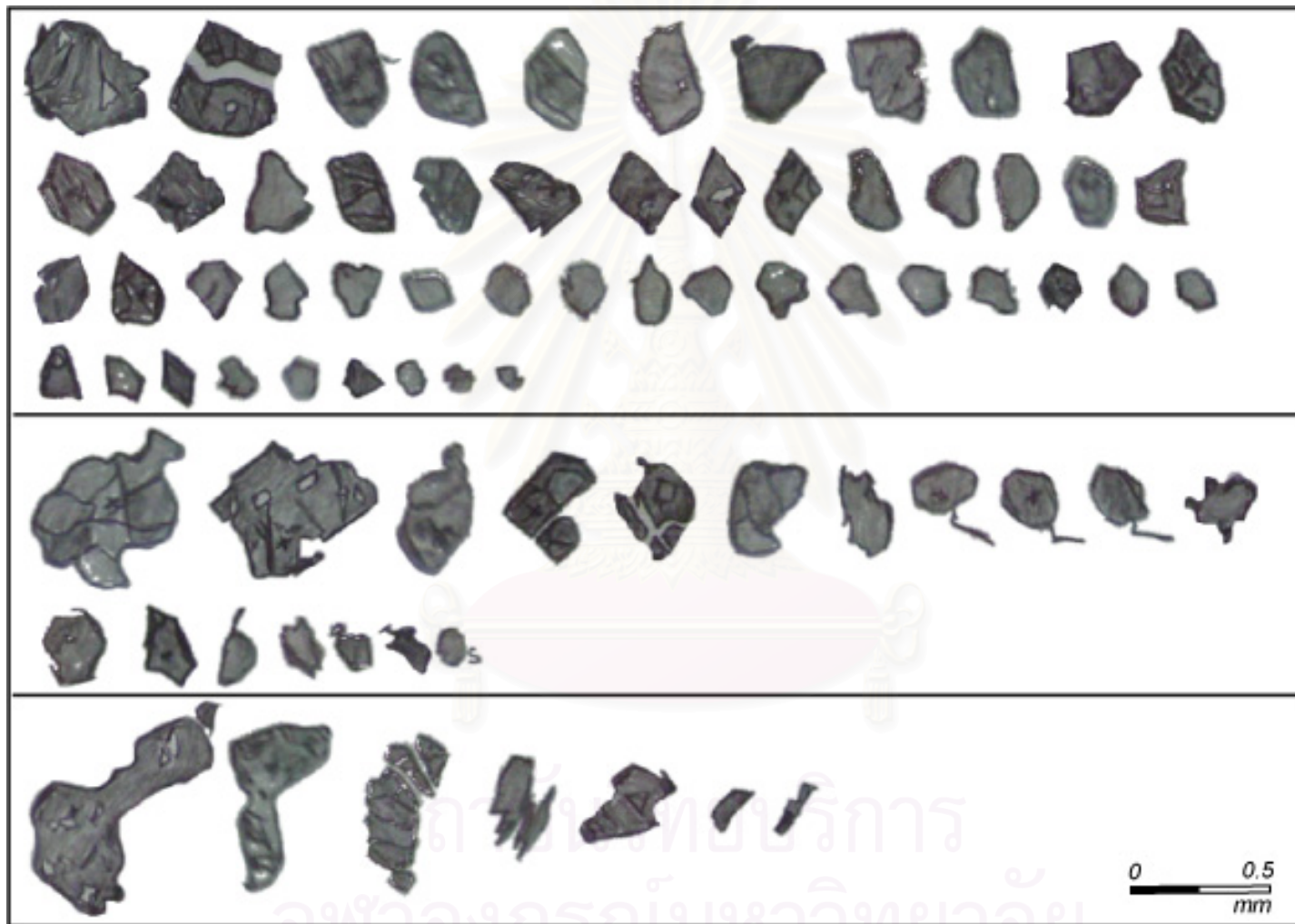


Figure 3.17 Sketch of the morphological characteristic of chromian spinels of Sra Kaeo.

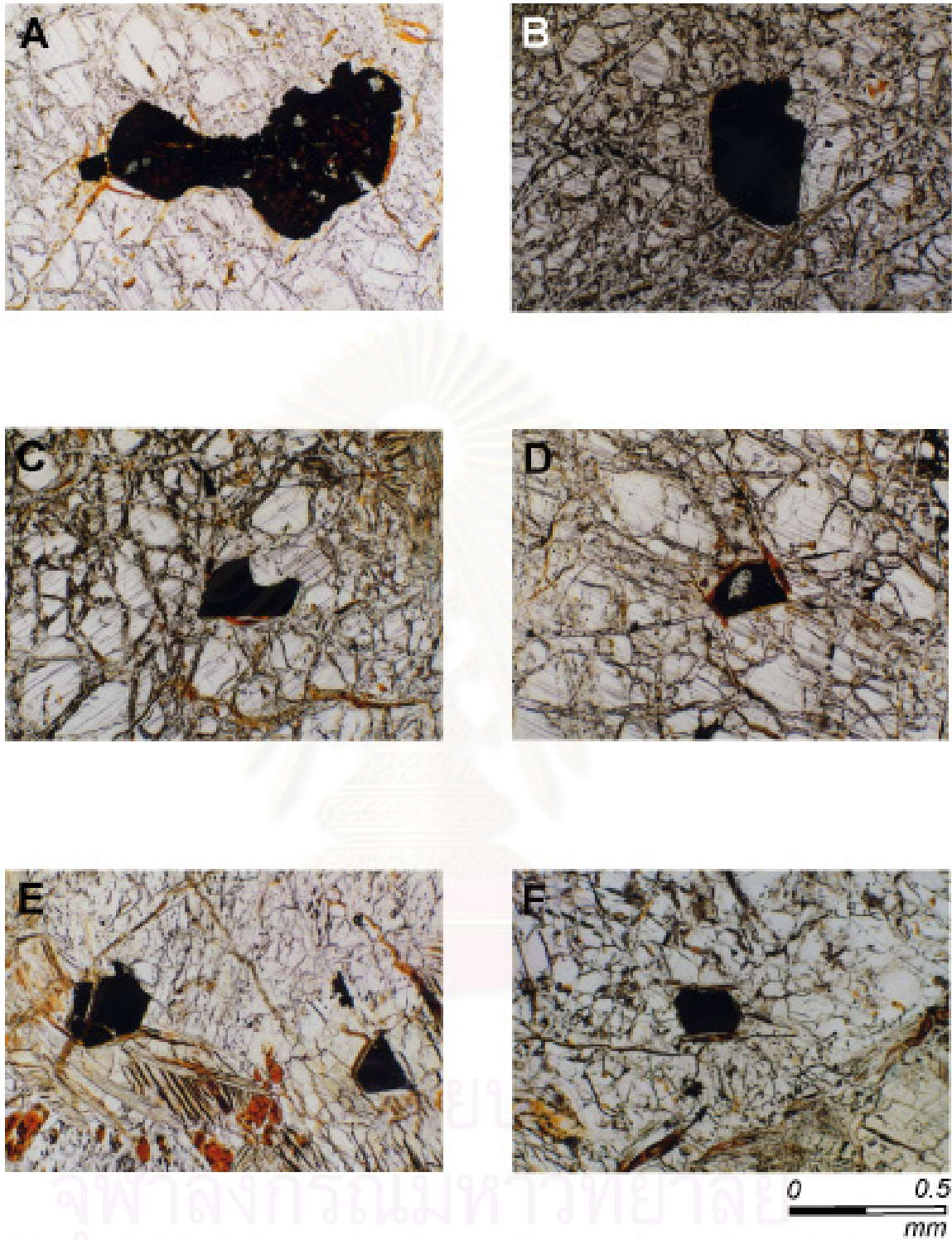


Figure 3.18 Photomicrographs of spinels from Sra Kaeo ultramafic host rocks showing isolated grains (E) subhedral (A and C) to euhedral (B, D, and F).

CHAPTER IV

GEOCHEMISTRY

4.1 EPMA Method

120 chromian spinel grains from Thailand and 106 grains from the other countries were selected for chemical analysis using EPMA (electron probe microanalysis) (model JEOL JXA 8621) at the Chemical Analysis Center, University of Tsukuba. Twelve major and minor oxides, including MgO, FeO, Fe₂O₃, Cr₂O₃, Al₂O₃, SiO₂, Na₂O, K₂O, CaO, TiO₂, MnO and ZnO, were analyzed for all of chromian spinel grains. Their weight percent can be useful in calculating partition values and plotting in standard diagrams. Method of calculation is explained below.

The most important oxides are ferric and ferrous oxides; which calculation is based on spinel stoichiometry. All Fe was calculated at first as FeO (total). All Ti was combined with Fe as ulvospinel molecule (Fe₂²⁺TiO₄). After subtraction of the ulvospinel molecule, the cation fractions of Mg, Fe²⁺, Cr, Al and Fe³⁺, were calculated assuming spinel stoichiometries. All Mn was added to total Fe prior to the calculation. Detailed equation is shown in appendix 1. Essential partition values used in the standard variation diagrams are chrome partition (Cr#) = Cr/(Cr+Al) and magnesium partition (Mg#) = Mg/(Mg+Fe²⁺). The other partition values of trivalent cations applied for variation triangular diagrams are Cr³⁺# = Cr/(Cr+Al+Fe³⁺), Al³⁺# = Al/(Cr+Al+Fe³⁺), and Fe³⁺# = Fe³⁺/(Cr+Al+Fe³⁺).

4.2 Geochemical results

4.2.1 Chiang Rai spinel

The EPMA result indicates that all the analysed spinels from the Chiang Rai area show a wide variation on major element concentrations. Cr₂O₃ ranges from 35 to 45 %. Al₂O₃ varies from 25 to 30 %. However, some grains have very low aluminar contents of about 8-9 %, suggesting high possibility of alteration effect which removed Al to form Al-hydrous mineral around spinel grains, such as chlorite. Total iron content ranges from 17 to 32 %, but mostly below 20%, whereas magnesium oxide is about 6-13 %. Other

elements are minor and generally lower than 0.1%. Some are lower than detection limit of probe. These elements are MnO, NiO, TiO₂, SiO₂, CaO, Na₂O and K₂O. It is important to note that TiO₂ of Chiang Rai spinel is very low compared with all area.

For major element partition calculation, it can be concluded that Cr# is about 0.4-0.5 and Mg# is about 0.3-0.7, but mostly concentrated within the range of 0.4-0.6. Cr³⁺# is about 0.45-0.68, Al³⁺# 0.2-0.55, and Fe³⁺ is slightly low 0.04-1.10 (table 4.1).

4.2.2 Nan-Uttaradit spinel

The EPMA result reveals that spinels from Nan-Uttaradit area have higher Cr content than that of the Chiang Rai area. The Cr content of Nan-Uttaradit spinels varies from 36 to 45 %. In contrast, the Nan-Uttaradit spinels have very low Al content 11 to 18 %, most of them are less than 15%. Total iron content is relatively high (30-38 %) whereas magnesium content is low (2-7 %). TiO₂ content (0.30.5 %) is higher than that of the Chiang Rai spinel. MnO content is very close to TiO₂. The other oxides, including CaO, Na₂O, K₂O NiO and SiO₂, are present in only trace amounts, about 0.001-0.1%.

Cr# can be divided into two ranges one about 0.3-0.5 and the other about 0.5-0.7. Mg# shows an average range of 0.3-0.4. Other element partitions show narrow distribution. Cr³⁺# varies from 0.55 to 0.6, Al³⁺# from 0.3 to 0.4. However Fe³⁺# value range (0.1-0.2) is obviously higher more than those of the other areas (table 4.2).

4.2.3 Loei spinel

Spinel from the Loei area have chrome contents relatively higher than those of the two earlier mentioned areas. The Cr contents vary from 45 to 50 %, only few grains have Cr content lower than 40%. Alumina contents (11-13 %), on the other hand, are also lower than those of the Nan-Uttaradit and Chiang Rai areas. Spinel with chromium contents lower than 40 % usually have high alumina contents (27-30 %). So both elemental compositions show reverse relation. Total iron is wide, extending from 25-46 %. Magnesium is quite high, 7-14 %. TiO₂ and MnO are also very high, 0.3-0.7%. CaO, Na₂O, K₂O, ZnO and SiO₂ are present in minor and trace amounts, and generally range from 0.001-0.1%.

Sample No	C2-4-		C2-6-		C9-2-		C10-					C11-		C11-					
	C2-4	2	C2-6	2	2	C9-3	C9-4	C10-2	C10-3	3-2	C10-4	C10-6	C11-1	3-2	C11-4	5-2	C11-7	C12-1	C12-2
SiO ₂	0.12	0.04	0.01	0.00	0.00	0.01	1.94	0.01	0.02	0.00	0.04	0.04	0.02	0.02	0.00	0.08	0.00	0.00	0.00
Al ₂ O ₃	24.65	25.53	25.58	25.25	31.90	31.43	28.68	28.17	30.24	30.20	26.65	28.74	28.29	29.90	28.75	30.01	28.45	25.95	25.09
TiO ₂	0.08	0.08	0.04	0.01	0.01	0.04	0.00	0.02	0.01	0.03	0.02	0.02	0.05	0.03	0.03	0.01	0.05	0.01	0.02
Cr ₂ O ₃	38.85	38.48	40.77	38.89	36.21	35.46	32.27	38.23	36.51	36.87	39.98	37.64	38.54	36.94	38.04	37.50	38.32	41.19	41.06
FeO	24.31	23.08	19.98	22.23	17.45	17.57	20.57	18.49	18.13	19.10	18.10	18.18	17.63	18.57	18.07	18.11	18.36	18.88	19.77
NiO	0.06	0.04	0.08	0.04	0.05	0.08	0.05	0.09	0.13	0.07	0.10	0.11	0.07	0.00	0.07	0.05	0.07	0.05	0.09
MnO	0.43	0.41	0.19	0.38	0.26	0.27	0.34	0.28	0.25	0.26	0.32	0.21	0.23	0.25	0.29	0.27	0.28	0.26	0.31
MgO	9.75	10.42	11.11	10.52	13.86	13.18	15.27	12.53	13.06	12.51	12.60	12.71	13.04	12.81	12.77	13.09	12.28	11.78	11.32
CaO	0.05	0.03	0.00	0.07	0.07	0.05	0.11	0.02	0.00	0.05	0.01	0.02	0.03	0.00	0.01	0.00	0.00	0.03	0.02
Na ₂ O	0.00	0.04	0.01	0.05	0.07	0.02	0.04	0.06	0.00	0.01	0.08	0.08	0.02	0.00	0.04	0.00	0.00	0.01	0.01
K ₂ O	0.02	0.00	0.02	0.00	0.01	0.03	0.02	0.01	0.02	0.00	0.00	0.00	0.02	0.00	0.01	0.00	0.01	0.01	0.00
Total	98.31	98.14	97.77	97.44	99.89	98.15	99.27	97.91	98.36	99.09	97.89	97.75	97.93	98.50	98.07	99.11	97.80	98.17	97.68
Cation	4 oxygens																		
Fe total	0.66	0.62	0.53	0.60	0.44	0.45	0.52	0.48	1.75	0.49	0.48	0.47	0.46	0.48	0.47	0.46	0.48	0.50	0.53
Fe*	0.66	0.62	0.53	0.60	0.44	0.45	0.52	0.48	1.75	0.49	0.48	0.47	0.46	0.48	0.47	0.46	0.48	0.50	0.53
Fe ²⁺	0.55	0.52	0.48	0.51	0.39	0.41	0.31	0.43	0.65	0.44	0.42	0.42	0.41	0.43	0.42	0.42	0.44	0.46	0.47
Fe ³⁺	0.11	0.10	0.05	0.09	0.05	0.04	0.21	0.05	1.10	0.05	0.06	0.05	0.05	0.05	0.05	0.05	0.04	0.04	0.05
TiO ₂	0.08	0.08	0.04	0.01	0.01	0.04	0.00	0.02	0.01	0.03	0.02	0.02	0.05	0.03	0.03	0.01	0.05	0.01	0.02
Cr#	0.51	0.50	0.52	0.51	0.43	0.43	0.43	0.48	0.45	0.45	0.50	0.47	0.48	0.45	0.47	0.46	0.47	0.52	0.52
Mg#	0.46	0.49	0.52	0.49	0.61	0.59	0.69	0.57	0.57	0.56	0.58	0.58	0.59	0.58	0.58	0.59	0.56	0.54	0.53
Cr ₃ #	0.49	0.48	0.50	0.48	0.42	0.42	0.38	0.46	0.29	0.44	0.49	0.46	0.47	0.44	0.46	0.45	0.47	0.51	0.51
Al ₃ #	0.46	0.47	0.47	0.47	0.55	0.56	0.51	0.51	0.35	0.54	0.48	0.52	0.51	0.53	0.52	0.53	0.52	0.47	0.46
Fe ₃ +3#	0.05	0.05	0.02	0.05	0.02	0.02	0.11	0.03	0.36	0.02	0.03	0.03	0.02	0.03	0.02	0.02	0.02	0.02	0.03

Table 4.1 Representative microprobe analyses of chromian spinels in ultramafic rock from Chiang Rai.

Sample No	N75-						N76-						U83-U84							
	N75-1	N75-2	N75-3	4-2	N75-5	N75-6	N76-1	2-2	N76-3	N76-4	N76-5	N76-6	U83-1	U83-2	U83-3	U83-4	U83-5	U83-6	U84-2	U84-3
SiO ₂	0.01	0.01	0.00	0.05	0.01	0.01	0.02	0.00	0.01	0.02	0.00	0.02	0.03	0.00	0.00	0.02	0.02	0.03	0.02	0.00
Al ₂ O ₃	18.20	15.18	12.89	16.56	16.83	18.18	16.16	16.84	11.22	14.65	14.65	12.67	13.45	13.49	13.23	12.86	15.18	14.56	12.46	12.54
TiO ₂	0.32	0.34	0.40	0.33	0.35	0.28	0.33	0.37	0.48	0.37	0.28	0.26	0.49	0.49	0.48	0.44	0.49	0.47	0.51	0.53
Cr ₂ O ₃	37.89	38.84	39.89	37.98	40.05	38.20	39.94	36.77	40.65	39.55	39.75	39.71	43.83	44.86	45.25	44.03	42.63	42.40	45.29	44.24
FeO	34.13	37.12	38.01	36.01	34.32	32.69	35.24	36.33	38.80	35.91	35.87	37.96	33.06	32.78	31.44	32.67	31.58	34.21	32.82	34.03
NiO	0.11	0.02	0.07	0.12	0.08	0.11	0.08	0.05	0.06	0.02	0.10	0.05	0.07	0.00	0.07	0.13	0.13	0.10	0.10	0.01
MnO	0.48	0.40	0.49	0.35	0.41	0.41	0.52	0.46	0.46	0.46	0.54	0.45	0.49	0.47	0.55	0.48	0.38	0.47	0.51	0.42
MgO	7.24	6.08	5.50	6.69	7.09	7.61	6.87	6.89	5.52	6.02	6.39	5.99	6.22	6.43	7.01	7.02	7.03	6.73	6.63	6.19
CaO	0.00	0.03	0.02	0.04	0.00	0.04	0.01	0.00	0.01	0.04	0.04	0.09	0.00	0.00	0.00	0.06	0.04	0.03	0.06	0.03
Na ₂ O	0.13	0.09	0.13	0.14	0.13	0.21	0.04	0.09	0.22	0.03	0.16	0.09	0.22	0.11	0.12	0.16	0.03	0.14	0.00	0.04
K ₂ O	0.00	0.00	0.00	0.00	0.00	0.00	0.01	0.01	0.00	0.02	0.03	0.01	0.00	0.00	0.01	0.01	0.00	0.00	0.00	0.00
ZnO	0.35	0.32	0.11	0.25	0.18	0.21	0.21	0.25	0.28	0.21	0.26	0.22	0.26	0.26	0.19	0.20	0.25	0.26	0.21	0.21
Total	98.85	98.43	97.49	98.51	99.44	97.95	99.41	98.06	97.71	97.29	98.06	97.52	98.11	98.89	98.36	98.07	97.74	99.39	98.62	98.22
Cation	4 oxygens																			
Fe total	0.98	1.10	1.16	1.05	0.99	0.94	1.02	1.07	1.19	1.08	1.07	1.15	0.98	0.96	0.93	0.97	0.92	1.00	0.97	1.01
Fe*	0.97	1.08	1.14	1.03	0.97	0.93	1.01	1.05	1.16	1.06	1.05	1.14	0.96	0.94	0.90	0.95	0.90	0.97	0.95	0.99
Fe ²⁺	0.66	0.72	0.74	0.69	0.67	0.64	0.68	0.68	0.74	0.71	0.70	0.72	0.69	0.68	0.65	0.65	0.65	0.68	0.67	0.70
Fe ³⁺	0.31	0.37	0.39	0.35	0.30	0.29	0.33	0.37	0.43	0.34	0.36	0.42	0.26	0.25	0.25	0.29	0.25	0.30	0.27	0.29
TiO ₂	0.32	0.34	0.40	0.33	0.35	0.28	0.33	0.37	0.48	0.37	0.28	0.26	0.49	0.49	0.48	0.44	0.49	0.47	0.51	0.53
Cr#	0.58	0.63	0.67	0.61	0.61	0.58	0.62	0.59	0.71	0.64	0.65	0.68	0.69	0.69	0.70	0.70	0.65	0.66	0.71	0.70
Mg#	0.36	0.31	0.28	0.33	0.35	0.38	0.34	0.34	0.29	0.31	0.32	0.31	0.32	0.33	0.36	0.36	0.36	0.34	0.34	0.32
Cr ³⁺	0.50	0.52	0.55	0.50	0.52	0.50	0.52	0.49	0.56	0.54	0.53	0.54	0.60	0.60	0.61	0.60	0.57	0.56	0.61	0.60
Al ³⁺	0.35	0.30	0.26	0.33	0.33	0.36	0.32	0.33	0.23	0.30	0.29	0.26	0.27	0.27	0.27	0.26	0.30	0.29	0.25	0.25
Fe ³⁺ #	0.15	0.18	0.19	0.17	0.15	0.14	0.16	0.18	0.21	0.17	0.17	0.20	0.13	0.12	0.12	0.14	0.12	0.15	0.13	0.14

Table 4.2 Representative microprobe analyses of chromian spinel in ultramafic rock from Nan-Uttaradit.

Cr# are divided into two narrow ranges-one at 0.4-0.5 and the other at 0.7-0.75. Mg# shows much wider variation, extending from 0.2-0.7. Cr³⁺ # range from 0.4 to 0.7, Al³⁺ # from 0.2 to 0.5 and Fe³⁺ # are very low, 0.01-0.12 (table 4.3).

4.2.4 Sra Kaeo spinel

Spinel from ultramafic rocks of the Sra Kaeo area have the highest chrome contents. They range from 48 to 62 %, mostly over 50%. Alumina contents are normal and average about 10-20%. Total iron concentration varies from 20-30 %. Magnesium is also normal (6-10 %) with slightly low manganese (0.04-0.6 %). Noteworthy is that major element compositions of this area are resembled with spinels from Loei. Only some minor elements are different, such as very low TiO₂ (0.03-0.2 %) and abnormally high ZnO (0.2-0.7 %). SiO₂, NiO, CaO, Na₂O and K₂O are also present in only trace amounts similar to those of the other areas.

Cr# are very high ranging from 0.6 to 0.95. Mg# extended from 0.2 to 0.5. Cr³⁺ # are widely consistent, ranging from 0.5 to 0.9, mostly within the range of 0.6-0.75. Al³⁺ # are 0.05-0.3, and the average range is from 0.2 to 0.3. Fe³⁺ # is slightly low (0.02-0.07), only few is high, up to 0.1 or 0.2 (table 4.4).

Sample No	L16-1	L16-2	L16-3	L16-4	L16-6	L19-1	L19-2	L19-3	L19-4	L19-5	L19-6	L19-7	L23-1	L23-2	L23-3	L23-4	L23-5
SiO ₂	0.03	0.07	0.01	0.00	0.02	0.02	0.03	0.01	0.01	0.05	0.04	0.03	0.01	0.03	0.01	0.03	0.00
Al ₂ O ₃	12.73	12.84	12.46	12.38	11.93	12.91	13.11	12.78	12.13	12.28	11.87	11.88	30.54	27.93	29.73	29.41	27.00
TiO ₂	0.46	0.48	0.55	0.59	0.56	0.64	0.58	0.56	0.65	0.58	0.56	0.51	0.01	0.04	0.02	0.00	0.00
Cr ₂ O ₃	45.26	45.91	46.58	46.18	45.12	46.47	45.18	45.34	45.66	46.00	46.65	46.54	35.64	38.29	39.14	38.46	41.98
FeO	31.67	31.87	31.86	32.43	34.07	31.96	31.66	32.40	32.06	32.30	31.96	32.16	18.00	15.79	16.99	18.27	16.31
NiO	0.07	0.07	0.00	0.11	0.00	0.05	0.06	0.07	0.07	0.06	0.04	0.07	0.06	0.12	0.09	0.09	0.07
MnO	0.47	0.45	0.48	0.55	0.54	0.43	0.47	0.50	0.46	0.50	0.44	0.46	0.37	0.24	0.25	0.21	0.25
MgO	6.77	7.31	6.81	6.38	5.92	7.04	6.90	6.95	6.83	6.43	6.98	6.27	13.42	14.77	13.81	13.29	13.71
CaO	0.05	0.03	0.03	0.03	0.06	0.00	0.06	0.02	0.00	0.09	0.02	0.03	0.04	0.05	0.01	0.00	0.01
Na ₂ O	0.11	0.15	0.00	0.06	0.04	0.17	0.08	0.22	0.17	0.15	0.00	0.11	0.15	0.04	0.08	0.08	0.11
K ₂ O	0.00	0.00	0.02	0.00	0.02	0.00	0.03	0.01	0.00	0.02	0.00	0.04	0.00	0.01	0.01	0.01	0.00
ZnO	0.23	0.19	0.31	0.25	0.26	0.34	0.17	0.40	0.18	0.21	0.18	0.34	0.29	0.13	0.15	0.20	0.16
Total	97.85	99.36	99.10	98.96	98.53	100.03	98.33	99.26	98.23	98.67	98.74	98.46	98.52	97.44	100.28	100.06	99.60
Cation	4 oxygens																
Fe total	0.94	0.93	1.27	0.33	1.02	0.93	0.93	0.95	0.95	0.96	0.94	0.96	0.47	0.41	0.43	0.46	0.42
Fe*	0.92	0.91	1.24	1.24	0.99	0.89	0.90	0.92	0.92	0.93	0.91	0.93	0.46	0.41	0.43	0.46	0.42
Fe ²⁺	0.66	0.64	1.01	1.01	0.71	0.65	0.66	0.89	0.66	0.68	0.65	0.68	0.40	0.33	0.39	0.41	0.38
Fe ³⁺	0.25	0.26	0.24	0.24	0.28	0.24	0.25	0.03	0.26	0.25	0.26	0.24	0.07	0.08	0.04	0.05	0.04
TiO ₂	0.46	0.48	0.55	0.59	0.56	0.64	0.58	0.56	0.65	0.58	0.56	0.51	0.01	0.04	0.02	0.00	0.00
Cr#	0.70	0.71	0.71	0.71	0.72	0.71	0.70	0.70	0.72	0.72	0.72	0.72	0.44	0.48	0.47	0.47	0.51
Mg#	0.35	0.37	0.26	0.25	0.31	0.36	0.35	0.29	0.35	0.33	0.36	0.32	0.60	0.67	0.61	0.59	0.62
Cr ₃ #	0.62	0.61	0.63	0.63	0.62	0.62	0.61	0.69	0.62	0.63	0.63	0.64	0.42	0.46	0.46	0.45	0.50
Al ₃ #	0.26	0.26	0.25	0.25	0.24	0.26	0.27	0.29	0.25	0.25	0.24	0.24	0.54	0.50	0.52	0.52	0.48
Fe ³⁺ #	0.13	0.13	0.12	0.12	0.14	0.12	0.12	0.02	0.13	0.12	0.13	0.12	0.03	0.04	0.02	0.03	0.02

Table 4.3 Representative microprobe analyses of chromian spinels in ultramafic rock from Loei.

Sample No	S46-1	S46-2	S46-2-3	S46-2-4	S46-2-5	S47-1	S47-3	S47-4	S47-5	S47-8	S48-3	S48-4	S89-1	S89-2	S89-3	S89-4	S89-5	S89-6	S91-1	S91-3	S91-4	S91-5	S91-6
SiO2	0.01	0.14	0.05	0.03	0.03	0.00	0.02	0.05	0.03	0.02	0.00	0.03	0.05	0.00	0.66	0.01	0.03	0.00	0.02	0.00	0.00	0.01	0.00
Al2O3	15.94	16.17	15.12	15.35	16.12	12.26	12.24	12.38	11.80	12.38	2.36	6.56	19.79	18.36	18.58	19.64	18.96	20.02	17.58	18.33	20.36	18.39	17.87
TiO2	0.11	0.14	0.08	0.19	0.10	0.11	0.12	0.13	0.10	0.07	0.18	0.15	0.05	0.02	0.03	0.03	0.08	0.03	0.05	0.08	0.04	0.08	0.05
Cr2O3	50.05	49.17	49.69	48.90	48.51	54.13	53.96	54.51	54.03	54.04	62.39	46.43	48.70	48.71	42.19	48.64	48.83	49.65	48.63	47.99	45.57	48.92	49.59
FeO	25.22	25.39	24.23	27.85	25.98	24.47	23.96	25.05	25.50	25.13	28.60	40.09	22.04	22.74	29.24	21.41	21.28	21.13	24.92	24.25	24.64	22.86	21.49
NiO	0.05	0.00	0.00	0.00	0.03	0.00	0.04	0.06	0.00	0.04	0.07	0.06	0.02	0.05	0.03	0.05	0.07	0.01	0.07	0.05	0.03	0.08	0.04
MnO	0.45	0.49	0.46	0.49	0.59	0.46	0.52	0.47	0.48	0.49	0.64	0.52	0.47	0.49	0.43	0.34	0.41	0.39	0.54	0.44	0.53	0.43	0.46
MgO	7.81	7.13	8.27	5.96	6.83	7.46	7.49	7.36	6.94	7.13	4.15	4.18	9.77	8.42	8.86	10.66	9.64	10.31	6.77	7.50	7.52	8.29	9.43
CaO	0.02	0.00	0.02	0.00	0.01	0.00	0.01	0.00	0.02	0.00	0.02	0.00	0.06	0.01	0.04	0.02	0.05	0.00	0.03	0.02	0.03	0.04	0.03
Na2O	0.00	0.01	0.09	0.03	0.00	0.00	0.02	0.09	0.01	0.04	0.00	0.11	0.04	0.04	0.00	0.15	0.01	0.10	0.00	0.07	0.06	0.00	0.08
K2O	0.00	0.00	0.00	0.00	0.01	0.01	0.00	0.02	0.00	0.01	0.01	0.01	0.00	0.00	0.00	0.00	0.01	0.01	0.01	0.00	0.02	0.00	0.00
ZnO	0.64	0.60	0.59	0.75	0.70	0.34	0.30	0.42	0.20	0.34	0.33	0.51	0.40	0.39	0.37	0.26	0.30	0.24	0.44	0.46	0.55	0.28	0.36
Total	100.31	99.24	98.61	99.54	98.90	99.24	98.68	100.55	99.10	99.67	98.74	98.66	101.39	99.23	100.44	101.19	99.63	101.89	99.05	99.18	99.33	99.38	99.40
Cation	4 oxygens																						
Fe total	0.71	0.72	0.69	0.80	0.75	0.71	0.70	0.71	0.74	0.72	0.89	1.26	0.59	0.63	0.81	0.57	0.56	0.63	0.71	0.68	0.69	0.63	0.60
Fe*	0.70	0.71	0.69	0.79	0.74	0.70	0.69	0.71	0.74	0.72	0.88	1.25	0.59	0.63	0.81	0.57	0.56	0.62	0.70	0.67	0.68	0.63	0.59
Fe2+	0.62	0.65	0.59	0.70	0.66	0.63	0.62	0.63	0.65	0.65	0.78	0.81	0.54	0.59	0.58	0.50	0.52	0.55	0.67	0.63	0.64	0.60	0.55
Fe3+	0.08	0.07	0.10	0.09	0.08	0.07	0.07	0.07	0.08	0.07	0.11	0.44	0.05	0.04	0.22	0.07	0.04	0.08	0.04	0.04	0.05	0.03	0.05
TiO2	0.11	0.14	0.08	0.19	0.10	0.11	0.12	0.13	0.10	0.07	0.18	0.15	0.05	0.02	0.03	0.03	0.08	0.03	0.05	0.08	0.04	0.08	0.05
Cr#	0.68	0.67	0.69	0.68	0.67	0.75	0.75	0.75	0.75	0.75	0.95	0.83	0.62	0.64	0.60	0.62	0.62	0.63	0.65	0.64	0.60	0.64	0.65
Mg#	0.38	0.35	0.41	0.30	0.34	0.37	0.38	0.37	0.35	0.36	0.22	0.22	0.46	0.41	0.42	0.50	0.48	0.46	0.33	0.37	0.36	0.40	0.46
Cr3#	0.65	0.65	0.65	0.65	0.64	0.72	0.72	0.72	0.72	0.72	0.90	0.65	0.61	0.63	0.54	0.60	0.61	0.60	0.64	0.62	0.59	0.63	0.63
Al3#	0.31	0.32	0.30	0.30	0.32	0.24	0.24	0.24	0.24	0.25	0.05	0.14	0.37	0.35	0.35	0.36	0.37	0.36	0.34	0.36	0.39	0.35	0.34
Fe3+3#	0.04	0.03	0.05	0.04	0.04	0.04	0.03	0.04	0.04	0.04	0.05	0.21	0.03	0.02	0.11	0.03	0.02	0.04	0.02	0.02	0.02	0.02	0.02

Table 4.4 Representative microprobe analyses of chromian spinels in ultramafic rock from Sra Kaeo.

CHAPTER V

INTERPRETATION

5.1 Geochemical Correlation Diagram

To determine tectonic setting of ultramafic origin for individual areas in Thailand, we applied standard variation diagrams. Relationship between chrome partition, magnesium partition, contents of titanium oxide and partition of trivalent cations, such as Cr^{3+} #, Al^{3+} # and Fe^{3+} #, were plotted on standard diagrams. In addition, the Cr # and Mg # values are compared with those of Haggerty (1976) (see Figure 5.5).

5.1.1 Chiang Rai Area

Plots of Cr # and Mg # indicate that more than 90 % were systematically distributed in Alpine-type peridotite field (Irvine, 1974) (Figure 5.1). Only 3-4 grains were located in a field of stratiform complex. Figure 5.1 shows that the same elemental partitions were plot in the mutual portions of the peridotite field. However, as in Figure 5.2 for the Cr #- TiO_2 diagram (Figure 5.2), the plots fall within the fore-arc tectonic setting. The triangular diagram of Fe^{3+} - Cr^{3+} - Al^{3+} contents indicates that the Chiang Rai spinel is mostly located in the Alpine-type peridotite field.

5.1.2 Nan-Uttaradit

Nan-Uttaradit spinels have wide range of chrome partition (0.3-0.8) but low range of magnesium partition (0.25-0.45) (Figure 5.3). Although half of the data are applied within the stratiform-complex field and the other half are located out side diagram fields. However, this characteristic indicates subsequence fractional crystallization under less differentiation environment. Moreover, it is likely that the overall trend follows or is almost parallel to the Alpine-peridotite trend. TiO_2 contents show obviously high expansion in the Cr #- TiO_2 diagram (Figure 5.4) and are splitted into two subfields (blue solid stars present data from Panjasawatwong, 1991). However both subfields indicated island arc setting, similar to the Cr#-Mg# relation of Haggerty diagram (Figure 5.5). It is considered that a wide Cr # suggest the alpine peridotite occurring in island arc setting.

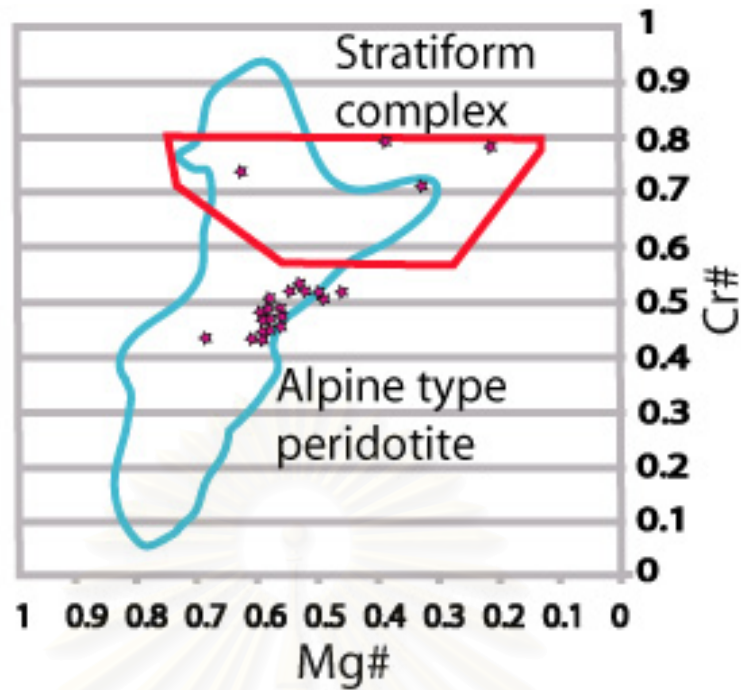


Figure 5.1 Cr# and Mg# plots of spinels from Chiang Rai mostly within Alpine type peridotite and some in stratiform complex field of ultramafic bodies (Irvine, 1974).

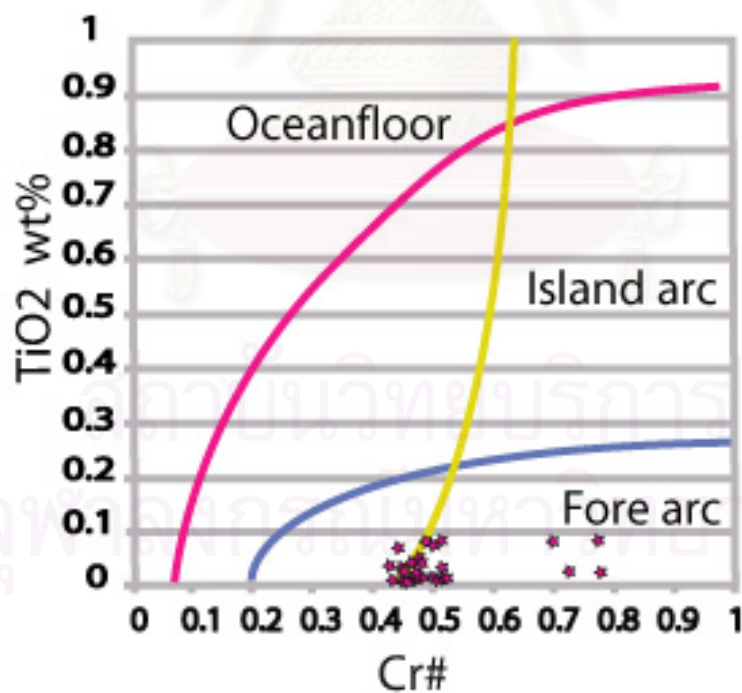


Figure 5.2 Cr#-TiO₂ relationship of chromian spinels from Chiang Rai mostly indicating fore-arc setting field (modified from Arai, 1992 and Charusiri 2000).

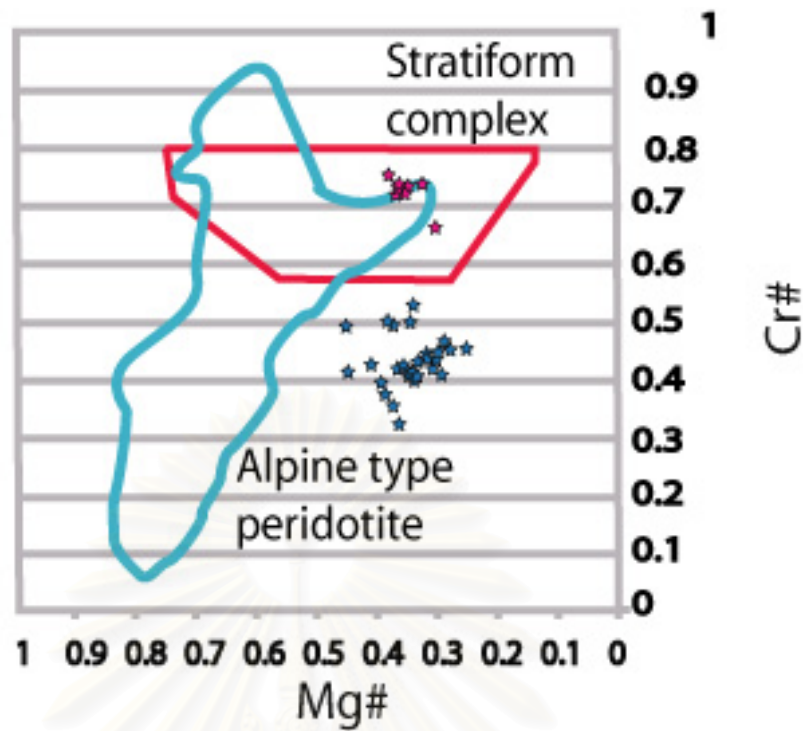


Figure 5.3 Cr# and Mg# plots of spinels from Nan-Uttaradit mostly outside but close to Alpine type peridotite with some minor stratiform complex ultramafic bodies (Irvine, 1974).

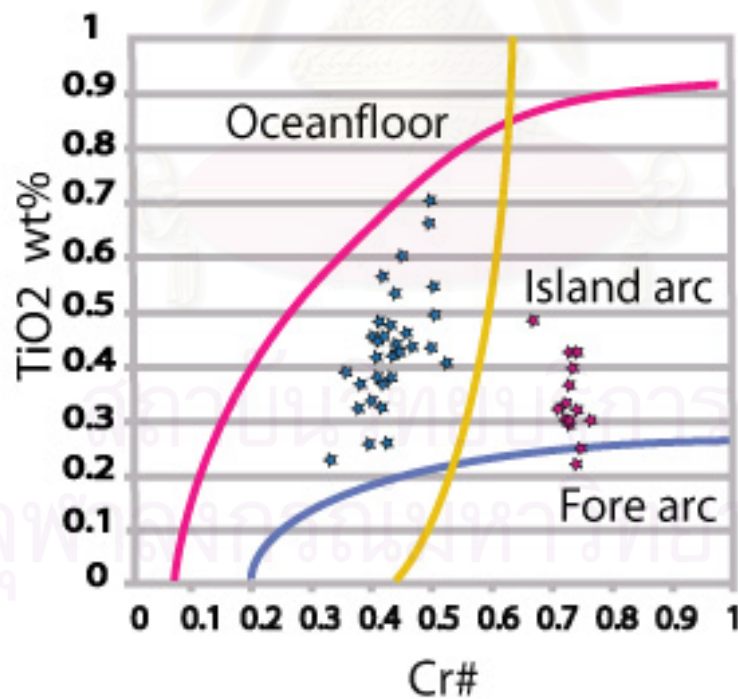
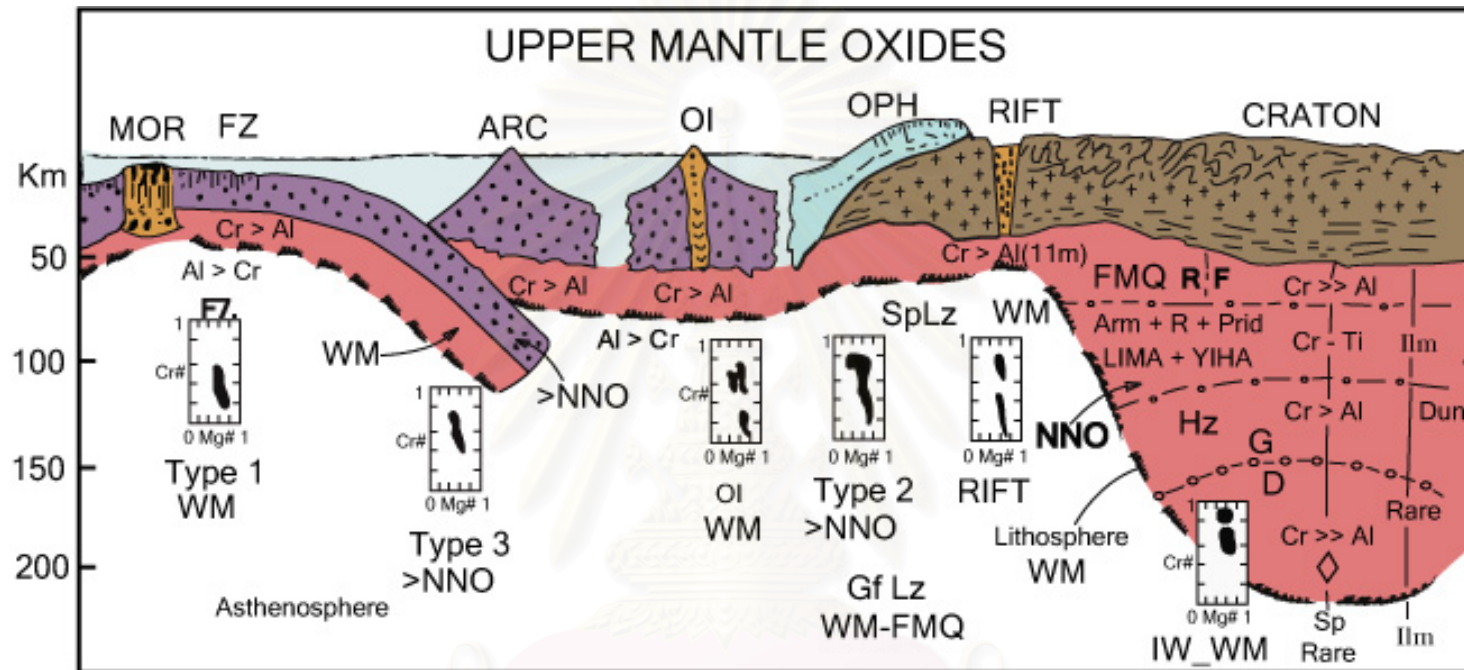


Figure 5.4 Cr#-TiO₂ relationship of chromian spinel from Nan-Uttaradit mostly within the island-arc tectonic setting field (modified from Arai, 1992 and Charusiri, 2000).



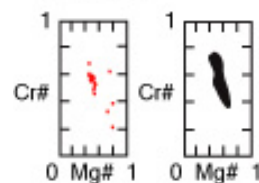
Type 1 : Mid Oceanic Ridge

Type 2 : Ophiolite Suite

Type 3 : Island Arc

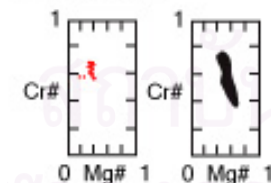
OI : Oceanic Island

Chiang Rai



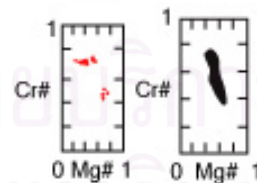
Type 3

Nan-Uttaradit



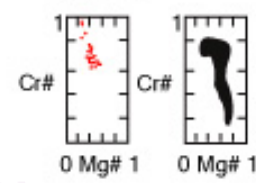
Type 3

Loei



Type 3

Sra Kaeo



Type 2

Figure 5.5 Cr# and Mg# plot of spinels from Thailand (left with red dots) in comparison with several models of spinel in ultramafic origin (black in right diagrams) from different tectonic setting (Haggerty, 1976).

5.1.3 Loei Area

As shown in Figure 5.6 Cr # and Mg # partitions of two narrow groups are observed. The first group was plotted in the field of Alpine type peridotite and the second was plotted in an area of stratiform complex. Mg # and Cr # plots also indicated two fields of igneous magma -one in the cumulate and the other in the harzburgite field. The graph of TiO₂ contents plotted against Cr # (Figure 5.7) indicate also two fields of plots -one in the fore arc setting and the other belonging to the island arc setting. Even though most values were located in area of arc setting, Also curve shape and a distribution pattern of Cr#-Mg# were resemble type III (subduction) and rifting setting of Haggerty (1976) (Figure 5.5).

5.1.4 Sra Kaeo

Chrome partition of Sra Kaeo approximately 80 % align in stratiform complex trend (Figure 5.8), the rest of the data falls outside the stratiform complex field. The Cr # and Mg # plots (Figure 5.11) indicate that spinels belong to cumulates field. In Haggerty diagram field of ophiolite (type II) should be suitable with their chemistry. Considering relationship of Cr# and TiO₂ (Figure 5.9), it is suggested that the values fall within the field of fore arc setting. The variation of Cr³⁺-Al³⁺-Fe³⁺# indicates the spinel plotting in the field of stratiform. So the chemical data of this area should be only a part belongs to fore arc obduction and effected later or generated by subduction.

5.2 Petrographic interpretation

To better understand chromian spinel host rock type in high weathering and alteration influence zone. Combinations between several factors are essential. Based on the basic model of ultramafic origin Arai, 2002, ultramafic rocks are divided into two main groups (Figure 3.3). The first group is called, restite or residual peridotites which leave part in magma chamber. These are produced from partial melting of mantle materials in the upper mantle. The second group is a differentiated liquid part (primary magma) from melting that move upon fractionation and form ultramafic cumulate layers. Ultramafic rock types in residual peridotite part are dominated by harzburgite and lherzolite. Ultramafic rocks in silicate cumulate generally show layered structures upon

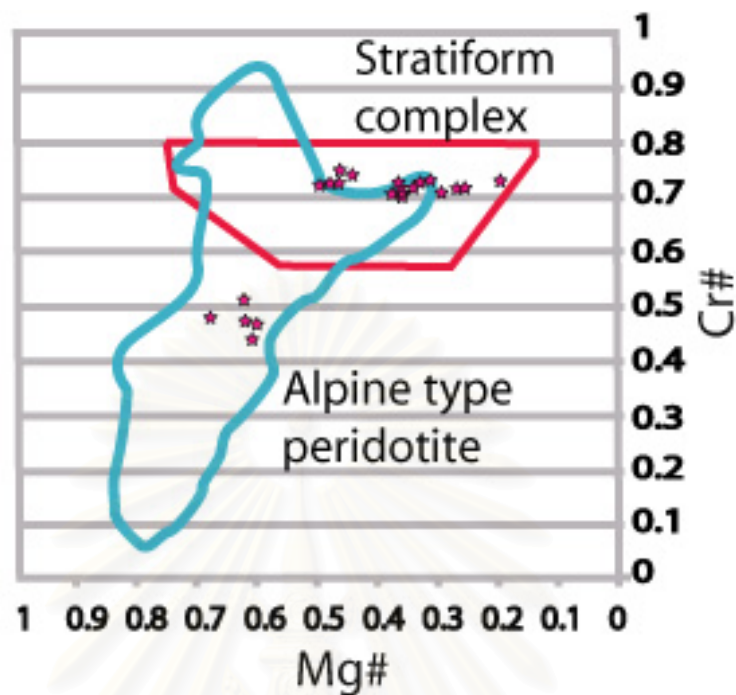


Figure 5.6 Cr# and Mg# plots of spinels from Loei mostly within the stratiform complex and some in Alpine-type peridotite ultramafic bodies (Irvine, 1974).

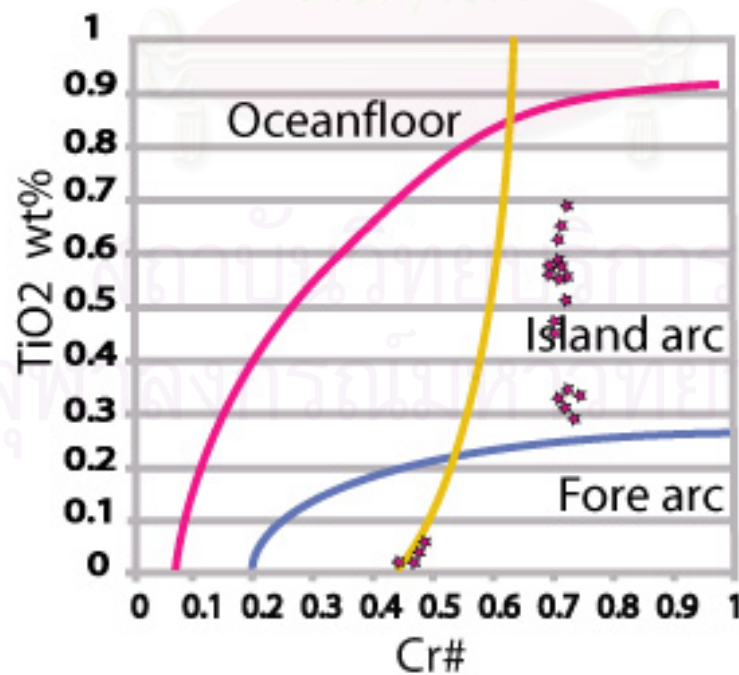


Figure 5.7 Cr#-TiO₂ relationship of chromian spinel from Loei mostly within the island-arc field and some in fore-arc tectonic setting field (modified from Arai, 1992 and Charusiri, 2000).

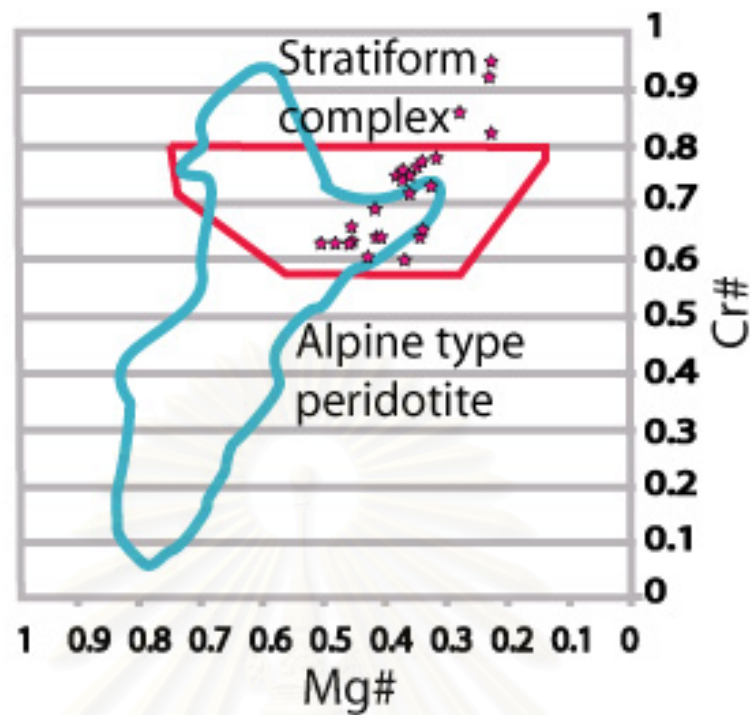


Figure 5.8 Cr# and Mg# plots of spinels from Sra Kaeo almost all within the Alpine-type peridotite and stratiform complex bodies, only few are outside these two fields (Irvine, 1974).

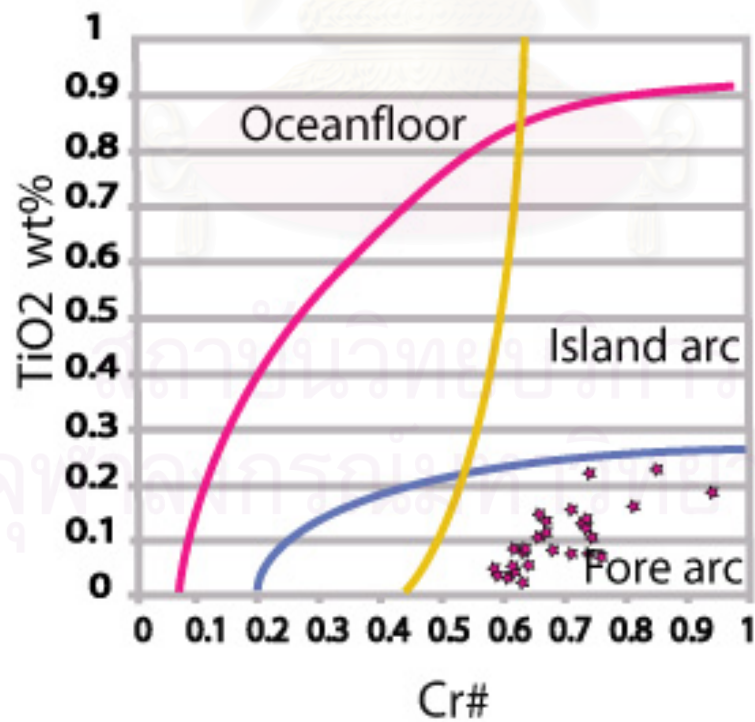


Figure 5.9 Cr#-TiO₂ relationship of chromian spinels from Sra Kaeo mostly located within fore-arc tectonic setting field (modified from Arai, 1992 and Charusiri, 2000).

Morphological and chemical variations of chromian spinel

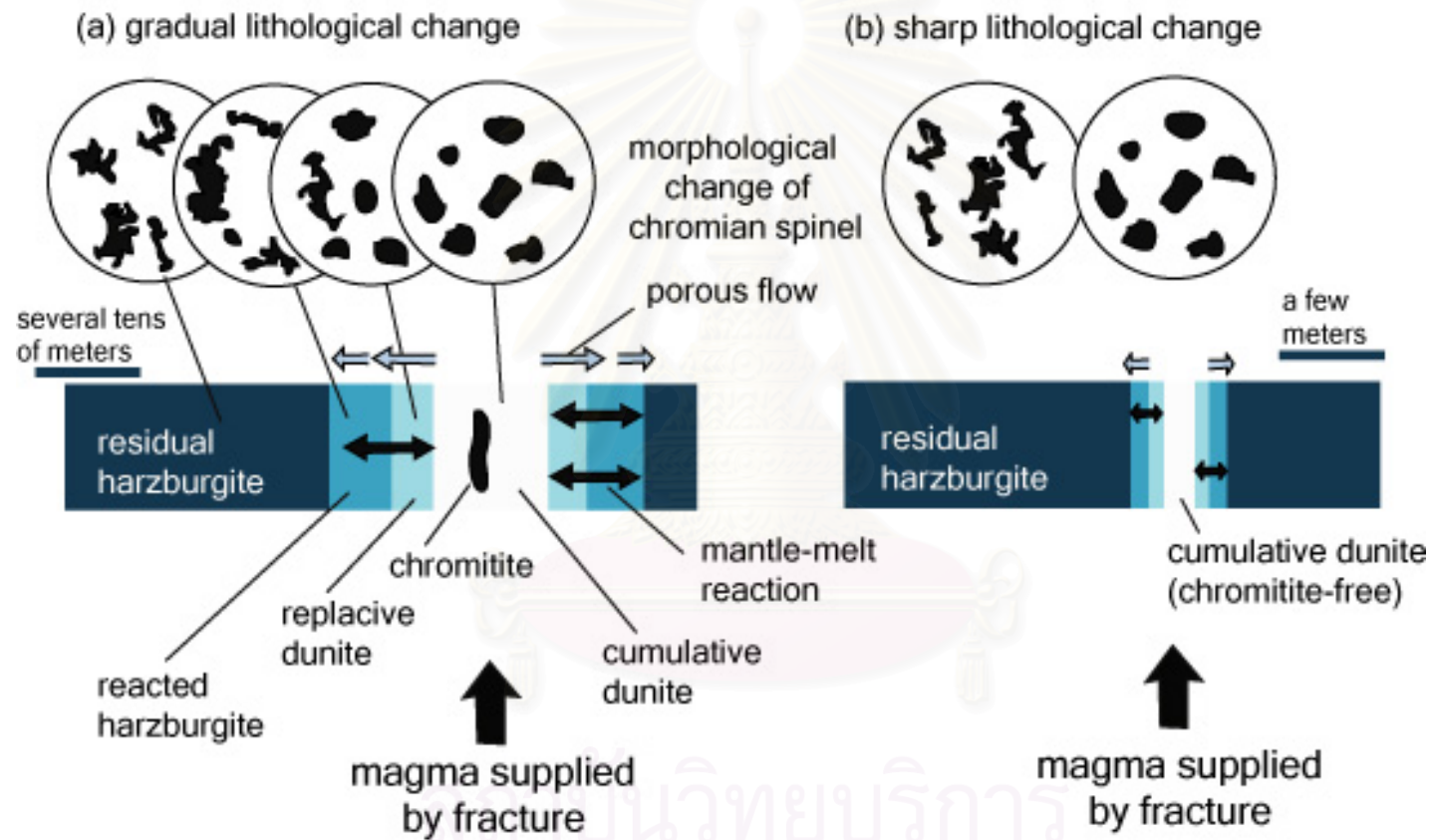


Figure 5.10 Schematic diagrams to show relationship between morphological change of chromian spinel and lithological variation due to mantle/melt interaction (Matsumoto and Arai, 2001).

fractionation and crystallization in crust. Order of rock types from lower to upper sequences are peridotite±dunite±chromitite, pyroxenite, and gabbro. The late stage liquid part which is remained in fractionation in turn becomes secondary magma and moves up to shallow part in the crust. Secondary magma will cool down to form any kind of mafic extrusive rock such as dolerite and basalt.

Arai and Matsumoto (2001) provided the relationship of chromian spinel (morphological change) and its ultramafic host rocks (lithological variation) (Figure 5.10). Spinel in residual peridotites invariably show irregular (vermicular) morphology to anhedral, but spinels in ultramafic cumulate layers frequently show good crystallinity which is indicated by almost subhedral to euhedral crystals. Cause of morphology variation is mainly due to crystallize in different condition. In deep residual peridotite, spinels are grown contemporaneously or very closed to partial melting time. A limited free space is considered as one controlling factor, so spinel crystallization has to follow the remained irregular and narrow spaces among mafic minerals. For cumulate layer chromian spinel can be extracted directly from secondary magma (completely liquid part). So the spinel crystal can grow without limited space boundary.

Chemical composition is the one important key to prove types of ultramafic host rocks. Based on relationship of several elements partitions, such as that of Pober and Faul (1988) classified chromian spinels in harzburgite and lherzolite host rocks from residual magmas and chromian spinels in ultramafic host rocks from cumulate layers. Trivalent cation of Cookenboo et al. (1997) which trivalent proportion of Cr^{3+} #, Al^{3+} # and Fe^{3+} are applied to distinguish fields of spinel compositions which occur in stratiform complex within abyssal peridotite, alpine type peridotite and Tulameen Alaskan type complex. From concept discussed above, we are able to conclude host rock types in each area below.

5.2.1 Chiang Rai Area

A relationship between Cr# and Mg# of Chiang Rai spinel were plotted in an overlap zone between the upper part of lherzolite and the lower part of harzburgite (Figure 5.11). Exception is for few grains that were located in areas of cumulate. This clearly presents in trivalent partition plot of Cookenboo et al. (Figure 5.12). Morphology

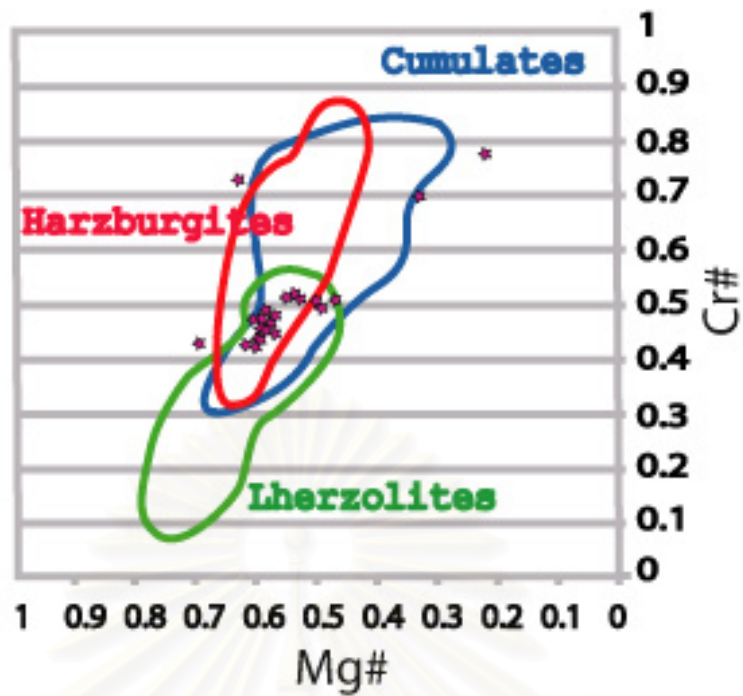


Figure 5.11 Cr# and Mg# plots of spinels from Chiang Rai showing plots in the compositional fields of lherzolite, harzburgite, and cumulate of spinels from ultramafic rock types (Pober and Faupl, 1988).

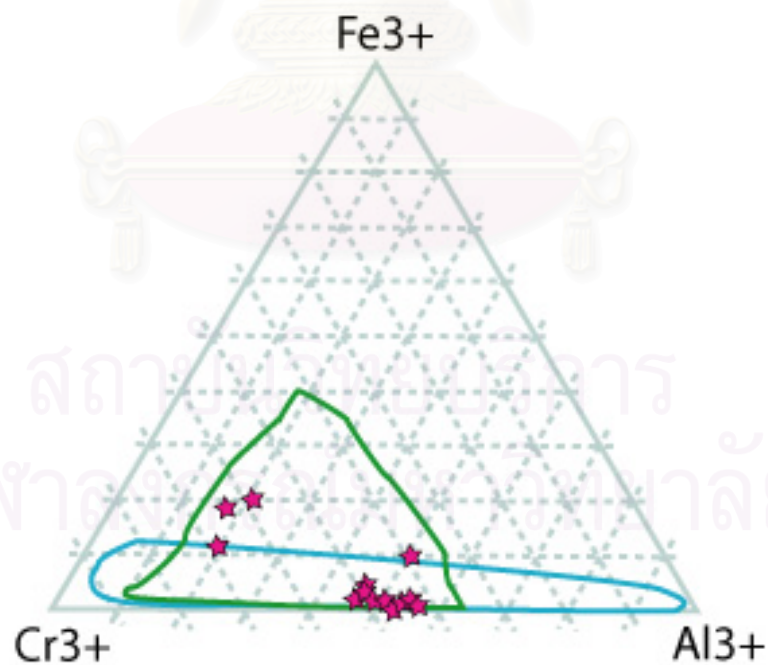


Figure 5.12 Trivalent partition plot of spinels from Chiang Rai showing trivalent plot mostly in arc setting (Cookenboo et al., 1997).

and chemical composition of spinels can support one another. Most of spinels which compositions plotted widely in the lower part of Alpine type peridotite have irregular grain shape in host rocks containing pyroxene relicts. This suggests that the ultramafic host rock of this area is residual harzburgite. The other few spinels with good crystallinity show their composition located in the upper part of stratiform complex field. These spinels also have large subhedral crystal faces and Fe^{3+} # higher than that of the first group. The ultramafic host rock of this group is ultramafic cumulate, although not dominant in population.

5.2.2 Nan-Uttaradit

For chemical data of the Nan-Uttaradit areas, we combined our spinel analysis data with those of Punjasawatwong (1991). Spinel of this area can be divided into two groups, the first is located in the upper part of cumulate field and the second they have quite similar the same Mg# as the first group but lower in Cr# and distribute in the right site out of the overlapping zone between cumulate field and lherzolite field in Pober and Faul (1983) (Figure 5.13) diagram. This second group also located around right site of stratiform rims in Cookenboo (1997) (Figure 5.14) diagram. Spinel here are mainly subhedral to euhedral and are very clean in an inner part of crystals. A dominant chemical composition occurs in stratiform boundary in Cookenboo plot. A homogeneous of serpentinite host texture, such as antigorite matrix and clinopyroxene relict, supported the idea that this ultramafic host rock should be dunite and wehrite in part of a cumulate layer.

5.2.3 Loei Area

Spinel from the Loei area can be subdivided into two groups based upon chemical compositions and diversity of morphology. The first spinel group is plotted on the upper part of cumulate field in Pober and Faul (1983) (Figure 5.15) diagram and shows large cumulate at the left lower field and extend to middle part of stratiform field in Cookenboo et al. (1997) (Figure 5.16) diagram. This spinel group has almost the similar crystal size, and is mainly subhedral-euhedral crystals disseminated in dominant antigorite matrix and associated with well distributed olivine relicts. The ultramafic host

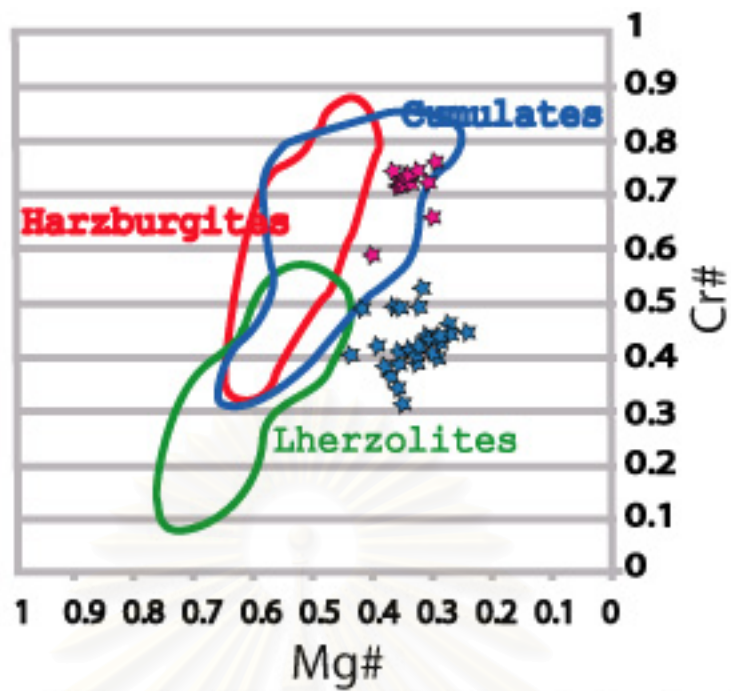


Figure 5.13 Cr# and Mg# plots of spinel from Nan-Uttaradit showing plots in the compositional fields of cumulates of spinels from ultramafic rock types (Pober and Faupl, 1988).

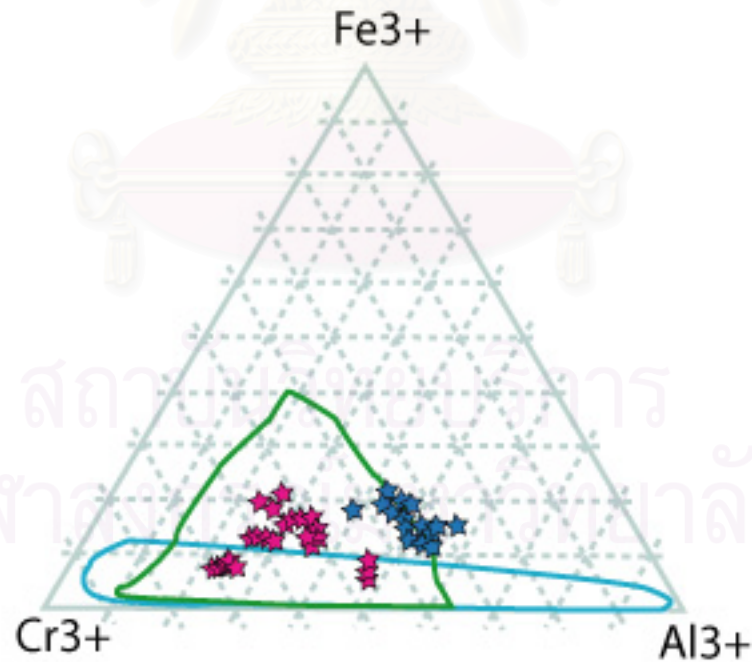


Figure 5.14 Trivalent partition plot of spinels from Nan-Uttaradit showing trivalent plot mostly in stratiform complex field (Cookenboo et al., 1997).

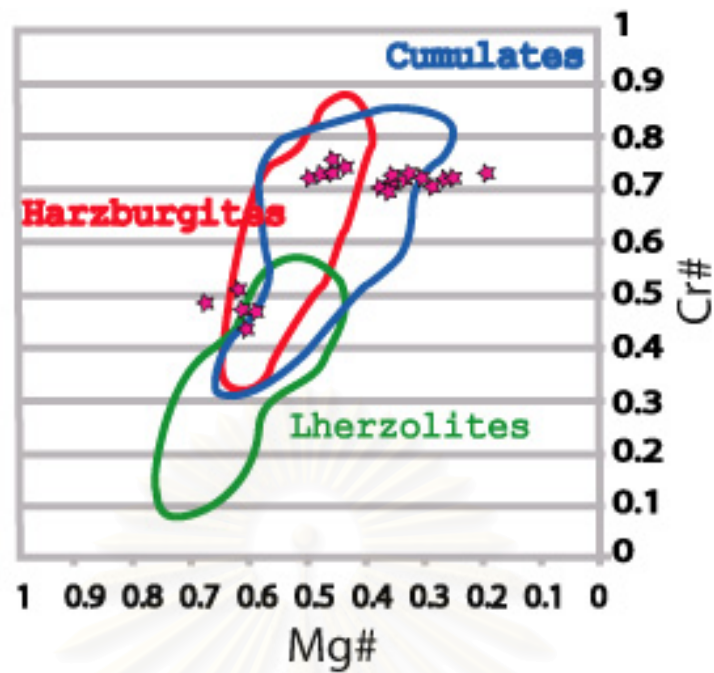


Figure 5.15 Cr# and Mg# plots of spinels from Loei showing plots in compositional fields of cumulates and some in harzburgite of spinels from ultramafic rock types (Pober and Faupl, 1988).

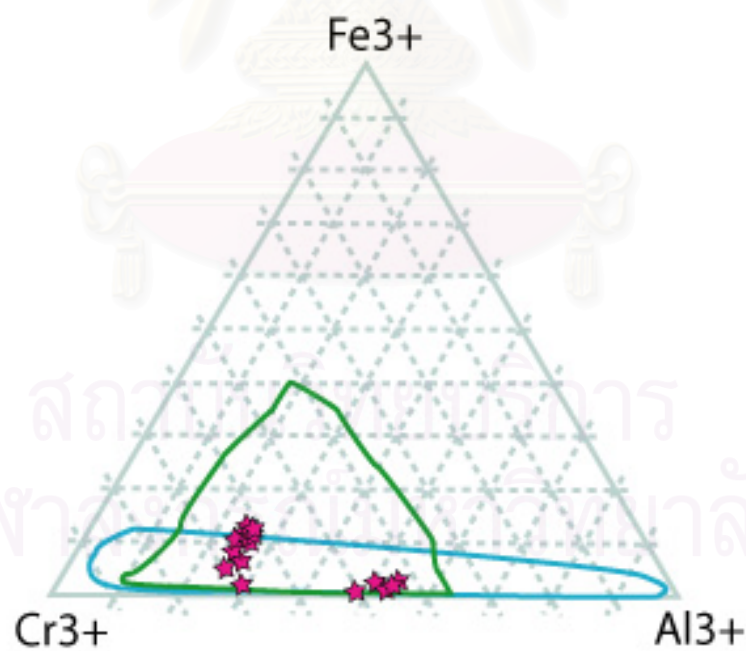


Figure 5.16 Trivalent partition plot of spinels from Loei showing trivalent plot mostly in stratiform complex and some in Alpine-type peridotite (Cookenboo et al., 1997).

rock of this area is considered as cumulate dunite. The other group, though not high amount, is located on right side of the harzburgite field rim in Pober and Faul (1983) (Figure 5.15) diagram and concentrates in a middle lower part of the Alpine type peridotite field in trivalent plot of Cookenboo. With its subvermicular morphology, multicrystal shapes and associated with orthopyroxene porphyroblast, we infer that ultramafic host rock of this group should be residual harzburgite.

5.2.4 Sra Kaeo Area

Most of spinel chemistry of Sra Kaeo area were plotted in cumulate field of Pober and Faul (1983) (Figure 5.17) diagram and located in the lower left of stratiform field in Cookenboo (1997) (Figure 5.18) diagram. Perhaps 2-3 grains were plotted in Alpine type peridotite boundary. Subhedral to euhedral spinel and well-defined crystal faces are normally characteristic in this area. High diversity in grain size and shape are vary, characteristic and reduced degree of origin in ultramafic cumulate layer. Considering serpentinite host rocks, we found sharp orthopyroxene porphyroblast disseminated in antigorite mesh without the appearance of olivine relict. This texture can be orthopyroxenite or harzburgite. We explain this as a transition zone between an upper part of residual peridotite and a lower part of cumulate layer in the magma chamber. This perhaps makes a difficulty in recognizing residual or cumulate in transition by texture only. Basically a general conclusion for this area is that, ultramafic host rocks may be cumulated orthopyroxenite or residual harzburgite, but a lower part of ultramafic cumulate, is also quite possible.

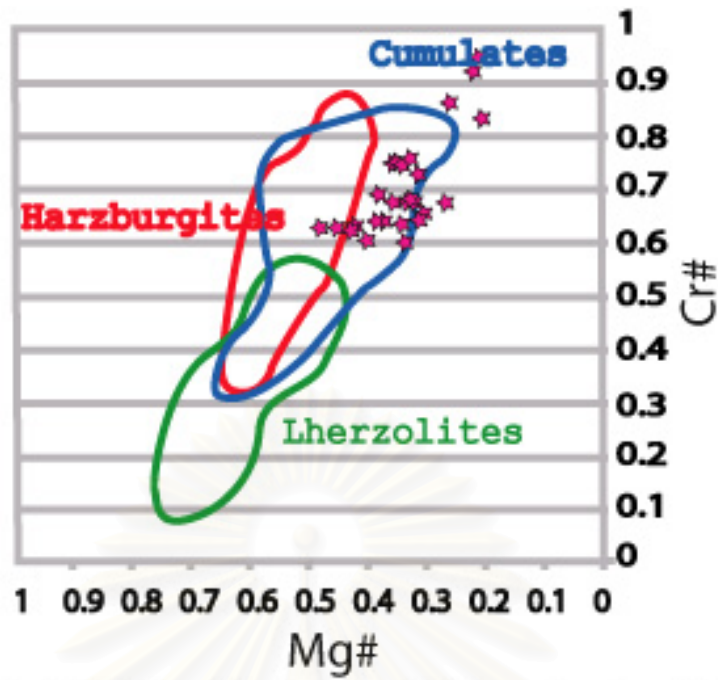


Figure 5.17 Cr# and Mg# plots of spinels from Sra Kaeo plotted mostly in cumulates field on compositional field of spinels from ultramafic rock types (Pober and Faupl, 1988).

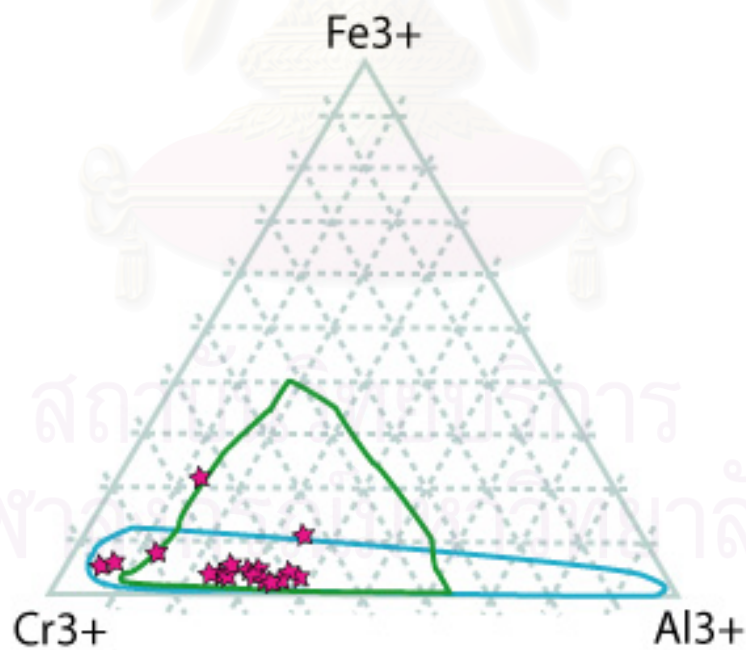


Figure 5.18 Trivalent partition plot of spinels from Sra Kaeo showing trivalent plot mostly in overlap zone between stratiform complex and Alpine-type peridotite (Cookenboo et al., 1997).

CHAPTER VI

DISCUSSION

6.1 Implication to tectonic setting

As stated in the previous chapter, both chemical and physical properties of chromian spinels can help in deciphering origin of ultramafic rocks that host spinels. Additionally chemical compositions of chromian spinels are able to indicate tectonic setting of ultramafic origin. These chemical controllers of spinel chemical proportion can be discussed below.

The Cr/Al ratio of Cr# [= Cr/(Cr+Al) atomic ratio of spinel] in residual peridotite depends largely on the degree of partial melting. The ratio of chromian spinel from the melt extracted from residual peridotite is changeable depending on degree of fractionation (or degree of magma solidification). The spinel crystallized first from the melt may have the same Cr# as that in residual peridotite but will change during crystallization process. Moreover, the Cr# may increase or decrease depending on the coprecipitating minerals. In general, the Cr# (and Mg#) will decrease as the degree of fractionation increase whereas Cr# will increase as the degree of partial melting increase. But the Cr# may increase if Si-rich mineral (garnet or plagioclase) coprecipitates with spinel (Arai, 2000). Similarly as shown in Figure 6.2, degree of partial melting increases as Cr³⁺ increase and Al³⁺ decreases. Like wisely, Fe³⁺ and Ti increases and Cr³⁺ decreases as the degree of fractionation increases.

The melting condition is changeable on the basis of difference in tectonic setting. Amount of water that can enhance the degree of partial melting of peridotite is available at the arc setting. Basically, the degree of partial melting may be relatively high at intraplate setting (or around mantle plume) and is relatively low at mid oceanic ridge setting (Arai, 2003). The composition of peridotite is one of the essential factors that inform geochemical source. In general peridotite is relatively poor in Ti at arc setting and is always high in Ti at intraplate setting (Arai, 2003) (Figure 6.3).

As stated earlier, different tectonic setting generated chemical variation of spinels and different rocks assemblages. Because geological mechanism directly concerns about degree of partial melting, pressure, temperature and peridotite source

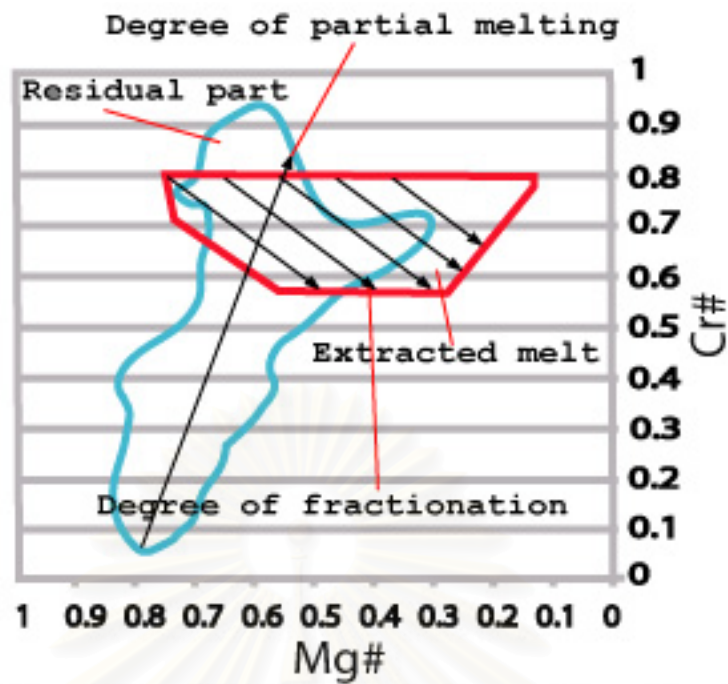


Figure 6.1 Variation of Cr# and Mg# in spinels during partial melting of mantle materials and during fractionation of extracted melt (primary magma). Arrows present trend of chemical variation.

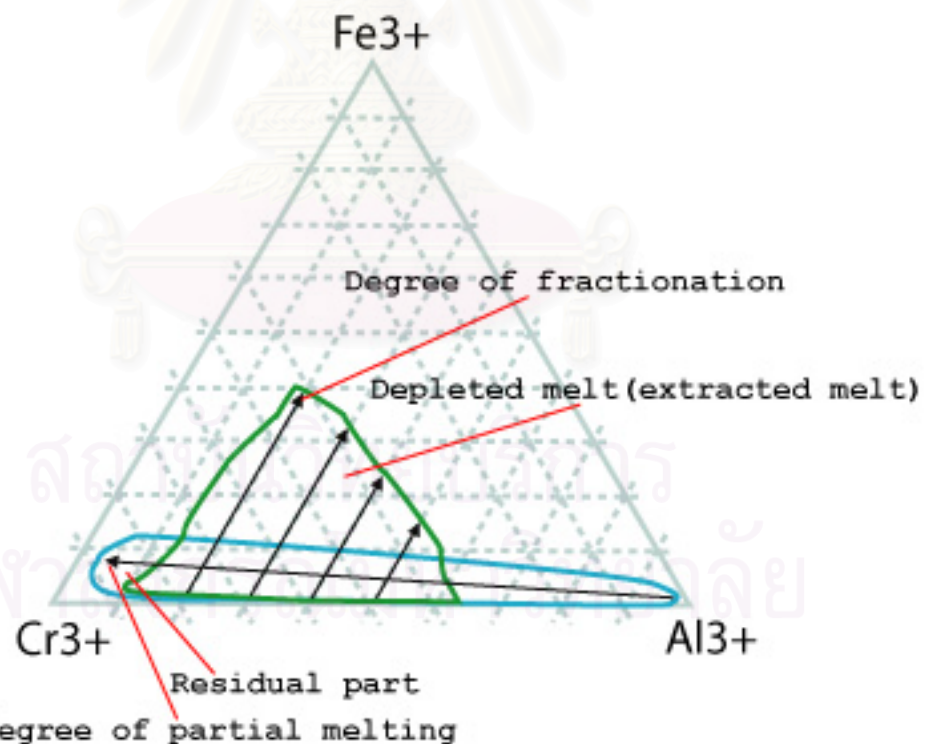


Figure 6.2 Variation of trivalent partition in spinels during partial melting of mantle materials and during fractionation of extracted melt (primary magma). Arrows present trend of chemical variation.

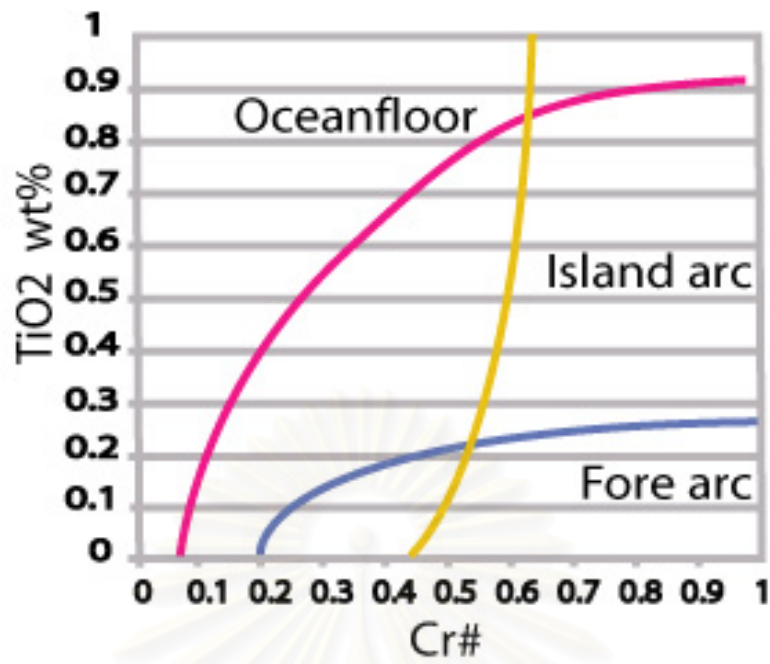


Figure 6.3 Relationship of Cr# to TiO₂ contents of mafic and ultramafic origins for the classification of tectonic setting (after Arai, 1992).



Figure 6.4 Diagram showing ranges of Cr# of spinel in peridotites from different tectonic settings. The heavy-line represents the majority of data plots.

character. The uppermost mantle is dominated by peridotite which harzburgite and lherzolite are the main rock types. Dunite, wehrlite, and eclogite may constitute part of the upper mantle. There are two main peridotite subtypes (Boudier and Nicolas, 1985 and Nicolas, 1986). The harzburgite subtype is associated with ophiolites and represents depleted mantle rock that underlies fast-spreading ridge. The lherzolite subtype, less depleted and less common in ophiolites, characterizes mantle diapir and slow-spreading ridges. Dunite and chromite pods, dikes, and layers are largely confined to the upper (near crust) part of the harzburgite subtype. A quite different range of composition in term of Cr# variation for the spinel of the less depleted lherzolites compared to the harzburgite that represent the different degree of partial melting. The depleted residual mantle peridotite that formed after the separation of basaltic (or mafic) liquid usually has harzburgite character (high degree of partial melting). On the other hand, lherzolite character normally derived from low degree of partial melting.

6.1.1 Abyssal peridotite

Abyssal peridotites are defined as peridotites of the actual oceanic crust, mainly generated at mid-oceanic ridges. They are usually interpreted as residuals of mantle, suggesting partial fusion and magma genesis (Dick and Bullen, 1984). Chrome spinels of these peridotites are limited by Cr# value of 0.6 and low or negligible TiO₂ contents (< 0.25 wt %).

6.1.2 Fore-arc peridotites

In the supra-subduction zone the upper mantle is dominated mainly by harzburgites, and the transitional zone between crust and mantle by dunite (Arai, 1994). Spinel in the fore-arc peridotite normally have Cr# ranging from 0.4 to 0.9, most frequently around 0.7 (Bloomer and Fisher, 1987). In addition, Mg # is negatively correlated with the Cr#, and Fe³⁺ # is very low, usually less than 0.1.

6.1.3 Back-arc peridotites

Back-arc basin peridotites have been reported from peridotite xenoliths in the Japan Sea (Ishii, 1987) and from Circum-Izu Massif peridotites (Arai, 1991). Data on

these peridotites suggest that the back-arc basin mantle comprises refractory lherzolite and harzburgite and spinels from these rocks show Cr# ranging from 0.4 to 0.6 (Arai, 1991). These values are slightly similar to those of the abyssal peridotite but within a more narrow range.

6.1.4 Subcontinental peridotites

Subcontinental peridotites are reported from xenoliths in alkaline basalts erupted on continental rift zone (Nixon, 1987). Although spinels from these peridotites cover a wide range from 0.05 to 0.8, fertile lherzolites with Cr# < 0.2 are more abundant than other kinds of peridotites in the subcontinental upper mantle.

6.1.5 Alpine-type peridotites

Alpine-type peridotites are mostly emplaced into their present position tectonically rather than by magmatic intrusion. Many of alpine-type peridotite often occur in close spatial association with gabbro, diabase, greenstone and pillow basalt as the basal member of ophiolite complexes, while others do not form part of an ophiolitic assemblage. Considering the tectonic mode of ophiolite emplacement, the latter may be interpreted as a dismembered one, but they are some alpine-type peridotites which are associated with none of ophiolitic rock types (Dick and Bullen, 1984). Alpine peridotites are usually divided into two categories, harzburgite (ophiolitic) and lherzolite (root zone) subtypes (Den Tex, 1969, Jackson and Thayer, 1972). The harzburgite subtype often forms the basal peridotite member of the ophiolite suite, usually associated with subordinate amounts of dunite, lherzolite and chromitite. The lherzolite subtype makes lherzolite dominate masses usually free from the so-called ophiolitic igneous sequence. Chromian spinels from on land alpine type peridotites exhibit a wide range of Cr# from 0.08 to 0.95. Peridotite which have Cr# about 0.5 are also predominant. Partition values of spinels can indicate their source rock in his Cr# and Mg# diagram 6.1.6 Spinel composition and Tectonics. Irvine (1974) divided chrome-spinels into alpine type and stratiform type. Cr# and Mg# in diagram of Haggerty (1976) separated tectonic setting of ultramafic origin into 6 different regions: 1 mid-oceanic ridge peridotite, 2 subduction or arc peridotite, 3 oceanic Island peridotite, 4 ophiolite sequence, 5 continental rift

peridotite, and 6 peridotite on stable craton. Cr# and TiO₂ weight percent in Arai (1992) diagram divided 3 types of spinel ultramafic host origin: 1 island arc, 2 fore arc, and 3 intraplate (ocean-floor). Cr# diagram by Arai (1994) used only Cr# for classified peridotites from different tectonic setting such as abyssal peridotite, fore-arc peridotite, back arc peridotite, ocean hot spot, sub continental peridotite (rift zone) and on-land alpine peridotite (Figure 6.4). The last diagram is that of Cookenboo et al (1997) which provides 3 groups of chromian spinels in different tectonic setting based on Cr³⁺, Al³⁺ and Fe³⁺ proportion, 1 alpine-type peridotite, 2 stratiform complex and 3 Alaskan-type (equivalent to arc affinity with high water contain and high oxygen facucity).

6.2 Comparison with other well-studied areas

Though, all of standard diagrams are widespread and useful for defining tectonic setting, these diagrams are applied to spinels from selected areas where tectonic setting are well-defined (Figure 6.5). Approximately 106 spinel grains from ultramafic rocks including 40 grains from Sohar Oman, 16 grains from Davas Switzerland, 20 grains from Indus Tibet, and 30 grains from Song Ma Suture Viet Nam were determined for major and minor oxide analysis using EPMA. Spinel grains were analyzed under the same condition as sample from Thailand.

Tectonic settings of each area are described below. Sohar (Oman) ophiolite represents a paleo oceanic crust at a spreading ridge or ophiolite slab. It already had effected from continental subduction in a late state of geological mechanism. Davos (Switzerland) ophiolite fragment is a part of an ancient ocean. It prefers oceanic affinity and belongs to continental transition from adjacent distal continental margin. Indus (Tibet) ophiolite has been a paleo-ophiolite that has been also disturbed by continental collision. Song Ma (Viet Nam) ophiolite is represented by the really paleo subduction zone.

The results of physical and chemical investigations of individual areas are described along with their geological information.



Figure 6.5 Geographic map of Asia showing locations where spinel-bearing ultramafic rocks were collected.

6.2.1 Sohar, Oman

6.2.1.1 Geologic setting

The Oman Mountains form an arcuate coastal chain that extends from the Musandam peninsular in the northwest to the surrounding region in the southeast of Oman, with a total length of about 700 km, and a width between 50 and 140 km. The mountains are bounded to the northeast by the Gulf of Oman and the Batinah plain, and flanked to the south by pebbly desert plains extending as far as the sands of the Rub al Khali. The geology of this chain is dominated by the small, best-preserved ophiolite complexes.

The so-called Samail Igneous Rocks (Lee, 1928) is part of the Peri-Arabian ophiolite belt that was emplaced on the Arabian carbonate platform in the Campanian-Maestrichtian (Late-Cretaceous) as a result of intra-oceanic thrusting. Its emplacement was accompanied by high-grade amphibolite facies metamorphism that affected the sole of the nappe, starting at about 90 Ma. The ophiolite nappe was disrupted into contiguous tectonic blocks during thrusting over the Arabian Platform. In the central part, the ophiolitic blocks are disposed on either side of the northwest/southeast regional anticline whose core is occupied by Jabal Akhdar and the Hawasina window. To the northeast are the Wadi Sarami, Haylayn, Rustaq blocks and to the southwest the Wuqbah, Maqniyat, and Bahlsa blocks. The outcrops of serpentized harzburgite at Jabal Misht and Jahm al Jubayl preserve former connections between the two groups of blocks. In the southeastern part, bounded to the west by the Samail Gap, are the large Samail and Samad blocks and the smaller Al Khawdh and Masqat blocks.

The composite structure of the volcanic units and the spatial organization of the hypabyssal dolerite dykes and successive plutonic sequences argue in favour of polyphase ophiolitic magmatism. As in most other ophiolites, two main magmatic stages are explained.

The first stage is characterized by products of early magmatism occurring throughout the chain and is related to the main stage of sea-floor spreading. They are composed, from base to top, of ultrabasic and gabbroic cumulates, resting on the palaeo-Moho followed by the dyke complex and the volcanic formation. The second stage, resulting from the later magmatism, is present irregularly along the chain. Several

suites can be defined in this second magmatic stage, which thus appears itself to have been polyphase. It is represented by distinct plutons intruded at different level in the crust by dykes, many of which are picritic, and by volcanic rocks in two main formations. Magmatic activity apparently decreased from the first to the second stage in response to the progressive closure of the oceanic basin. The early magmatism is thus generally referred to as the main spreading (the axis set) event and the later magmatism to the arc set, formed in response to an evolving geotectonic environment. The late-stage magmatism was generated in a more depleted mantle than the early magmatism and is more generally contaminated by subduction-related components in the source.

Le Me'tour et al. (1989) separated the geodynamic evolution of the Samail Nappe into 3 stages below.

- 1) Creation of new oceanic crust at a spreading ridge (first stage magmatism) within a basin that opened in pre-existing Neo-Tethyan lithosphere, probably induced by sinistral slip between the Eurasian and African continents.
- 2) Immediately after this short spreading phase, second-stage magmatism produced volcanic rocks and plutonic intrusive bodies that cut the newly created oceanic crust. Products of this late magmatic activity were emplaced preferentially along pre-existing faults in the early crust. Ceuleneer et al.(1989) emphasize the relationships between movement on north-south subvertical faults, related to the initiation of obduction, and the injection of late intrusives. Their geochemical characteristics, which are typical of forearc magmatism, lead to the hypothesis of northeastward subduction of the older Neo-Tethys crust beneath the juvenile oceanic crust of the Samail Nappe. This new dynamic system is seen as related to increasing convergence between Eurasia and Africa.
- 3) Intra-oceanic detachment at the boundary between the young and old oceanic lithospheres.

6.2.1.2 Chromian spinel

Spinel from the Oman ophiolite is generally subhedral-euhedral and reddish brown color, the average size is about 0.3 mm. Most spinel crystals are euhedral and

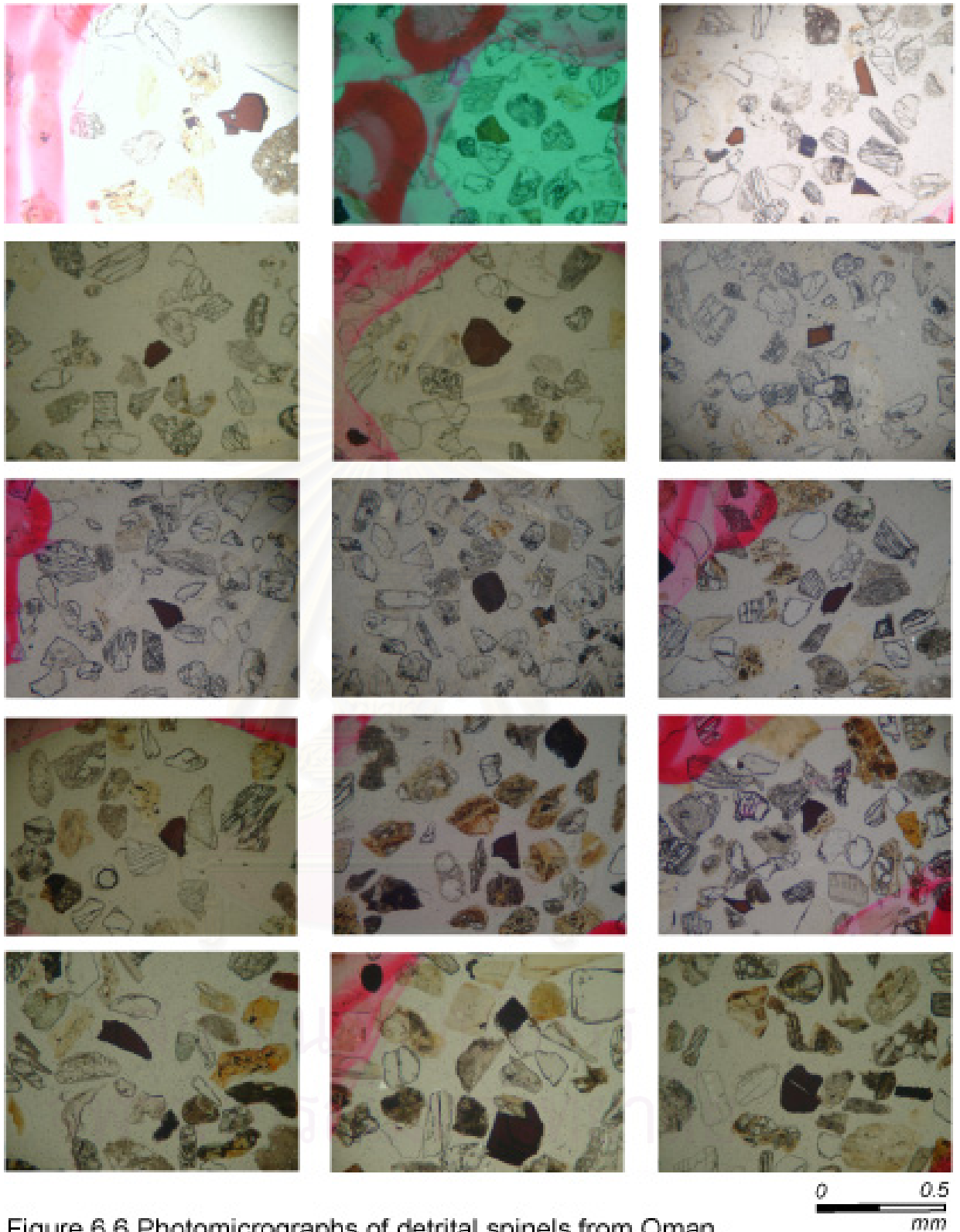


Figure 6.6 Photomicrographs of detrital spinels from Oman.

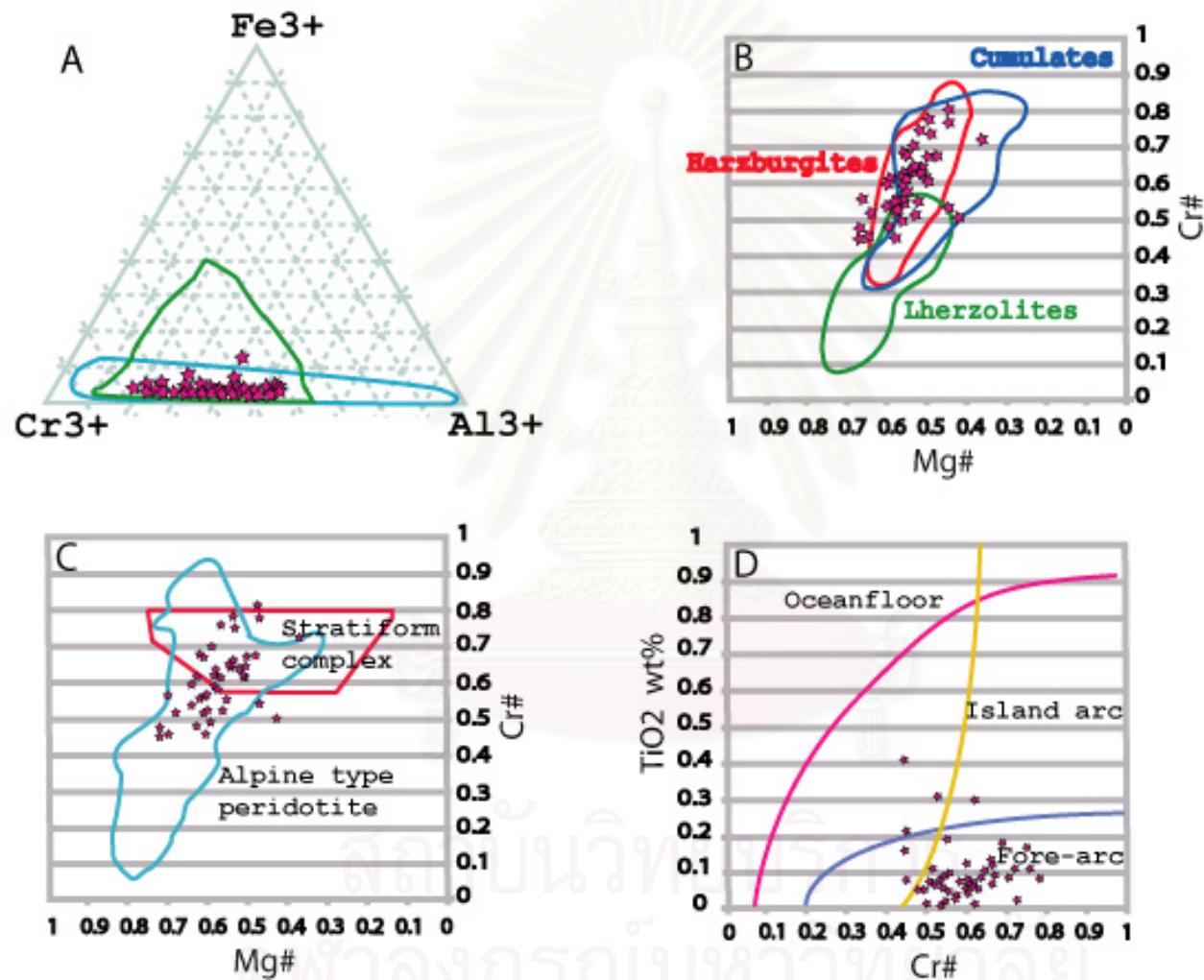


Figure 6.7 Chemical relation plots of spinels from Oman. A) Ternary plot of the major trivalent cation, B) $Cr\#$ and $Mg\#$ plot on compositional field of spinel from ultramafic rock type, C) $Cr\#$ and $Mg\#$ relation plot with Alpine type peridotite and stratiform complex ultramafic bodies, and D) $Cr\#$ - TiO_2 relationship compared with tectonic-setting field.

subhedral (Figure 6.6). Cr# and Mg# plot indicates that the spinel host rocks are harzburgite which generated from lower part of ultramafic cumulate in ophiolite sequence (Figure 6.7). Based on their physical and chemical characteristics, fractional crystallization is the dominated magmatic process. The tectonic setting is likely to be related to oceanic subduction. Cr# and TiO₂ % plot suggests that spinels from Oman Ophiolite are subduction- related rather than belonging to ocean floor. These lines of physiochemical evidences supported the geologic interpretation from the field survey.

6.2.2 Davos, Switzerland

6.2.2.1 Geologic setting

Based on the study of Bernoulli et al. 2001, the geology and tectonic interpretation are discussed below. In eastern Switzerland, ophiolitic fragment (part of ocean floor) and associated oceanic rocks are preserved in the south – Pennine platta nappe in the Aroza zone, a highly complex zone comprising imbricates derived from an ancient ocean–continent transition and form the adjacent distal continental margin. The platta nape nappe and the Aroza zone are sandwiched between the Middle Pennine and Austroalpine nappes which are derived from the northwestern and the southeastern margin of the alpine segment of the Tethys ocean, respectively. Along the upper and lower boundaries of Aroza zone as well as within the zone, tectonic – mélanges are widespread within the Aroza zone. The Totalp imbricate near Davos shows the clearest relationship between the basement of the ocean – continent transition and the overlaying oceanic sediments. In the Tatalp imbricate, only traces of possibly Mesozonic igneous rocks are observed. However, in the platta nappe to the south, gabbros intruded the already serpentinized mantle rocks at shallow depth 161 Ma ago. Basaltic flows and pillow lavas stratigraphically overlie the exhumed subcontinental mantle rocks and the tectonic sedimentary breccias relate to the exhumation of both mantle rocks and gabbros. Gabbros and basalts are derived from an asthenospheric MORB – type source and appear to document the onset of sea – floor spreading across and exhumed subcontinental mantle during the earliest evolutionary stage of a slow-spreading ridge.

The major part of the Totalp serpentinite is a variable serpentinized lherzolite (where our samples were collected) with narrow pyroxenite dike. Peridotite–mylonites

indicate deformation at mantle depth which is possibly related to a pre-Mesozoic event. $^{40}\text{Ar}/^{39}\text{Ar}$ dating result shows that the mantle rocks were uplifted to about 10 km depth in the late middle Jurassic. Initial serpentinization accompanied exhumation and deformation under decreasing temperatures during Jurassic rifting. This evolution is documented by serpentinite mylonites, deformed under greenschist facies conditions that were cataclastically deformed and partially calcitized under lower temperature. Differences in hydrogen isotope ratios between serpentinites and ophiocalcites suggest that serpentinization zones and to zone of ophiocalcite formation and continued during the Alpine orogeny.

6.2.2.2 Chromian spinel

Our petrographic determination on colour and shapes of spinels from Davos, Switzerland shows thermal alteration effect in some parts of grain (Figure 6.8). So host rocks type and tectonic setting may not be easily recognized. Coordinate between Cr# and Mg# is difficult to interpret because Al and Fe are sensitive with thermal effect.. Anyway TiO_2 and petrographic evidence found one important key around spinel grains. This point is the main key to explain why Cr# of this area that should very low but it prefer high. In chloritization water and thermal alteration were extract Al from spinel grained and use in reaction. This chemical mechanism reduced aluminar percentage in spinel so $\text{Cr}\# = \text{Cr}/(\text{Cr} + \text{Al})$ be higher than previous. In Cr# and TiO_2 weight percent diagram (Figure 6.9), all of plots are in the ocean floor field and island arc boundary. We therefore interpret that Davos spinel may have occurred in the ocean-floor setting and thermal effect of spinel was probably caused by subsequent ductile deformation.

6.2.3 Song Ma, Viet Nam

6.2.3.1 Geologic setting

The Song Ma-Song Da region of northern Vietnam contains the Song Ma – Anticlinorium, a poly deformed, poly metamorphosed, early Palaeozo Island arc / fore arc Terrance accreted to the south china plate in siluro – Devonian times (Findlay,1999). The Song Ma fault is merely one of many northwest-trending, post-cretaceous, high angle reverse oblique-slip faults and thrusts responsible for Cenozoic shortening and

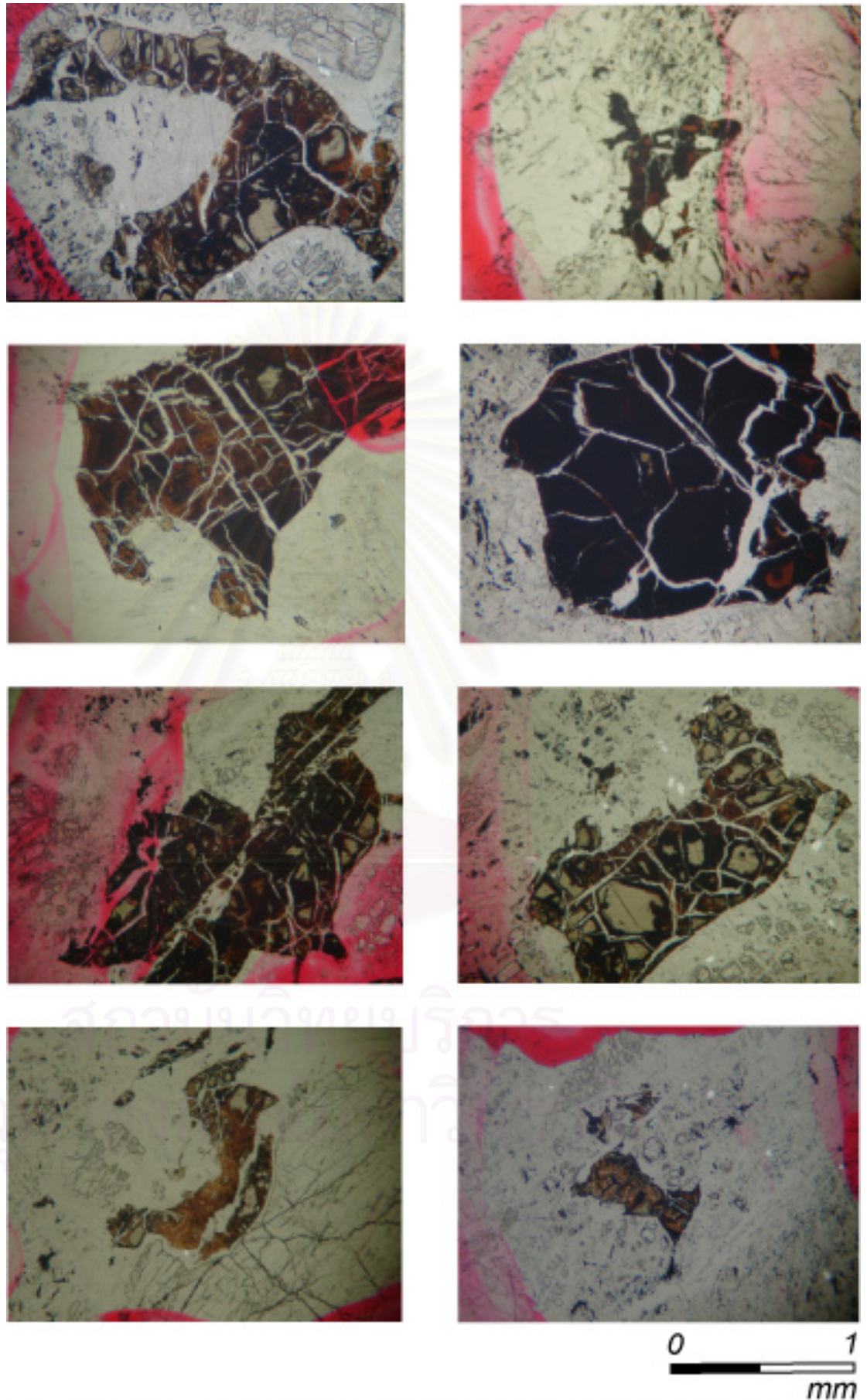


Figure 6.8 Photomicrographs of spinels from Switzerland ultramafic rocks.

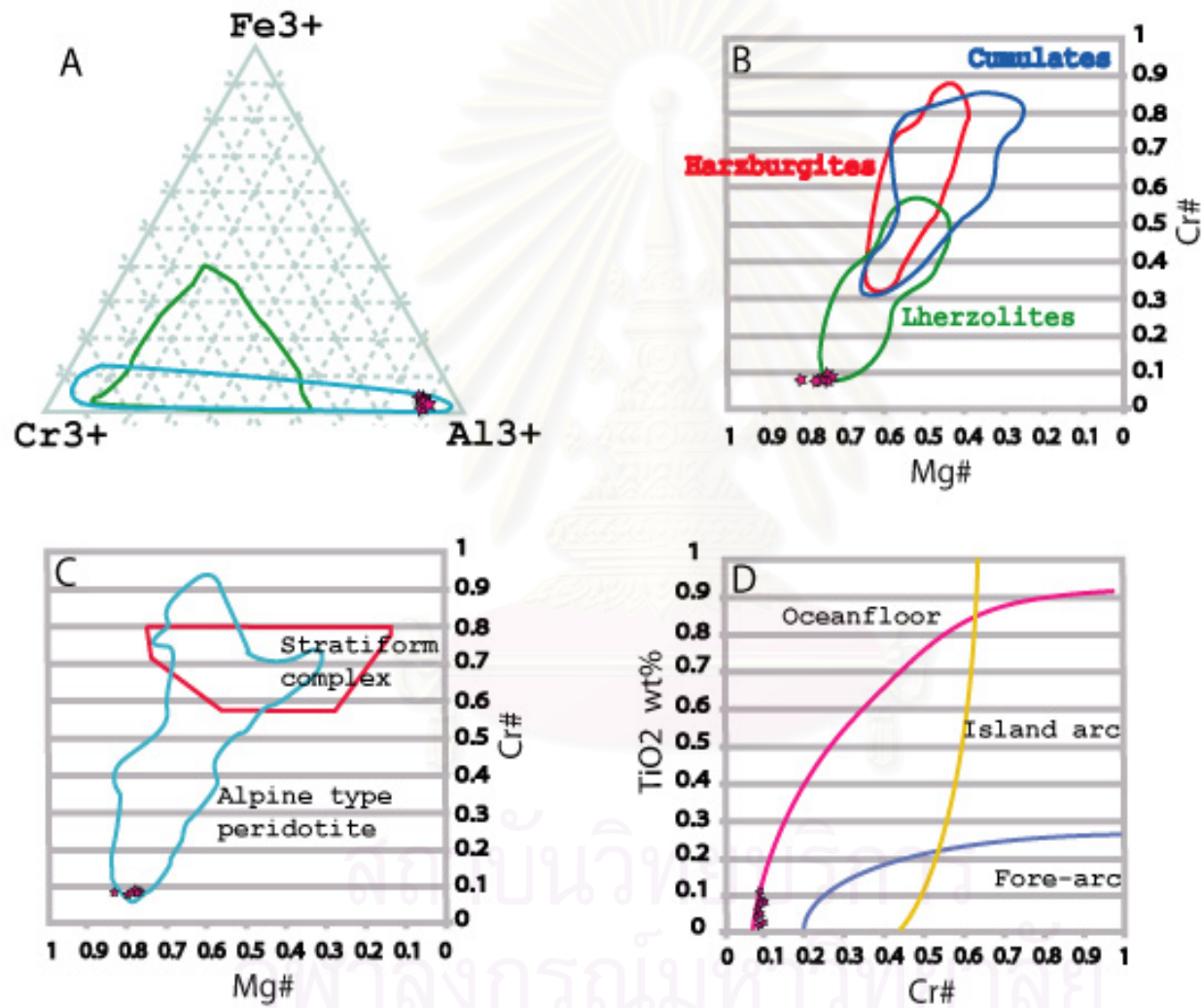


Figure 6.9 Chemical relation plots of spinels from Switzerland. A) Ternary plot of the major trivalent cation, B) $Cr\#$ and $Mg\#$ plot on compositional field of spinel from ultramafic rock type, C) $Cr\#$ and $Mg\#$ relation plot with Alpine type peridotite and stratiform complex ultramafic bodies, and D) $Cr\#$ - TiO_2 relationship compared with tectonic-setting field.

strike-slip transition of northern Vietnam. The Song Ma Anticlinorium and Song Ma fault, therefore, act as an Indosinian geosuture between the south china and Indochina plates; In particular indentified the Song Ma Fault is currently identified as paleo subduction zone (Findlay, 1999).

The Nui Nua ultramafic massif, where the collected sample was collected, has also been included in the Song Ma Anticlinorium. This ultramafic body which occupies about 60 km², has not been metamorphosed and invariably displays cumulus textures. This body is thus very different from small serpentinized and magnetised ultramafic body in the southern flank of Song Ma Anticlinorium (Finley, 1999). Furthermore, the only deformation structures are small faults confined to the northeastern margin, although shear zone are known also in the northwestern part of the body. This lack of deformation contrasts in the ultramafic bodies in the southern flank of the anticlinorium. Therefore, the ultramafic bodies at Nui Nua is probably younger than those in the Song Ma anticlinorium, and it may be a Permian intrusive emplaced tectonically by younger faulting rather than being an integral part of the Song Ma Formation.

6.2.3.2 Chromian spinel

Chromian spinel is generally reddish brown and subhedral-euhedral. Spinel ranges in size from 0.3 to 1 mm and averages 0.6 mm. Less commonly grains are subvermicular, and sometimes are equant grains with sharp grain boundaries (Figure 6.10). In particular few grains contain large circular inclusions. Fifty percent of Cr# and Mg# were plotted on Alpine-type peridotite field but they were spread in lateral conforming with special characteristic of stratiform peridotite pattern (Figure 6.11). Host rocks of this area are likely to be ultramafic cumulates. In triangular plot, chemical compositions are narrow range with variable Cr and Al and located only the lower part of diagram. Subhedral-euhedral spinel shape supported origin in ultramafic cumulate sequence. Cr# and TiO₂ weight percent plot and Haggerty (1976) (Figure 6.12) diagram suggest the origin of chrome spinel in the Song Ma area related to island arc setting.



Figure 6.10 Photomicrographs of spinels from Vietnam ultramafic rocks.

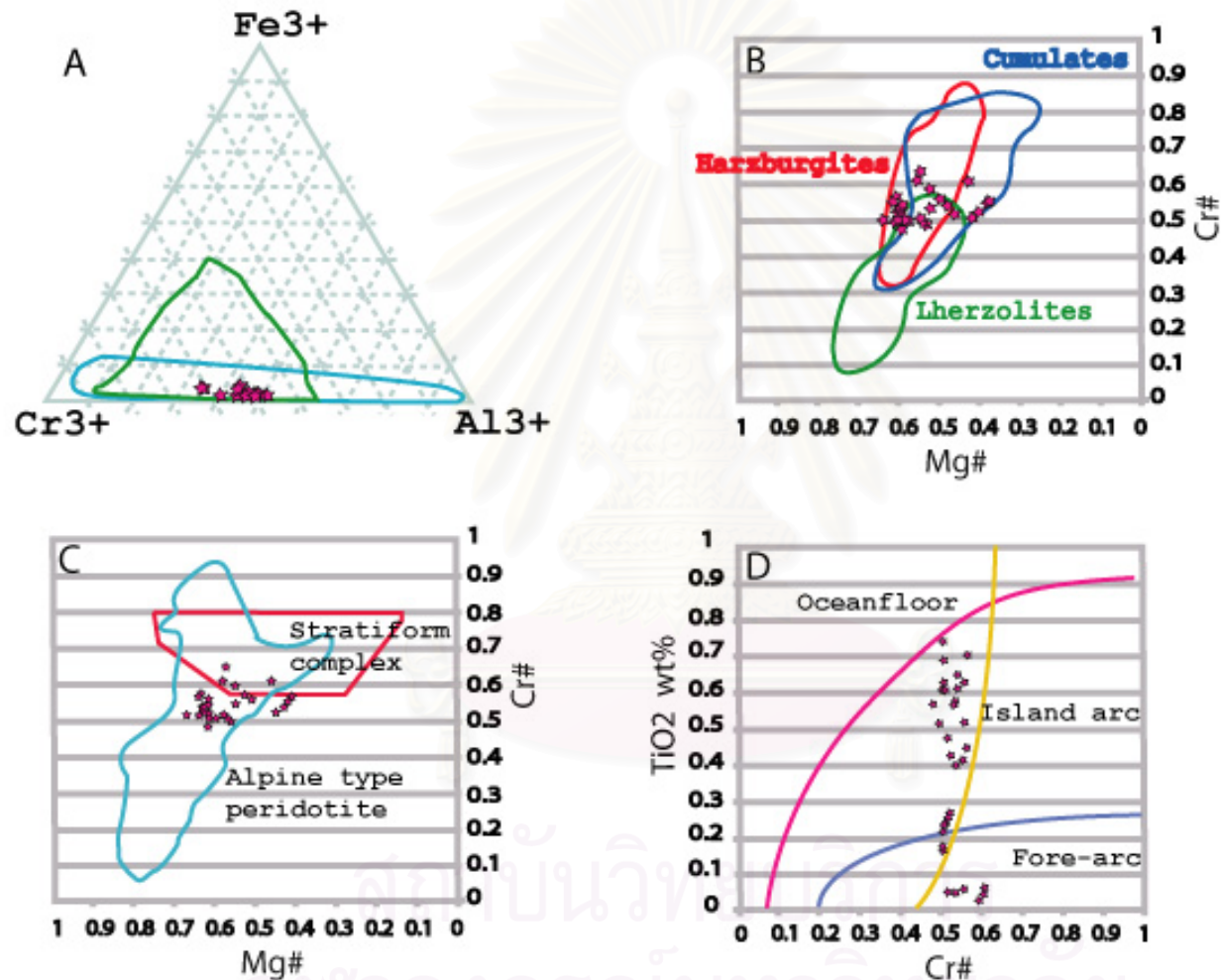
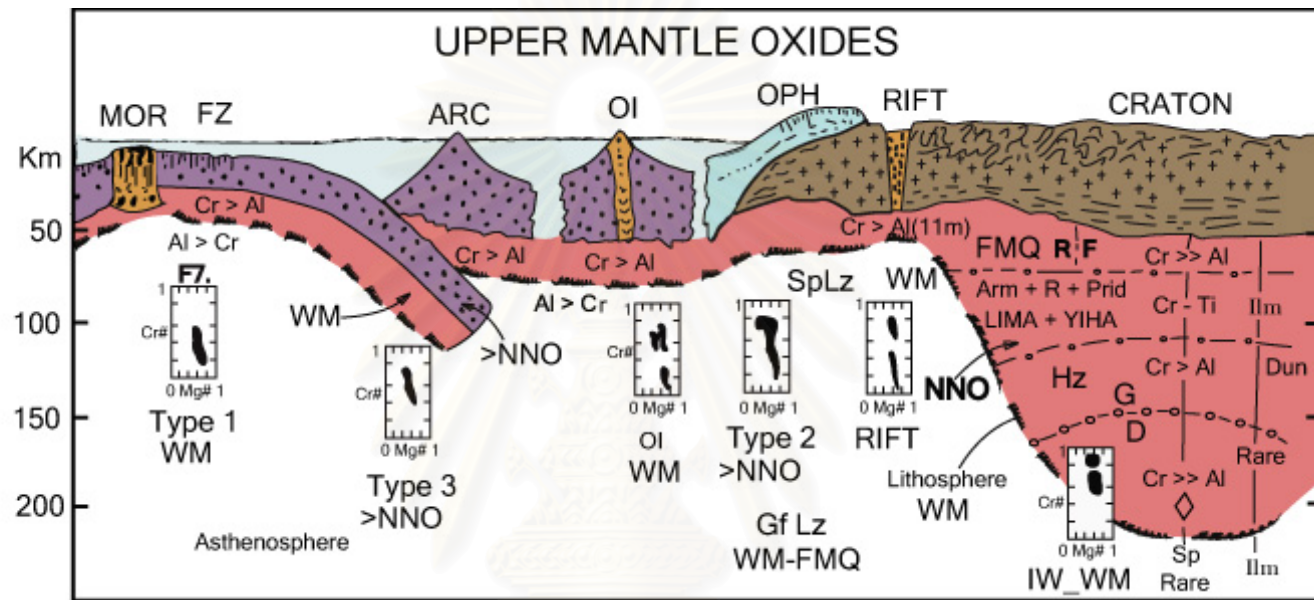


Figure 6.11 Chemical relation plots of spinels from Vietnam. A) Ternary plot of the major trivalent cation, B) $Cr\#$ and $Mg\#$ plot on compositional field of spinel from ultramafic rock type, C) $Cr\#$ and $Mg\#$ relation plot with Alpine type peridotite and stratiform complex ultramafic bodies, and D) $Cr\#$ - TiO_2 relationship compared with tectonic-setting field.



Type 1 : Mid Oceanic Ridge Type 2 : Ophiolite Suite Type 3 : Island Arc OI : Oceanic Island

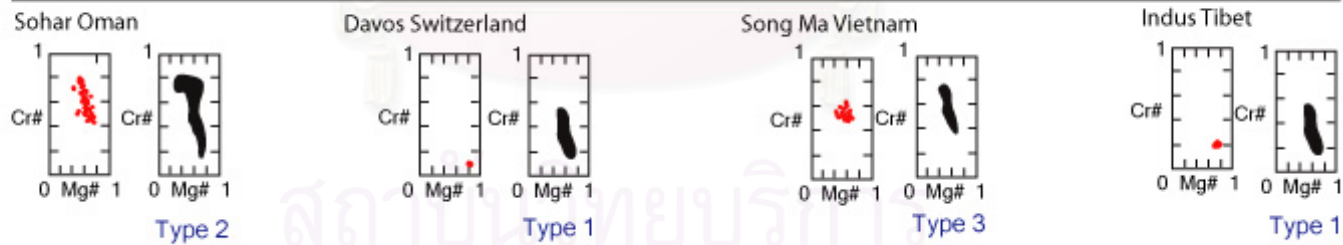


Figure 6.12 Cr# and Mg# plot of spinels from several countries (left with red dots) in comparison with several models of spinel in ultramafic origin (black in right diagrams) from different tectonic setting (Haggerty, 1976).

6.2.4 Indus, Tibet

6.2.4.1 Geologic setting

The Indus-Yarlung-Zangbo Suture Zone as a major geological structure (Wang et al, 2000) in Tibe, is well known as the locus of tectonic emplacement of the Tethyan ophiolites. Current models propose that most of the East Tethyan oceanic lithosphere was subducted within a single subduction zone during the Middle or Cretaceous. This was their completed during the Paleogene collision between India and Asia (Wang et al. 2000). The Early Cretaceous sediment of the Giabulin Formation in southern Tibet, includes conglomeratic member that contain ultramafic and mafic plutonic rocks, as well as radiolarian chert clasts, that recorded the erosion of oceanic lithosphere involved in subduction event which occurred earlier than previously believed.

The Indus-Yalung-Zangbo Suture Zone is a major lineament in Tibet that is accepted as the collision zone between India and Asia. It includes seven different tectonic sedimentary units. The ophiolitic massif including Xigaze ophiolites is form the basement of the Xigase Group. Current models suggest that most of the East Tethyan oceanic lithosphere was subducted within single subduction zone during the Middle or Late Cretaceous and closed during Paleogene continental collision. The occurrence of ultramafic pebbles indicates the existence of an Indus-Yalung-Zangbo paleo-ophiolites as the source of the conglomeratic unit within the Giabulin Formation.

The mineral and whole rock geochemical data suggest that the source of the Giabulin Formation ultramafic pebbles and the Yalung-Zangbo ophiolite were formed in different genetic environments. The composition of the Giabulin Formation spinels and clinopyroxenes suggests the host peridotite were fertile implying they had undergone a very low degree of partial melting. In comparision, the mineral chemistry of spinel and clinopyroxene, and geochemistry of Yarlung-Zangbo peridotites, is characteristic of a more refractory uppermantle. The possible initial geodynamic setting for the Yarlung-Zangbo ophiolite are within a spreading ridge over depleted mantle and a supra-subduction zone including back-arc and arc environment.



Figure 6.13 Photomicrographs of spinels from Tibet ultramafic rocks.

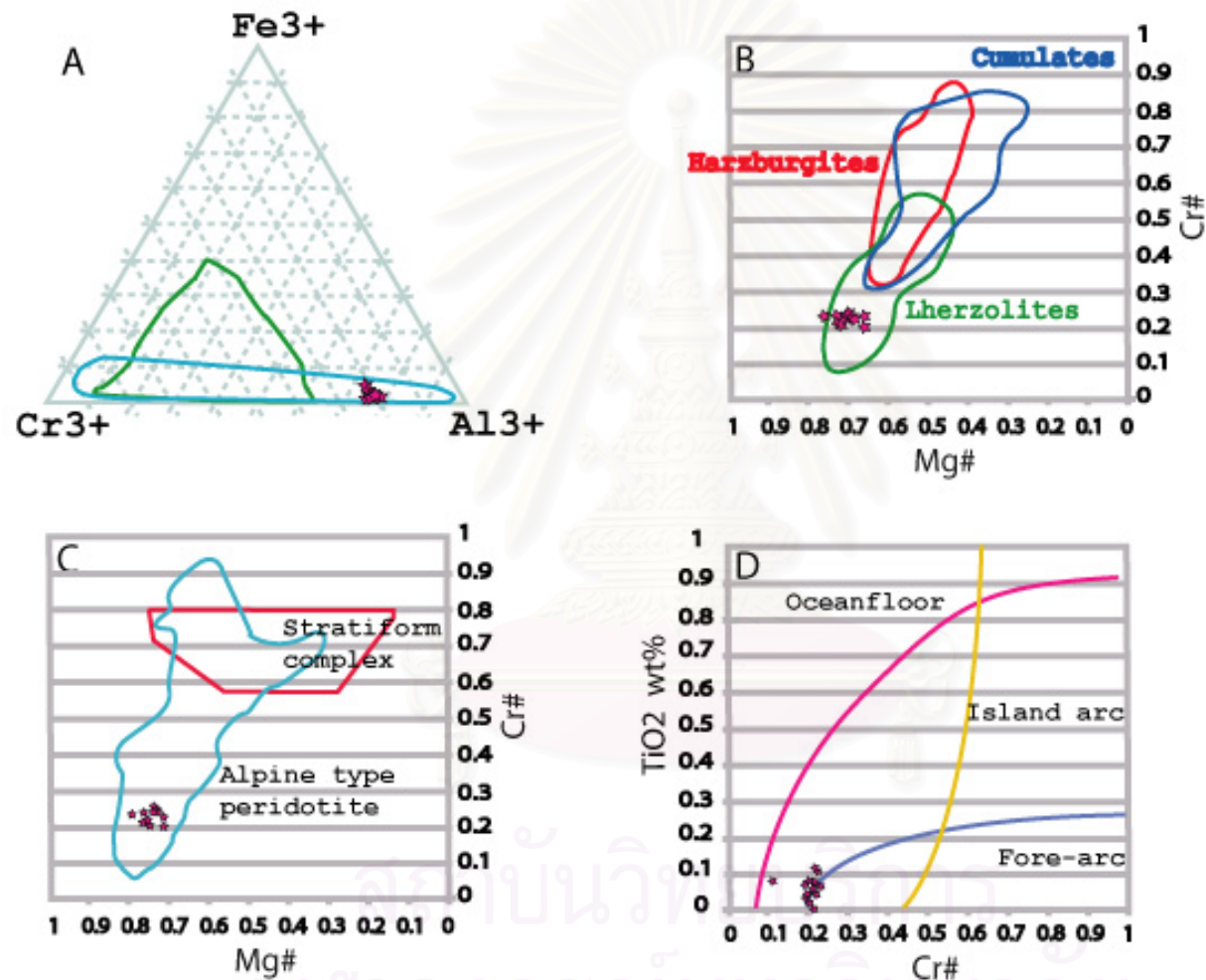


Figure 6.14 Chemical relation plots of spinels from Tibet. A) Ternary plot of the major trivalent cation, B) $Cr\#$ and $Mg\#$ plot on compositional field of spinel from ultramafic rock type, C) $Cr\#$ and $Mg\#$ relation plot with Alpine type peridotite and stratiform complex ultramafic bodies, and D) $Cr\#$ - TiO_2 relationship compared with tectonic-setting field.

6.2.4.2 Chromian spinel

Petrographic investigation reveals that thermal alteration is one effect on spinel chemistry in this area but the effect is much less than that of the Davos area. Chromian spinels are almost anhedral, yellowish brown color (Figure 6.13), and have very low Cr# but high Mg#. These properties indicate residual lherzolite host rock (less depleted peridotite) for spinel host rocks. In particular diagram (Figure 6.14), the plots are mainly between Island arc and ocean floor. Very high aluminar contents are essentially due to thermal alteration. So spinels of the Indus area are indicated ocean floor peridotite (Haggerty type I).

6.2.5 Diagram test conclusion

Samples from Sohar (Oman) and Song Ma (Viet Nam) suggest clearly that there exists a concordance between host-rock types and tectonic setting. Host rocks of Sohar Oman are harzburgite which probably originated from or belong to lower part of cumulate layer in ophiolite suite. Song Ma (Viet Nam) spinels also suggest peridotite host rocks that belong to the lower part of cumulate layer. Also a high possibility of origin related to island arc environment cannot be ruled out-Indus (Tibet) shows a few thermal alteration effects as indicated by slightly low Al content. However chemical data of spinel suggest the ultramafic host being residual lherzolite (less depleted peridotite) and originated in part of ocean floor. Spinel of Davos (Switzerland) was also disturbed by very high degree of thermal alteration. But the overall data point to residual peridotite for the ultramafic host with low degree of partial melting. This character is specific for oceanic plate affinity.

From the systematic diagrams presented above, it is concluded that all of spinel plots can be applied to indicate tectonic setting which is responsible for generation of ultramafic host rocks in each area. In addition, the other diagrams that can be well confirm the chromian spinel significant in tectonic setting implication work is Cr# plot for peridotites by Arai 1994 (Figure 6.15).

6.3 Comparison of the results between Thai and overseas spinels

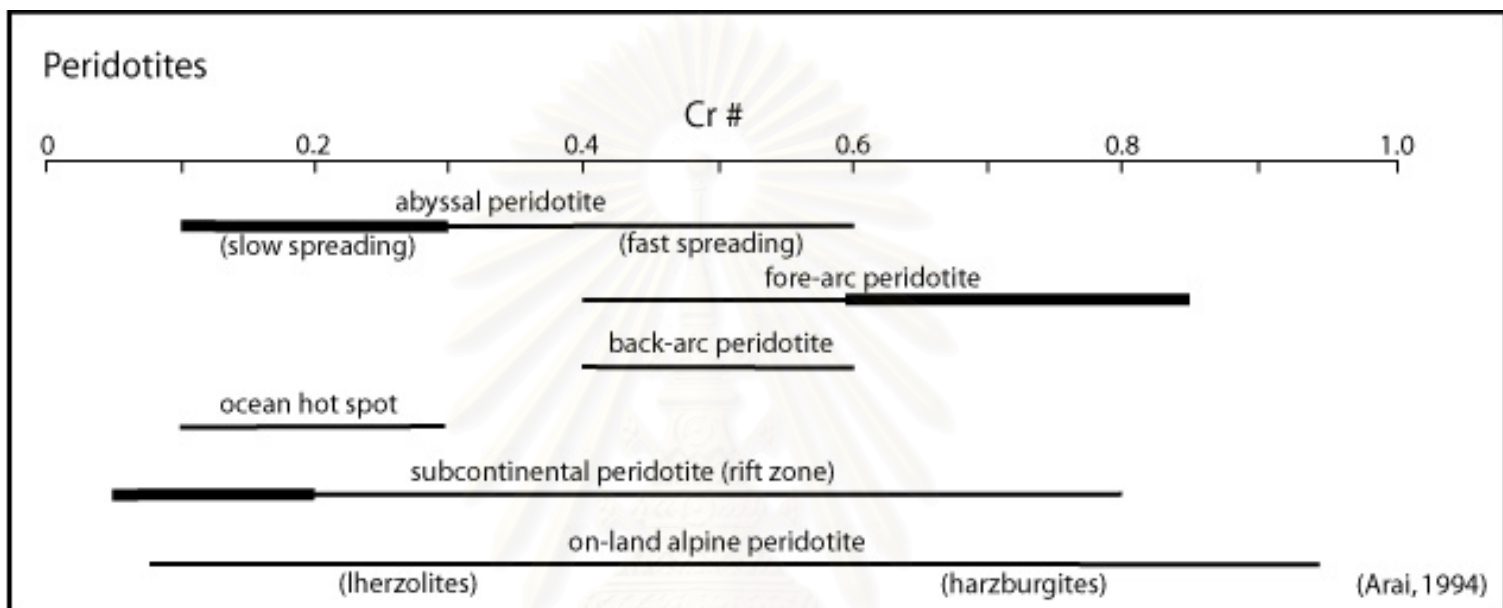
The next part emphasizes a comparison between Thai and overseas areas based on the results on 6.2, which the areas resemble in tectonic setting. Comparison is made between Nan-Uttaradit and Song Ma Viet Nam, and Sra Kaeo and Sohar Oman. Chiang Rai and Loei have not match with our examples.

6.3.1 Nan-Uttaradit VS Song Ma Viet Nam

In Irvine (1974)'s diagram spinels from Viet Nam show a widely lateral distribution, which is typical for stratiform complex. For Nan-Uttaradit, a lateral distribution is not much obvious but slightly vertical continuous trend of Cr# and Mg#, relation implicating continuous fractional crystallization. This mechanism generally occurs in the cumulate layer or stratiform peridotite. Song Ma (Viet Nam) host rocks are harzburgite in lower part of ultramafic cumulate, so it does not present clearly fractionation both in Pober and Faul (1983)'s and Cookenboo (1997)'s diagram. Noteworthy, all of plots were located in overlapping part of residual peridotite and ultramafic cumulate. In contrast Nan-Uttaradit is perfectly present part of ultramafic cumulates and have a strongly continuous degree of fractionation. Both of the areas are narrow spreading and located in type II of Haggerty (1976)'s, revealing island-arc setting. So we consider that Nan-Uttaradit ultramafic rocks, occurred in island-arc setting but Song Ma Viet Nam took place between Island arc and ocean floor settings.

6.3.2 Sra Kaeo VS Sohar Oman

Spinel from Sra Kaeo and Sohar Ultramafic rocks have very high chrome contents: Sra Kaeo-about 0.6-0.95 and Oman-about 0.45-0.8. These indicate very high degree of partial melting in origin. In Irvine (1974)'s diagram Sra Kaeo spinels are plotted mostly in a field of stratiform but Oman spinel plot mostly align following a field of alpine-type peridotite. For ultramafic host rocks Sra Kaeo are certainly a part of cumulate peridotite and Sohar Oman may originate in a lower part of ultramafic cumulate or residual harzburgite. Results from both chemical and physical properties reveal that both areas have a high possibility for ultramafic rocks occurring in the lower part of ultramafic cumulate. For tectonic setting, based on Hargetty (1976)'s and Arai



Chiang Rai
 Nan-Uttaradit
 Loei
 Sra Kao
 Davos Switzerland
 Sohar Oman
 Indus Tibet
 Song Ma Vietnam

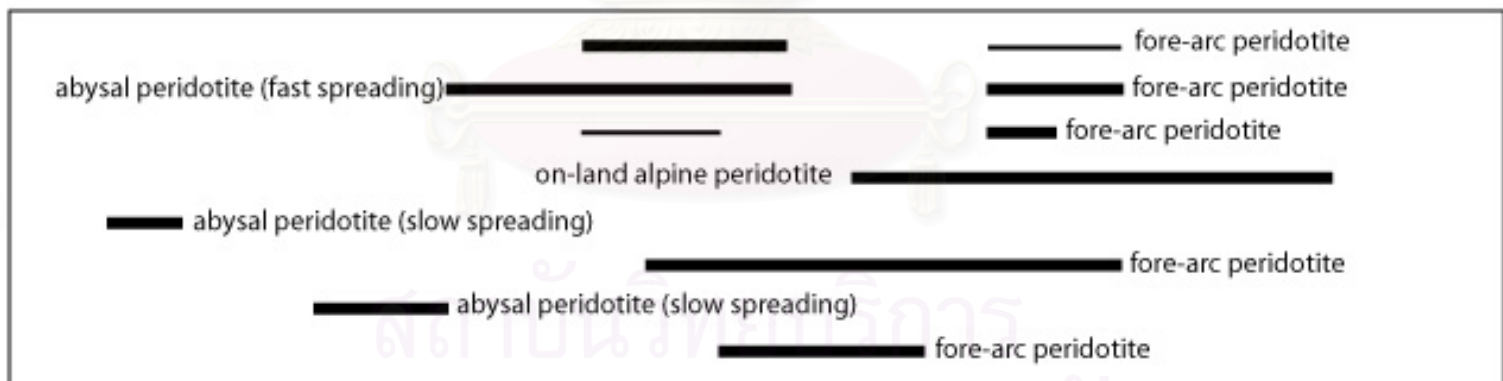


Figure 6.15 Diagram showing Cr# plot of all areas compare ranges of Cr# of spinel in peridotites from different tectonic settings (Arai, 1994). The heavy-line part represents the majority of data plots.

(1992)'s diagram, high Cr# and very low TiO₂ contents of spinels point to fore-arc tectonic setting.

Subsequent complex tectonic setting of Oman ophiolite, started from the opening of new oceanic crust in an early stage by mantle plume and later tectonic setting largely changed to convergent, volcanic activity and partial melting from subduction became much active in this belt. A partial melting in this stage could be affected old oceanic crust chemical composition. The last stage is thrusting of oceanic slab to appear as modern Oman ophiolite (oceanic floor). A subduction effect should be the important factor which makes Cr# value of Oman ophiolite a wider range than any general oceanic slab.

6.4 Tectonic setting of individual sutures

6.4.1 Chiang Rai

The inferred Permo-Triassic Chiang Khong volcanic rocks are constituted by felsic to mafic volcanic rocks and pyroclastic equivalents. Least-mobile element and REE from basaltic suite suggest that the Chiang Khong volcanics have formed in a continental volcanic arc. It can be concluded that the Chiang Khong-Tak volcanic belt consists of two magmatic series that have formed in a continental volcanic-arc environment. These include tholeiitic series and alkalic series (Punjasawatwong et al., 2003). Tak-Lampang-Phrae-Chiang Khong volcanic belt includes pre-Cenozoic volcanic rocks exposed from southeast of Tak northward to Lampang, Phrae, Nan and Chiang Khong. Rock east and southeast of Tak are rhyolite with flow bands, porphyritic rhyolite, aphanitic andesite, tuff and agglomerate. They are dated as Late Triassic-Early Triassic. In the Lampang-Phrae area, the rocks include Late Permian-Early Triassic andesite rhyolite, and tuff. These rocks are intruded by shallow intrusive of Triassic diorite, granodiorite, and granite (Tulyatid and Charusiri, 1999). According to Bunopas (1981) these volcanic rocks are Late Permian to Early Triassic and they indicate the presence of a Triassic volcanic arc between Lampang-Phrae. Field data confirm the existence of serpentinite in the Chiang Khong area.

Ultramafic masses of this area were located at least of Chiang Khong volcanic belt. They were classified as alpine type peridotite, and have been related, to some

extent, to subduction. Slightly low Cr# implied less depleted harzburgite host that was formed by slightly low degree of partial melting. Very low TiO₂ wt % indicates the locations within the fore arc setting. According to the model of alpine-type serpentinite emplacement (Lockwood, 1972) (Figure 1.4), much Alpine-type serpentinite is derived from oceanic crust or uppermost mantle, that has been subducted beneath a continental crust along the continental margin. Serpentinite mass moved down to the uppermost of mantle and was disturbed by high-pressure and high-temperature conditions. Partial dehydration and mantle peridotite mixing support the process of contamination from mantle materials. Although in an area of subduction, faults in overriding plates are to be expected and may provide ultramafic protrusion channels so ultramafic protrusions mostly appear as large and elongate bodies bounded by major faults.

6.4.2 Sra Kaeo

Sra Kaeo-Chanthaburi volcanic belt comprises a western chert-clastic belt, middle serpentinite-mélange belt and eastern granitic belt (Chutakosikanont, 2004). The western belt appears to form a stack of imbricate thrust slice and is dated as a Middle Triassic by radiolarians. The serpentinite mélange belt is composed of a wide variety of rock units, including rocks of oceanic, island arc, and continental affinities of various ages (Hada et al., 1994). Structures indicate east-directed accretionary thrusting and westward directed subduction. Rocks of the suture zone are overlain unconformably by Jurassic red bed sandstone and post Triassic basaltic lavas. The basalt disconformably overlies the suture and is interplate continental basalt (Punjasawatwong and Yaowanoyothin, 1993). Eastern granitic belt is composed mainly of two major granites. The first is of I-type granitoid rocks emplaced in Early Jurassic, and the second is tentatively inferred to have involved in movement on the Mae Ping fault zone in the Eocene (Charusiri et al., 1992).

Ultramafic masses of this area were located west of Chanthaburi granitic belt. A tectonic setting of ultramafic origin in this area was defined by a part of fore arc setting like Chiang Rai. But ultramafic characters are much different due to physical mechanism and degree of partial melting. High degree of partial melting can produced voluminous

extracted magma. This assumption can be confirmed by very high Cr# chromian spinel in the cumulate orthopyroxenite which belongs to a lower part of ultramafic cumulate.

6.4.3 Nan-Uttaradit

The largest body of the Nan River mafic-ultramafic belt consists mainly of metabasalt and metabasaltic andesite flows and tuffs overlying metagabbro transitional into epidote amphibolite. Ultramafic rocks along the southeast side of the body include metahornblendite, metapyroxenite and serpentinite lens within garnet amphibolite. Geochemical studies suggest that the mafic rocks closely resemble calc-alkali basalts formed in a volcanic arc, rather than in an oceanic environment. Lacking oceanic affinities, this group of mafic-ultramafic rocks should probably be termed a volcanic arc suite with associated fault-emplaced ultramafic bodies (Macdonald and Barr, 1984). The intimate association of ultramafic and metagabbroic rocks in the Nan River belt suggests that the ultramafic rocks have a mainly cumulate origin. The mafic rocks in the Nan River belt are chemically similar to basalts formed at spreading centers close to subduction zones (supra-subduction) although the geochemical characteristics are more suggestive of a converging rather than diverging plate margin (Barr and Macdonald, 1987).

Following two groups of chemical characteristics of chromian spinels we proposed the evolution of ultramafic origin into two steps (Robertson, 2004). The first group represents ultramafic masses that have formed by spreading above subduction zones, so called suprasubduction peridotite (Figure 1.5). They are characterized by moderate to high TiO_2 and slight low Cr# and intruded during early stage of oceanic-oceanic plate subduction. The second group has higher Cr# value and indicates higher degree of partial melting. Therefore it is quite possible to conclude, based upon physiochemical properties of spinels, that for mean tectonic setting has changed from supra-subduction in the Permo-Triassic period to island-arc setting in the Triassic period.

6.4.4 Loei

The Loei volcanic rocks are mainly Permian-Triassic rhyolite in the west and Late Devonian tholeiites in the east. The eastern sequence likely represents the ancient

Paleotethys that was destroyed by the collision between Indosinian and Cathaysia during Permo-Triassic times. Previous interpretation of the belt have assumed that the igneous rocks were the result of subduction associated with the Permo-Triassic closure of Tethys and the suturing of the Indochina and Shan Thai cratonic blocks. The petrochemical results from the Lam Narai volcanic province indicate that the belt is not a single subduction-related volcanic arc. The absence of Permo-Triassic igneous rocks in the center of volcanic belt argues against eastward dipping subduction beneath the Indosinia block in that part of the belt during the closure of Tethys. The absence of continuous subduction zone along the western margin of Indosinia requires a more complex plate margin (Intasopa and Dunn, 1993).

This area contains both ultramafic types -residual harzburgite and cumulates dunite. Their chemical compositions represent island arc peridotite or fore arc peridotite. An ultramafic source was generated by high degree of partial melting at deep level subduction and may have occurred or emplaced onto the accretionary prism of possibly arc affinity. The oceanic plate has been subducted into the Indochina plate during the Permo-Triassic.



สถาบันวิทยบริการ
จุฬาลงกรณ์มหาวิทยาลัย

CHAPTER VII

CONCLUSION

Based on physiochemical data of chromian spinels from each suture combined with previous tectonic models of Thailand. We can conclude the model of ultramafic origin of main sutures in Thailand as below (Figure 7.1).

7.1 Chiang Rai

Chiang Rai ultramafic masses are mainly less depleted harzburgite. They were generated in early stage of Permo-Triassic subduction event. Paleo-oceanic crust which eastern part of Shan Thai moved eastward subducted beneath western margin of Lampang-Chiang Rai microoceanic plate. The uppermost part of mantle materials that are mostly peridotite were moved and followed a fault break which acts as a channel by compression pressure. So ultramafic mass in this area appears as elongate bodies bounded by major fault included in accretionary zone. The eastward subduction was keep going, the paleo-oceanic part of Shan Thai sudducted to deep underneath. The results of deep partial melting and magmadifferentiation were created Chiang Khong volcanic arc in Permo-Triassic.

7.2 Nan-Uttaradit

According to two different groups of chromian spinel, one-formed by spreading above subduction zones (suprasubduction) and the other-formed in island arc setting. It is concluded that, in early Permo-Triassic Nakhon Thai plate was westward subducted underneath the eastern part of Lampang-Chiang Rai plate. Low degree partial melting of oceanic material at the shallow depth formed a spreading center close to subduction zones. Then converging setting was progress and changed spreading center to island arc environment until Late Triassic. Subsequently, tectonics continental collision is in the final but age of collision is still uncertain.

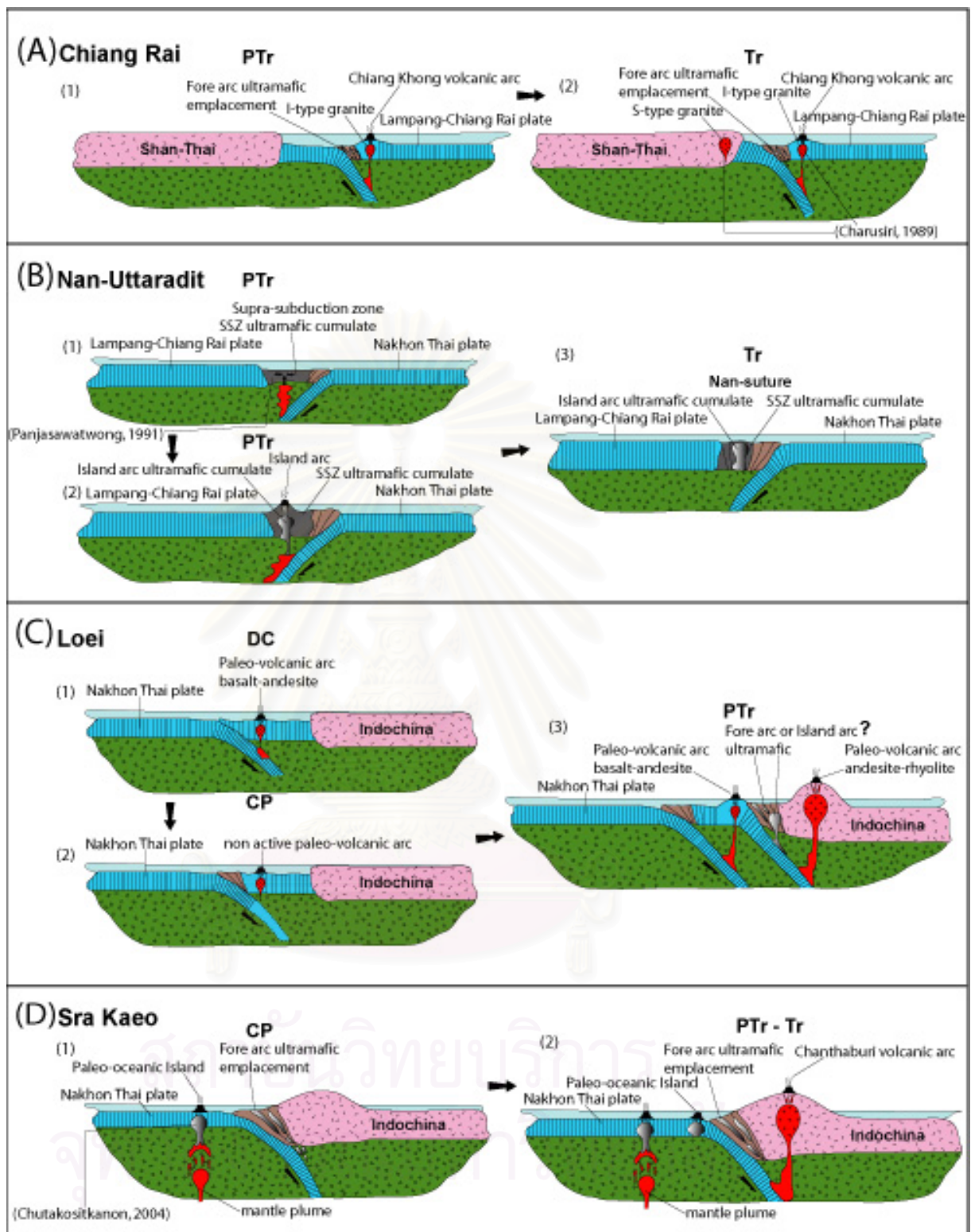


Figure 7.1 The conclusive models of ultramafic origins from each interpreted suture zone
 A) Chiang Rai : Fore arc setting B) Nan-Uttaradit : (1) SSZ ultramafic and (2) Island arc peridotite
 C) Loei : Fore arc or island arc ultramafic peridotite D) Sra Kaeo : Fore arc peridotite

7.3 Loei

The chemical composition of chromian spinels represents island arc and fore arc peridotite. An ultramafic source was generated by high degree of partial melting at deep level subduction. They were emplaced onto the island arc in Devonian-Carboniferous and accretionary zone in Permo-Triassic. The eastern margin of Nakhon Thai plate was subducted beneath Indochina formed the basaltic andesite volcanic arc by Devonian-Carboniferous. Subsequently, the passive margin on western side of Indochina was broken and subducted to east direction in Permo-Triassic then created fore arc ultramafic emplacement and andesitic-rhyolitic volcanic arc. Volcanic activity stilled active until Triassic age and island arc mafic-ultramafic sequence became to a large scale block of tectonic inclusion.

7.4 Sra Kaeo

An eastern subduction of Nakhorn Thai plate underneath Indochina and volcanic seamount activity on the western side were active simultaneously during Late Paleozoic. Since Carboniferous-Permian, high degree of partial melting extracted magma emplaced to subduction front (fore-arc environment) along major fault zone. An eastward subduction was responsible for the formation of Chanthaburi volcanic arc during Permo-Triassic. A volcanic seamount and oceanic rocks sequence also moved to east follow subduct direction and became to tectonic inclusion between accretionary zones by the same age with volcanic arc activity.

Table 7.1 Classified ultramafic host rocks and tectonic setting of each areas from Thailand by chromian spinel chemistry.

Areas	Ultramafic host rocks	Tectonic setting
Chiang Rai	Harzburgite	Fore arc
Nan-Uttaradit	Dunite and wehrlite	Island arc
Loei	Harzburgite	Island arc
SraKaeo	Orthopyroxenite	Fore arc

REFERENCES

- Arai, S. 1978. Dunite-Harzburgite-chromitite complexes as Refractory Residual in the Sangun-Yamaguchi Zone, Western Japan. Journal of Petrology 21: 141-165.
- Arai, S., 1992. Chemistry of chromian spinel in volcanic rocks as a potential guide to magma chemistry. Mineralogical Magazine 56: 173-184.
- Arai, S., 1994. Compositional variation of olivine-chromian spinel in Mg-rich magmas as a guide to their residual spinel peridotites. Journal of Volcanology and Geothermal Research 59: 279-293.
- Arai, S. and Abe, N. 1995. Reaction of orthopyroxene in peridotite xenoliths with alkali-basalt melt and its implication for genesis of Alpine-type chromitite. American Mineralogist 80: 1041-1047.
- Arai, S. and Kodoshima, K. 1999. Primary petrological characteristics of peridotites in the Sangun zone of northern Kyushu: a preliminary note from detrital chromian spinels. Journal of Mineral Petrology and Economic Geology 94: 97-108.
- Arai, S. and Kyoko, M. 1996. Petrology of the Gabbro-Troctolite-Peridotite complex from Hess deep, Equatorial Pacific: Implications for mantle-melt interaction within the Oceanic lithosphere. Proceedings of the Ocean Drilling Program, Scientific Results 147: 135-155.
- Barr, S.M. and Macdonald, A.S. 1987. Nan River suture zone, northern Thailand, Geology 15: 907-910.
- Barr, S.M., Tantisukrit, C., Yaowanaiyothin, W. and Macdonald, A.S. 1990. Petrology and tectonic implications of Upper Paleozoic volcanic rocks of the Chiang Mai belt, northern Thailand. Journal of Southeast Asian Earth Sciences 4: 37-47.
- Bernoulli, D., Manatschal, G., Gretchen, L., Green, F., and Weissert, H. 2001. Birth of an Ocean. IAS Davos Excursion guide book 5.
- Bunopas, S. and Vella, P. 1983. Tectonic and geologic evolution of Thailand. In : Nutalaya, P. (ed.). Proc. Of the Workshop on Stratigraphic correlation of Thailand and Malaysia. 8-10 Sept. Haad Yai, Thailand, Tech. Paper 1: 307-323.
- Bunopas, S. and Vella, P. 1992. Geotectonics and Geologic Evolution of Thailand, National Conference on Geologic Resources of Thailand: Potential for Future

- Development, 17-24 November, Department of Mineral Resources, Bangkok, Thailand: 209-228.
- Charusiri, P., Daorerk, V., Archibald, D., Hisada, K. and Ampaiwan, T. 2002. Geotectonic evolution of Thailand: A new synthesis. Journal of the Geological Society of Thailand : 1-20.
- Charusiri, P., Clark, A.H., Farrar, E., Archibald, D. and Charusiri, B. 1993. Granite belts in Thailand: evidence from the $^{40}\text{Ar}/^{39}\text{Ar}$ geochronological and geological syntheses. Journal of Southeast Asian Earth Sciences 8: 127-136.
- Charusiri, P., Hisada, K., Arai, S., Chutakositkanon, V. and Daorerk, V. 2000. Chromian Spinel: An Indicator Mineral to Tectonic Setting of Thailand-A Preliminary Synthesis. Symposium on Mineral, Energy, and Water Resources of Thailand: Toward the year 2000, October 28-29, Bangkok, Thailand: 217-220.
- Charusiri, P., Pongsapitch, W., Daorerk, V. and Charusiri, B. 1992. Anatomy of Chantaburi granitoids: Geochronology, Petrochemistry, Tectonic and Associated Mineralization. National Conference on Geologic Resources of Thailand: Potential and Future Development, 17-24 November: 383-392.
- Charusiri, P., Daorerk, V., Sutthirat, C., Charoenthitirat, T. and Choowong, M. 2005. Tectonic setting of northern Thailand, A Final Report submitted to Chulalongkorn University (in Thai with English abstract).
- Chutakositkanon, V., Hisada, K., Charusiri, P. and Arai, S. 2001. Tectonic significance of detrital chromian spinels in the Permian Nam Duk Formation, Central Thailand. Geosciences Journal 5: 89-96.
- Chutakositkanon, V. 2004. Detrital chromian spinels from the Sa Kaeo-Chanthaburi accretionary complex, eastern Thailand: tectonic evolution of the western margin of Indochina. Doctoral dissertation, The University of Tsukuba, Japan (unpublished).
- Cookerbo, H.O., Bustin, R.M. and Wilks, K.R., 1997. Detrital chromian spinel compositions used to reconstruction the tectonic setting of provenance: Implications for orogeny in The Canadian Cordillera. Journal of Sedimentary Research 67: 116-123.

- Dick, H.J.B. and Bullen, T., 1984. Chromian spinel as a petrogenetic indicator in abyssal and alpine-type peridotites and spatially associated lavas. Contribution to Mineralogy and Petrology 86: 54-76.
- Findlay, R.H. 1999. Review of the Indochina-South china plate boundary problem; structure of the Song Ma-Song Da Zone. Gondwana Dispersion and Asian Accretion: 341-361.
- Fruh-Green, G.L., Scambelluri, M. and Vallis, F. 2001. O-H isotope ratios of high pressure ultramafic rocks: implications for fluid sources and mobility in the subducted hydrous mantle. Contribution Mineral Petrology 141: 145-159.
- Hada, S., Bunopas, S., Ishi, K., and Yoshikura, S. 1997. Rift and drift history and the amalgamation of Shan-Thai and Indochina/East Malaya Blocks. In: Dheeradilok, P. and other (eds.), Proceedings of the International Conference on Stratigraphy and Tectonic Evolution of Southeast Asia and the South Pacific. Department of Mineral Resource, Ministry of Industry, Bangkok, Thailand, Aug. 19-24: 273-286.
- Hutchison, C.S. 1973. Tectonic Evolution of Sundaland: A Phanerozoic Synthesis. Geological Society Malaysia, Bulletin 6: 61-86.
- Hutchison, C.S. 1975. Ophiolite in Southeast Asia. Geological Society of America Bulletin 86: 797-806.
- Hutchison, C.S. 1989. Geological Evolution of South-east Asia, New York, United States: Oxford University Press: 368 p.
- Intasopa, S. and Dunn, T., 1990a. Petrology and geochronology of Loei province volcanics, central Thailand volcanic belt. EOS April 24.
- Intasopa, S. and Dunn, T. 1990b, $^{40}\text{Ar}/^{39}\text{Ar}$ geochronology of the central Thailand volcanic belt. EOS April 24.
- Irvine, T.N. 1974. Petrology of the Duke Island ultramafic complex, southeastern Alaska. Geological Society of America Memoir 138: 240 p.
- Lee, Y.I. 1999. Geotectonic significant of detrital chromian spinel: a review. Geosciences Journal 3: 23-29.
- Lockwood, J.P., 1972. Possible Mechanisms for the emplacement of Alpine-Type Serpentinite. The Geological Society of America Inc. Memoir 132: 273-287.

- Lockwood, J.P., 1971. Sedimentary and Gravity Slide Emplacement of Serpentinite. Geological Society of American Bulletin 82: 919-936.
- Macdonald, A.S., and Barr, S.M. 1984. The Nan River mafic-ultramafic belt, northern Thailand: Geochemistry and tectonic significance. Geol. Soc. Malaysia. Bulletin 17: 209-224.
- Matsumoto, I. and Arai, S. 2000. Morphological and chemical variations of chromian spinel in dunite-harzburgite complexes from the Sangun zone (SW Japan): implication for mantle/melt reaction and chromitite formation processes. Mineralogy and Petrology 73: 305-323.
- Metcalfe, I., Spiller, F.C.P, Benpei, L., Haoruo, W. and Sashida, K. 1999. The Paleotethys in Mainland East and Southeast Asia: Contribution from radiolarian studies. Gonwana dispersion and Asian Accretion: 259-280.
- Metcalfe, I. 2000. The Bentong-Raub Suture Zone. Journal of Asian Earth Sciences 18: 691-712.
- Mitchell, A.H.G. 1986. Mesozoic and Cenozoic regional tectonic and metallogenesis in Mainland SE-Asia. Geological Society Malaysia. Bulletin. Geosea Proceeding 2: 221-239.
- Neawsuparp, K. and Charusiri, P. 2002. New Discovery of Ultramafic Rocks and the Major Thrust Fault in Loei-Nong Bua Lumpu Area, NE Thailand Using Enhanced Aeromagnetic Data (Abstract). Their Crustal Evolution, Emplacement and Natural Resources Potential. Fourth Symposium of IGCP Project, 17-25 November: 44-45.
- Nesse, W.D. 1991, Introduction of Optical Mineralogy, Second Edition, New York, United States, Oxford University Press, Inc: 335 p.
- Panjasawatwong, Y. 1991. Petrology, geochemistry and tectonic implications of Igneous rocks in the Nan suture, Thailand and an empirical study of the effects of Ca/Na and H₂O on plagioclase-melt equilibria AT 5-10 KB pressure. Doctoral Dissertation, University of Tasmania Hobart, Australia (unpublished).
- Pober, E. and Faupl, P. 1988. The chemistry of detrital chromian spinels and its implications for the geodynamic evolution of the Eastern Alps. Geologische Rundschau 77: 641-670.

- Robertson, A., 2004. Development of concepts concerning to genesis and emplacement of Tethyan ophiolites in the Eastern Mediterranean and Oman regions. Earth-Science Review 66: 675-690.
- Singharajwarapan, S. and Berry, R. 1999. Tectonic implications of the Nan Suture Zone and its relationship to the Sukhothai Fold belt, Northern Thailand. Journal of Asian Earth Sciences 18: 663-673.
- Srinak, N. 2003. Lithostratigraphy of some Triassic clastic rocks in southern part of Amphoe Muang Mae Hong Son, Changwat Mae Hong Son, Northern Thailand. Master thesis, Department of Geology Faculty of Science, Chulalongkorn University (Unpublished).
- Sukiyama, M. 1999. Collisional event between Sibumasu and Indochina based on detrital chromian spinels. Master thesis, graduate school of education, University of Tsukuba, Japan (unpublished).
- Tan, B.K. 1996. Suture zone in peninsular Malaysia and Thailand: implications for palaeotectonic reconstruction of Southeast Asia. Journal of Southeast Asian Earth Sciences 13: 243-249.
- Tegyey, M. 1986, Ophiolite and Metamorphic Rock of the Oman Mountains: A Petrographic Atlas, Elsevier Science publishers: 124 p.
- Tulyatid J. and Charusiri, P., 1999. The ancient Tethys in Thailand as indicated by nationwide airborne geophysical data. International Symposium Shallow Tethys(ST) 5, 1-5 February: 335-350.
- Ueno, K. and Igo, H. 1997. Late Paleozoic foraminifers from the Chiang Dao area, Northern Thailand: Geologic age, faunal affinity, and paleobiogeographic implications. PRACE PANSTWOWEGO INSTYTUTU GEOLOGICZNEGO CLVII, Proceedings of the XIII International Congress on the Carboniferous and Permian: 339-352.
- Ueno, K. 2003. The Permian fusulinoidean faunas of the Sibumasu and Baoshan blocks: their implications for the paleogeographic and paleoclimatologic reconstruction of the Cimmerian Continent. Elsevier 193: 1-24.

Wang, C., Liu, Z. and H'ebert, R. 2000. The Yarlung-Zangbo paleo-ophiolite, southern Tibet: implication for the dynamic evolution of the Yarlung-Zangboo Suture Zone. Journal of Asian Earth Sciences 18: 651-661.

Wang, X., Metcalfe, I., Jian, P., He, L. and Wang, C. 2000. The Jinshajiang-Ailaoshan Suture zone, China: tectonostratigraphy, age and evolution. Journal of Asian Earth Sciences 18: 675-690.



สถาบันวิทยบริการ
จุฬาลงกรณ์มหาวิทยาลัย



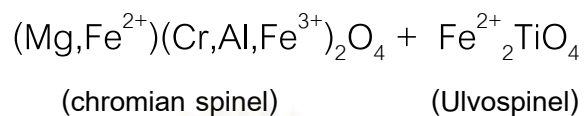
APPENDICES

สถาบันวิทยบริการ
จุฬาลงกรณ์มหาวิทยาลัย

Appendix I

How to calculate ferric and ferrous in chromian spinel by spinel stoichiometry.

Solid solution



How to calculate Fe^{2+} and Fe^{3+}

- 1) $\text{Mn} + \text{Fe} = \text{Fe total}$
- 2) $\text{Fe total} - 2\text{Ti} = \text{Fe}^*$
- 3) Solve simultaneous equation

$$2(\text{Mg} + \text{Fe}^{2+}) = \text{Cr} + \text{Al} + \text{Fe}^{3+}$$

$$\text{Fe}^{2+} + \text{Fe}^{3+} = \text{Fe}^*$$

$$2\text{Mg} + 2\text{Fe}^{2+} = \text{Cr} + \text{Al} + \text{Fe}^{3+}$$

$$\text{Fe}^{3+} = 2\text{Mg} + 2\text{Fe}^{2+} - \text{Cr} - \text{Al}$$

$$\text{Fe}^{2+} + 2\text{Mg} + \text{Fe}^{2+} - \text{Cr} - \text{Al} = \text{Fe}^*$$

$$3\text{Fe}^{2+} + 2\text{Mg} - \text{Cr} - \text{Al} = \text{Fe}^*$$

$$\text{Fe}^{2+} = (\text{Fe}^* + \text{Cr} + \text{Al} - 2\text{Mg})/3$$

สถาบันวิทยบริการ
จุฬาลงกรณ์มหาวิทยาลัย

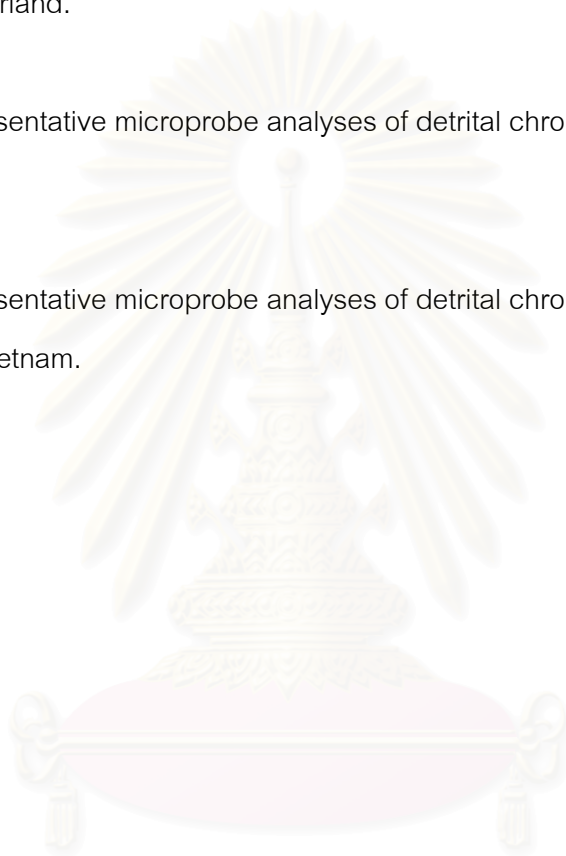
APPENDIX II

Table II.1 Representative microprobe analyses of detrital chromian spinels from Sohar, Oman.

Table II.2 Representative microprobe analyses of detrital chromian spinels from Davos, Switzerland.

Table II.3 Representative microprobe analyses of detrital chromian spinels from Indus, Tibet.

Table II.4 Representative microprobe analyses of detrital chromian spinels from Song Ma, Vietnam.



สถาบันวิทยบริการ
จุฬาลงกรณ์มหาวิทยาลัย

Sample No	O31-1	O31-2	O31-3	O32-4	O32-6	O32-7	O32-8	O32-9	O32-11	O31-12	O32-3-2	O33-2	O33-4	O33-6	O33-9	O33-11	O33-13	O33-15	O33-16
SiO ₂	0.00	0.03	0.00	0.01	0.00	0.00	0.00	0.00	0.00	0.03	0.04	0.00	0.19	0.02	0.02	0.11	0.03	0.06	0.00
Al ₂ O ₃	30.27	18.45	23.24	13.58	25.16	26.01	29.77	29.86	20.73	19.89	20.58	14.64	12.66	24.96	15.91	26.58	30.09	18.90	23.48
TiO ₂	0.41	0.06	0.10	0.08	0.11	0.01	0.16	0.08	0.05	0.04	0.08	0.19	0.11	0.06	0.09	0.07	0.22	0.01	0.02
Cr ₂ O ₃	36.16	48.15	44.21	52.32	41.32	38.96	35.98	36.39	47.80	46.60	46.86	51.23	52.55	41.54	50.94	41.70	36.60	48.48	43.82
FeO	15.73	18.78	17.88	23.51	18.25	22.98	16.54	18.61	18.14	20.26	20.04	20.79	21.37	18.58	18.59	15.70	17.16	18.49	17.04
NiO	0.15	0.13	0.10	0.06	0.16	0.04	0.11	0.09	0.05	0.02	0.04	0.08	0.03	0.07	0.10	0.10	0.16	0.02	0.06
MnO	0.19	0.30	0.29	0.51	0.27	0.36	0.20	0.24	0.24	0.29	0.28	0.38	0.28	0.27	0.30	0.26	0.22	0.26	0.25
MgO	15.83	11.69	12.72	7.40	13.09	9.32	15.20	13.51	12.39	11.05	11.09	11.08	10.31	12.96	12.01	15.01	13.30	11.74	12.97
CaO	0.03	0.05	0.01	0.02	0.00	0.03	0.02	0.03	0.00	0.00	0.02	0.04	0.10	0.04	0.05	0.07	0.08	0.06	0.04
Na ₂ O	0.06	0.00	0.00	0.00	0.06	0.05	0.00	0.03	0.02	0.00	0.00	0.01	0.00	0.01	0.02	0.00	0.03	0.01	0.04
K ₂ O	0.01	0.01	0.00	0.00	0.01	0.00	0.00	0.00	0.00	0.01	0.00	0.03	0.00	0.02	0.00	0.00	0.02	0.01	0.02
ZnO	0.12	0.18	0.21	0.23	0.12	0.41	0.09	0.26	0.16	0.22	0.20	0.07	0.21	0.20	0.11	0.08	0.22	0.20	0.14
Total	98.93	97.82	98.76	97.72	98.54	98.17	98.07	99.09	99.57	98.42	99.23	98.53	97.81	98.74	98.14	99.69	98.12	98.23	97.88
Cation	4 oxygens																		
Fe total	0.40	0.52	0.47	0.68	0.48	0.62	0.42	0.48	0.48	0.55	0.54	0.55	0.61	0.49	0.52	0.40	0.44	0.50	0.45
Fe*	0.38	0.51	0.47	0.68	0.48	0.62	0.42	0.47	0.48	0.55	0.54	0.49	0.60	0.49	0.51	0.40	0.43	0.50	0.45
Fe ²⁺	0.30	0.44	0.41	0.63	0.40	0.56	0.32	0.40	0.42	0.48	0.48	0.44	0.49	0.41	0.42	0.33	0.39	0.44	0.40
Fe ³⁺	0.08	0.07	0.06	0.05	0.08	0.06	0.09	0.08	0.06	0.07	0.06	0.06	0.11	0.08	0.09	0.07	0.04	0.06	0.05
TiO ₂	0.41	0.06	0.10	0.08	0.11	0.01	0.16	0.08	0.05	0.04	0.08	0.19	0.11	0.06	0.09	0.07	0.22	0.01	0.02
Cr#	0.44	0.64	0.56	0.72	0.52	0.50	0.45	0.45	0.61	0.61	0.60	0.70	0.74	0.53	0.68	0.51	0.45	0.63	0.56
Mg#	0.70	0.56	0.59	0.37	0.60	0.44	0.68	0.61	0.58	0.53	0.52	0.56	0.51	0.60	0.58	0.67	0.60	0.56	0.60
Cr ₃ #	0.43	0.61	0.54	0.70	0.50	0.49	0.43	0.43	0.59	0.59	0.59	0.68	0.69	0.51	0.65	0.49	0.44	0.61	0.54
Al ₃ #	0.53	0.35	0.43	0.27	0.46	0.48	0.53	0.53	0.38	0.37	0.38	0.29	0.25	0.45	0.30	0.47	0.54	0.36	0.43
Fe ₃ +3#	0.04	0.04	0.03	0.03	0.04	0.03	0.05	0.04	0.03	0.04	0.03	0.03	0.06	0.04	0.04	0.03	0.02	0.03	0.03

Table II.1 Representative microprobe analyses of detrital chromian spinels from Sohar Oman.

Sample No	D3-1	D3-2	D3-3	D3-4	D3-5	D3-6	D3-7	D3-8	D3-9	D3-10	D8-2
SiO ₂	0.00	0.47	0.03	0.00	0.03	0.03	1.28	0.00	0.00	0.02	0.00
Al ₂ O ₃	59.38	60.00	59.80	59.76	59.61	59.64	55.91	59.68	58.32	57.78	62.18
TiO ₂	0.02	0.03	0.11	0.07	0.04	0.01	0.04	0.05	0.03	0.08	0.09
Cr ₂ O ₃	8.78	6.91	7.03	7.66	7.30	7.61	7.26	7.26	9.51	7.57	7.33
FeO	10.73	12.42	11.57	11.36	11.18	11.39	10.80	10.51	11.62	11.00	11.79
NiO	0.39	0.32	0.31	0.37	0.37	0.35	0.33	0.42	0.29	0.38	0.41
MnO	0.06	0.07	0.09	0.15	0.16	0.11	0.15	0.15	0.10	0.13	0.11
MgO	20.08	20.97	19.88	19.89	19.70	19.76	20.58	20.13	18.96	19.44	21.43
CaO	0.00	0.02	0.04	0.03	0.00	0.00	0.01	0.00	0.00	0.03	0.00
Na ₂ O	0.03	0.00	0.00	0.08	0.01	0.06	0.00	0.00	0.00	0.03	0.02
K ₂ O	0.00	0.02	0.00	0.02	0.00	0.00	0.00	0.00	0.01	0.00	0.00
ZnO	0.12	0.13	0.19	0.22	0.11	0.08	0.21	0.16	0.16	0.05	0.07
Total	99.58	101.36	99.05	99.59	98.52	99.04	96.58	98.35	99.01	96.49	103.42
Cation	4 oxygens										
Fe total	0.23	0.27	0.25	0.25	0.25	0.25	0.24	0.23	0.25	0.25	0.25
Fe [*]	0.23	0.26	0.25	0.25	0.25	0.25	0.24	0.23	0.25	0.25	0.24
Fe ²⁺	0.22	0.20	0.23	0.23	0.23	0.23	0.17	0.22	0.26	0.23	0.21
Fe ³⁺	0.01	0.06	0.02	0.02	0.01	0.02	0.07	0.01	0.00	0.02	0.04
TiO ₂	0.02	0.03	0.11	0.07	0.04	0.01	0.04	0.05	0.03	0.08	0.09
Cr#	0.09	0.07	0.07	0.08	0.08	0.08	0.08	0.08	0.10	0.08	0.07
Mg#	0.77	0.80	0.77	0.77	0.77	0.77	0.83	0.78	0.74	0.77	0.79
Cr ₃ #	0.09	0.07	0.07	0.08	0.08	0.08	0.08	0.07	0.10	0.08	0.07
Al ₃ #	0.91	0.90	0.92	0.91	0.92	0.91	0.89	0.92	0.90	0.91	0.91
Fe ₃₊₃ #	0.00	0.03	0.01	0.01	0.01	0.01	0.04	0.01	0.00	0.01	0.02

Table II.2 Representative microprobe analyses of chromian spinels in ultramafic rock from Davos Switzerland.

Sample No	I11-2	I11-3	I11-4	I11-7	I12-1	I12-2	I13-2	I13-3	I13-5
SiO ₂	0.01	0.02	0.00	0.00	0.01	0.01	0.02	0.02	0.03
Al ₂ O ₃	47.32	48.30	47.67	48.56	48.77	46.94	47.92	46.98	46.21
TiO ₂	0.06	0.11	0.03	0.05	0.06	0.00	0.08	0.10	0.07
Cr ₂ O ₃	21.54	20.15	20.72	19.86	18.09	19.56	18.62	20.09	18.33
FeO	12.98	13.16	13.36	13.23	15.40	15.38	11.63	12.67	13.41
NiO	0.26	0.26	0.29	0.23	0.23	0.18	0.23	0.22	0.22
MnO	0.11	0.09	0.22	0.10	0.17	0.14	0.13	0.20	0.14
MgO	18.25	18.10	18.09	17.93	16.93	16.72	18.09	17.95	17.71
CaO	0.01	0.03	0.00	0.00	0.00	0.00	0.02	0.01	0.03
Na ₂ O	0.03	0.03	0.00	0.00	0.04	0.05	0.03	0.02	0.00
K ₂ O	0.00	0.01	0.01	0.00	0.00	0.00	0.00	0.02	0.01
ZnO	0.12	0.25	0.29	0.23	0.42	0.37	0.10	0.24	0.16
Total	100.69	100.50	100.70	100.20	100.12	99.35	96.87	98.50	96.32
Cation	4 oxygens								
Fe total	0.30	0.30	0.31	0.30	0.36	0.36	0.27	0.30	0.32
Fe [*]	0.29	0.30	0.31	0.30	0.35	0.36	0.27	0.29	0.32
Fe ²⁺	0.26	0.27	0.27	0.28	0.31	0.31	0.25	0.26	0.26
Fe ³⁺	0.03	0.03	0.04	0.02	0.04	0.05	0.02	0.03	0.06
TiO ₂	0.06	0.11	0.03	0.05	0.06	0.00	0.08	0.10	0.07
Cr#	0.23	0.22	0.23	0.22	0.20	0.22	0.21	0.22	0.21
Mg#	0.74	0.73	0.73	0.72	0.69	0.69	0.75	0.74	0.74
Cr ₃ #	0.23	0.22	0.22	0.21	0.20	0.21	0.20	0.22	0.20
Al ₃ #	0.75	0.77	0.76	0.78	0.78	0.76	0.79	0.76	0.77
Fe ₃ +3#	0.01	0.01	0.02	0.01	0.02	0.02	0.01	0.02	0.03

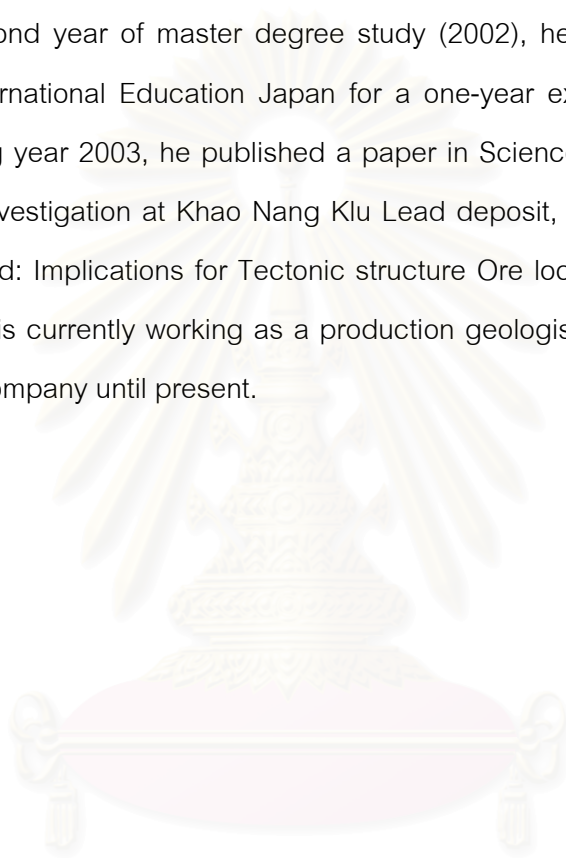
Table II.3 Representative microprobe analyses of chromian spinels in ultramafic rock from Indus Tibet.

Sample No	S57-1	S57-2	S57-3	S57-4	S58-1	S58-2	S58-3	S58-4	S59-2	S59-3	S62-1	S62-2	S65-2	S65-3	S69-1	S69-3	S70-1	S70-4	S70-5	S70-6	S72-1	S72-5
SiO ₂	0.00	0.09	0.04	0.02	0.00	0.02	0.00	0.00	0.03	0.05	0.00	0.07	0.00	0.00	0.01	0.02	0.03	0.00	0.03	0.04	0.01	0.02
Al ₂ O ₃	26.77	27.89	26.32	26.87	26.78	28.67	27.07	27.05	21.52	18.77	25.38	25.97	24.19	23.35	26.84	26.20	23.22	24.88	25.37	23.90	23.74	23.02
TiO ₂	0.48	0.52	0.61	0.63	0.69	0.57	0.75	0.61	0.02	0.00	0.04	0.04	0.00	0.05	0.24	0.25	0.71	0.58	0.57	0.63	0.52	0.45
Cr ₂ O ₃	42.10	40.20	41.16	40.44	40.81	38.73	40.77	40.62	45.93	49.61	42.43	40.72	43.56	42.83	41.15	41.05	44.99	42.29	42.45	44.31	44.35	43.83
FeO	15.80	18.51	17.08	17.26	16.81	16.76	14.91	18.06	18.62	17.63	22.18	21.35	19.93	22.76	16.08	16.77	16.11	16.58	16.20	15.04	15.58	19.36
NiO	0.13	0.06	0.07	0.13	0.10	0.08	0.07	0.07	0.02	0.12	0.08	0.07	0.04	0.05	0.09	0.04	0.10	0.09	0.05	0.13	0.09	0.07
MnO	0.27	0.28	0.31	0.26	0.27	0.23	0.23	0.28	0.29	0.31	0.51	0.39	0.32	0.46	0.20	0.24	0.32	0.31	0.26	0.24	0.26	0.37
MgO	13.47	12.11	13.62	13.22	13.65	13.47	14.44	12.95	11.52	11.93	8.97	9.24	10.72	8.38	13.90	13.27	13.43	13.42	13.29	13.59	13.54	10.91
CaO	0.03	0.02	0.02	0.05	0.00	0.00	0.00	0.00	0.01	0.00	0.01	0.01	0.00	0.00	0.01	0.03	0.00	0.00	0.01	0.00	0.02	0.02
Na ₂ O	0.00	0.06	0.01	0.06	0.00	0.00	0.02	0.03	0.00	0.00	0.02	0.00	0.06	0.01	0.00	0.00	0.00	0.03	0.05	0.04	0.00	0.00
K ₂ O	0.01	0.00	0.00	0.03	0.00	0.01	0.00	0.00	0.00	0.02	0.00	0.01	0.00	0.00	0.00	0.00	0.00	0.00	0.01	0.00	0.00	0.00
ZnO	0.17	0.18	0.22	0.34	0.25	0.25	0.21	0.18	0.19	0.16	0.53	0.73	0.34	0.46	0.23	0.31	0.21	0.21	0.24	0.12	0.10	0.28
Total	99.22	99.91	99.45	99.30	99.36	98.78	98.46	99.86	98.14	98.59	100.15	98.59	99.14	98.35	98.76	98.17	99.11	98.37	98.52	98.04	98.19	98.32
Cation	4 oxygens																					
Fe total	0.41	0.48	0.44	0.45	0.43	0.43	0.38	0.47	0.50	0.48	0.59	0.57	0.53	0.62	0.42	0.44	0.42	0.44	0.42	0.40	0.41	0.52
Fe*	0.39	0.45	0.41	0.42	0.40	0.40	0.35	0.44	0.50	0.48	0.59	0.57	0.53	0.62	0.40	0.43	0.39	0.41	0.40	0.37	0.39	0.50
Fe ²⁺	0.38	0.44	0.37	0.39	0.37	0.38	0.33	0.40	0.46	0.43	0.58	0.56	0.50	0.60	0.37	0.39	0.37	0.37	0.38	0.36	0.36	0.48
Fe ³⁺	0.01	0.01	0.04	0.03	0.03	0.02	0.02	0.03	0.04	0.04	0.01	0.01	0.03	0.02	0.04	0.04	0.03	0.04	0.02	0.01	0.02	0.03
TiO ₂	0.48	0.52	0.61	0.63	0.69	0.57	0.75	0.61	0.02	0.00	0.04	0.04	0.00	0.05	0.24	0.25	0.71	0.58	0.57	0.63	0.52	0.45
Cr#	0.51	0.49	0.51	0.50	0.51	0.48	0.50	0.50	0.59	0.64	0.53	0.51	0.55	0.55	0.51	0.51	0.57	0.53	0.53	0.55	0.56	0.56
Mg#	0.62	0.55	0.62	0.61	0.63	0.62	0.66	0.59	0.54	0.57	0.42	0.44	0.50	0.40	0.63	0.61	0.63	0.62	0.62	0.64	0.63	0.52
Cr ₃ #	0.51	0.49	0.50	0.49	0.50	0.47	0.50	0.49	0.58	0.63	0.53	0.51	0.54	0.54	0.50	0.50	0.56	0.52	0.52	0.55	0.55	0.55
Al ₃ #	0.48	0.50	0.48	0.49	0.49	0.52	0.49	0.49	0.40	0.35	0.47	0.48	0.45	0.44	0.48	0.48	0.43	0.46	0.47	0.44	0.44	0.43
Fe ³⁺ #	0.00	0.01	0.02	0.02	0.02	0.01	0.01	0.02	0.02	0.02	0.01	0.01	0.02	0.01	0.02	0.02	0.01	0.02	0.01	0.01	0.01	0.01

Table II.4 Representative microprobe analyses of chromian spinels in ultramafic rock from Song Ma Viet Nam.

BIOGRAPHY

The author graduated with his Bsc. (geology) from the Department of Geology Chulalongkorn University, Bangkok, Thailand in 2000. His senior project required for completing the degree was “Geophysical investigations of Lead deposit at Khao Nang Klu, Ban Kli Ti, Kanchanabury”. After graduation, he continued his study in the same institute. In second year of master degree study (2002), he got scholarship from the Association International Education Japan for a one-year exchange research student program. During year 2003, he published a paper in Science Asia Journal in the topic “Geophysical Investigation at Khao Nang Klu Lead deposit, Ban Kli Ti, Kanchanabury, Western Thailand: Implications for Tectonic structure Ore localization and Exploration”. Since 2003, he is currently working as a production geologist at Chatree gold Mine, of Akara Mining Company until present.



สถาบันวิทยบริการ
จุฬาลงกรณ์มหาวิทยาลัย